Fakultät für Medizin

Institut für Molekular Immunologie

The role of IKKα during diet-induced obesity and glucose intolerance in insulin sensitive tissues.

The role of glycosylation during intestinal carcinogenesis

Jessica Sylvie Pascale Heringer

Vollständiger Abdruck der von der Fakultät für Medizin der Technischen Universität München zur Erlangung des akademischen Grades eines

Doctor of Philosophy (Ph.D.)

genehmigten Dissertation.

Vorsitzender: Univ.-Prof. Dr. Jürgen Ruland

Bertreuerin: Priv.-Doz. Melek Canan Arkan-Greten, Ph.D.

Prüfer der Dissertation:

1. Univ.-Prof. Dr. Gabriele Multhoff
2. Univ.- Prof. Dr. Florian Richard Greten

Die Dissertation wurde am 04.02.2014 bei der Fakultät für Medizin der Technischen Universität München eingereicht und durch die Fakultät für Medizin am 26.06.2014 angenommen.

Table of Contents

LIST OF FIGURES AND TABLES

LIST OF ABBREVIATIONS

ABC	Avidin biotin complex
A/B	acrylamide/bisacrylamide
ACC	Acetyl-CoA carboxylase
AGEs	advanced glycated end products
Akt	=PKB protein kinase B
AMPK	5' adenosine monophosphate-activated protein kinase
AOX	alternative oxidase
APC	*Adenomatous polyposis coli or* Allophycocyanin
APS	*ammonium persulphate*
ATP	adenosine triphosphate
BAFF	B-cell activation factor
Bcl3	B-cell CLL/lymphoma3
B4galt6	Beta-1,4-Galactosyltransferase 6
BMI	Body mass index
BrdU	5'-Bromo 2' deoxyuridine
BSA	bovine serum albumin
cAMP	Cyclic adenosine monophosphate
CBP	CREB-binding protein
CCK	Cholecystokinin
cDNA	complementary DNA
c-IAP	cellular inhibitor of apoptosis
CD	cluster of differentiation
CD40L	CD40 ligand
CHUK	conserved helix-loop-helix ubiquitous kinase
Ckmm	Creatine kinase
Co	Control
CoA	Coenzyme A
COS	Columbia agar
Cpt1α	Carnitine palmitoyltransferase I
CRC	Colorectal cancer
DAB	3, 3′-Diaminobenzidine
DAPI	4', 6-diamidino-2-phenylindole
DC	dendritic cells
DC-SIGN	Dendritic Cell-Specific Intercellular adhesion molecule-3-Grabbing Non-integrin
dH_2O	distilled water
DEPC	Diethylpyrocarbonate
Dgat1	Diglyceride acyltransferase 1
dl	decilitre
DMSO	Dimethyl sulfoxide
DNA	deoxyribonucleic acid

DNase	deoxyribonuclease
dNTP	*deoxy*Nucleoside triphosphate
DTT	Dithiothreitol
ECL	enhanced chemiluminescent
EDTA	ethylenediaminetetraacetic acid
EGTA	ethylene glycol tetraacetic acid
ELISA	Enzyme linked immunosorbent assay
EMA	ethidium monoazide
Fabp4	fatty acid binding protein 4
FACS	fluorescence activated cell sorting
FBPase	fructose 1, 6-biphosphatase
FCS	foetal calf serum
FFA	Free fatty acid
FITC	fluorescein isothiocyanate
Fut	Fucosyltransferase
G6Pase	glucose 6-phosphatase
GAPDH	glyceraldehyde 3-phosphate dehydrogenase
GCG	Glucagon
Gcnt3	glucosaminyl (N-acetyl) transferase 3
GDP	guanosine di-phosphate
GEF	guanine nucleotide exchange factor
GIP	Gastric inhibitory polypeptide
GlcNAc	N-acetyl-D-glucosamine
GLUT	glucose transporter molecules
GLP	Glucagon-like peptide
GS	glycogen synthase
GSK3	glycogen synthase kinase 3
GTP	guanosine triphosphate
GTT	Glucose tolerance Test
H&E	Haematoxylin and eosin
H_2O	water
H_2O_2	hydrogen peroxide
HCl	hydrochloric acid
HFD	High fat diet
HGIEN	high-grade intraepithelial neoplastic
HNPCC	Hereditary nonpolyposis colon cancer
HSL	Hormone sensitive lipase
HSP70	Heat shock protein 70
IHC	immunohistochemistry
IκB	inhibitors of NF-κB

IKK	IκB kinase
IL	interleukin
IL1R	interleukin 1 receptor
Ins	Insulin
IR	insulin receptor
IRS	insulin receptor substrate
JNK	c-Jun N-terminal kinase
kDa	Kilo dalton
kg	kilogram
KO	Knock-out
K-ras	Kirsten-ras
LGIEN	low-grade intraepithelial neoplasia
LP	Lamina Propria
LPS	lipopolysaccharide
LPL	Lipoprotein lipase
LT	Lymphotoxin
M	mol/L
m^2	square meter
mA	mili Ampere
Mcad	Medium-chain acyl-CoA dehydrogenase
MCK	MacConkey agar
MCP	monocyte chemotactic protein
MEFs	Mouse embryonic fibroblasts
mg	milligram
Mgat4c	mannosyl (alpha-1, 3-)-glycoprotein beta-1, 4-N-cetylglucosaminyltransferase, isozyme C
MHC	major histocompatibility complex
min	min
ml	millilitre
MLN	mesenteric lymph nodes
mRNA	messenger RNA
Mttp	Microsomal triglyceride transfer protein
MUC	Mucin
NaCl	sodium chloride
ND	Normal diet
NEMO	NF-κB essential mediator
NF-κB	Nuclear Factor kappa B
ng	nanogram
NIK	NF-κB inducing kinase
NLS	nuclear localization signal

nm	nanometre
n.s	non-significant
OD	optical density
OGT	O-GlcNAc transferase
PAS	Periodic acid Schiff
PB/405	Pacific blue 405
PBS	phosphate buffered saline
PBS-T	phosphate buffered saline-tween
PDE3B	phosphodiesterase 3B
PE	Phycoerythrin
PEPCK	phosphoenolpyruvate carboxykinase
PI3K	phosphatidylinositol-3 kinase
PIP2	Phosphatidylinositol 4, 5-biphosphate
PIP3	Phosphatidylinositol 3, 4, 5-triphosphate
PKA	Protein kinase A
PKB	protein kinase B= Akt
PKC	Protein kinase C
pmol	picomol
PMSF	Phenylmethylsulfonyl Fluoride
PP	Pancreatic polypeptide or Peyer’s Patches
PP2A	protein phosphatase 2
PTEN	phosphatase and tensin homolog
PVDF	polyvinylidene difluoride
Raf	rapidly accelerated fibrosarcoma
RAS	rat sarcoma
RBC	red blood cell
Reg3a	regenerating islet-derived 3 alpha
RHD	REL homolog domain
RNA	ribonucleic acid
rpm	revolutions per min
RPMI	Roswell Park Memorial Institute medium
RT	room temperature
RTK	receptor tyrosine kinase
RT-PCR	real time-polymerase chain reaction
s	second
SBA	Small bowel adenocarcinoma
SCS	Schaedler agar
SDS	sodium dodecyl sulfate
SEM	standard error of the mean
SNVS	Schaedler-KV agar
SRC	Steroid receptor co-activator
STAT	signal transduction and activator of transcription

SteCoA	stearyl-*coenzyme A*
St3Gal IV	ST3 Beta-Galactoside Alpha-2, 3-Sialyltransferase 4
TAX1BP1	human T-cell leukaemia virus type I binding protein 1
TCR	T-cell receptor
TEMED	Tetramethylethylenediamine
TLR	Toll-like receptor
Tm4sf4	transmembrane 4 L six family member 4.
TNFα	tumour necrosis factor α
TNFR	tumour necrosis factor receptor
TRAF	TNF receptor-associated factor
Tregs	regulatory T cells
TSA	traditional serrated adenoma
V	Volt
VIP	Vasointestinal peptide
WB	western blot
WHO	World Health Organization
ZP103	Acetylated Galβ1→4GlcNAcβ-O-naphthalenmethanol
µ	micro
°C	degree celsius

1. INTRODUCTION

1.1 Obesity: epidemiology, definition, aetiology

The prevalence of obesity has increased dramatically in the last decades. According to World Health Organization (WHO), since 1980 the number of overweight individuals worldwide has more than doubled reaching 1.4 billion in 2008, among those 500 million are defined as obese. The numbers are expected to increase further and the estimates suggest 1.12 billion obese people by 2030 (Popkin et al. 2011).

Obesity is characterised as an excessive accumulation of fat tissue in the body. The most commonly used criteria to assess obesity is the Body Mass Index (BMI), which is defined as weight expressed in kilograms divided by height expressed in square metres. Normal BMI is defined as 18 to 25 kg/m², while overweight is between 25 and 30 kg/m². While BMI of 30 to 35kg/m² is defined as obesity BMI over 35 and 40 kg/m² is referred to morbid obesity (WHO).

Obesity is in most cases due to an imbalance between energy intake and energy expenditure. The increase in obesity prevalence over the last decades can mostly be explained by a change in the daily life style. Indeed, during the last decades, the technology permitted to decrease the efforts necessary to perform everyday tasks. Therefore, the amount of physical exercise decreased so as the energy expenditure. Moreover, the eating habit of people also had changed. A switch from a fruit-and-vegetable rich to a sweetener-fat-meat-rich diet (the so-called “Western diet”) took hold of during the last decades (Popkin et al 2011). However, genetic reasons can also explain obesity. Actually genetic disorders such Bardet-Biedl syndrome, or Prader-Willi syndrome, leads to obesity (OMIM entry n° 601665).

1.2 Metabolic syndrome: definition

The combination of obesity with increased circulating free fatty acids, high fasting glucose levels and hypertension is known as the metabolic syndrome. The distribution of adipose tissue in the body has diverse consequences. The sub-cutaneous fat does not lead to metabolic syndrome. Contrary to that, the abdominal fat tissue surrounding the organs in the abdominal cavity correlates well with the appearance of metabolic syndrome (Capurso et al 2012).

The excess accumulation of fat in the body has a lot of deleterious effects. These

consequences make obesity the fifth leading cause of death in the world (World Health Organization). A high BMI is a risk factor for the development of diabetes, gastrointestinal cancers (Li et al 2009; Agadjan et al 2012; Sung et al 2010) as well as cardiovascular diseases (Reaven 2012). Nowadays, a significantly increased incidence of type 2 diabetes, heart disease and cancer can already be attributed to obesity. Consequently, obesity leads to an increase of health costs and fighting against the obesity pandemic is therefore becoming a worldwide challenge.

1.3 Obesity is a low grade inflammatory condition

During obesity, hypertrophic adipose tissue is infiltrated with macrophages, which are polarized towards a phenotype (M1 phenotype) with increased pro-inflammatory cytokine secretion. TNFα, produced by the adipocytes and the macrophages infiltrating the adipose tissue, is a well-known pro-inflammatory cytokine. The production of TNFα can trigger activation of the NF-κB pathway. Fat tissue secretes IL-6 as well, which is known to be pro-inflammatory. Importantly, leptin stimulates the production of TNFα and IL-6 (Grundfeld et al 1996). Adiponectin, on the contrary is an anti-inflammatory adipokine. It inhibits the activation of NF-κB by Toll-like receptors (Yamagushi et al 2005). Moreover, it stimulates the production of IL10, an anti-inflammatory cytokine, produced by macrophages (Scarpellini et al 2012).

A study showed that recruitment of macrophages to adipose tissue via overexpression of the macrophages attracting chemokine, MCP1, is sufficient to cause insulin resistance. (Kanda et al 2006) Moreover, weight loss improves chronic inflammatory condition. When the storage capacity of adipose tissue is exceeded then the excess fat gets accumulated in other tissues such as pancreas, muscle and liver. Indeed, the constant production of pro-inflammatory adipokines by the hypertrophic fat tissue or by the infiltrating macrophages is believed to be the major sources for the systemic low-grade inflammation seen during obesity (Antuna-Puente et al 2008).

1.4 Glucose homoeostasis

Glucose homoeostasis is a very tightly regulated process. A disorder in glucose homoeostasis leading to hypo or hyperglycaemia can have severe consequences. As the major

source of energy for the brain is glucose, a hypoglycaemic condition can lead to central nervous system dysfunction and when prolonged to cell death (Ebert el al 2003, Cryer 2007). Temporary hyperglycaemic condition does not have damaging effects, however, chronic hyperglycaemia is the major feature of diabetes. The pancreas is the main player in the regulation of glucose homoeostasis as the two major hormones; glucagon and insulin, involved in the regulation of glycaemia are synthesised by the endocrine pancreas.

Glucagon is a 29 amino acids hormone produced by the α-cells of the endocrine pancreas. It is secreted in response to a low blood glucose level. Glucagon promotes gluconeogenesis, which is the conversion of liver glycogen to glucose in order to increase glycaemia and keep it at physiological level (Thomsen et al 1972).

Insulin is a 51 amino acids hypoglycaemic hormone produced by the β-cells of the endocrine pancreas (also called Langerhans islets) that is composed of a dimer of an A-chain and a B-chain. It is first produced as a pro-hormone called pro-insulin, which is then processed into insulin. During this process, 35 amino acids are removed from the pro-insulin to form insulin. 31 amino acid forms the C-peptide, which the levels are used to determine the insulin resistance (Nicol and Smith 1960).

The regulation of glucose homoeostasis involves different insulin sensitive tissues, which play a role in the balance of glycaemia. The skeletal muscle is the most important organ where glucose disposal takes place via an insulin-dependent mechanism. Liver, upon the stimulation of insulin, regulates around one third of the glucose uptake to produce glycogen via the glycogenesis. Finally, the adipose tissue is the organ where the fatty acid synthesis takes place under the control of insulin. Insulin resistance is the inability of an organ to uptake and clear the glucose. A deregulation of the insulin signalling leading to decreased glucose uptake in the insulin sensitive tissues conduces to insulin resistance (Sundsten and Ortsäter 2009) (Figure 1.1).

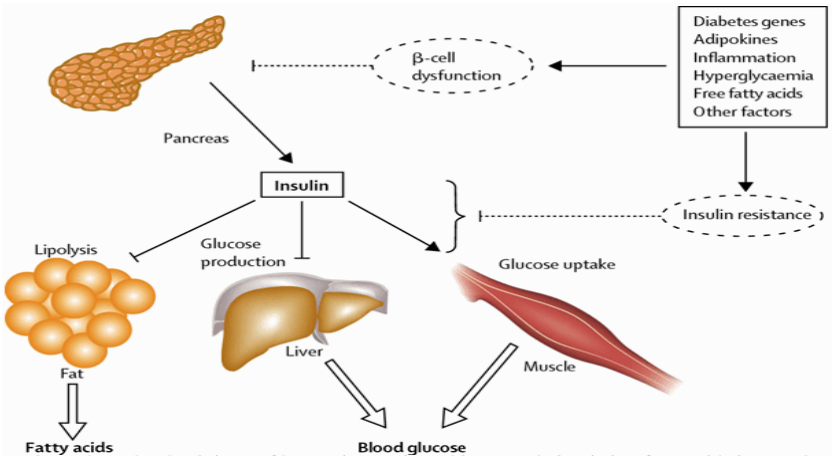

Figure 1.1 The regulation of glycaemia by insulin and the effects of insulin resistance and β-cell dysfunction (from http://jordan-tesch.wikispaces.com/Chapter+eight)

1.5 Insulin signalling pathway

During postprandial state the blood glucose level increases, which stimulates the production of insulin by the β-cells of the pancreas. The production of insulin then triggers the insulin signalling pathway to normalise the hyperglycaemia. To decrease the blood glucose level down to physiological level, insulin acts on different organs to stimulate the glucose uptake or the glycogenesis.

The insulin signalling pathway is complex and involves different sub-pathways leading to translocation of GLUT4 (Glucose transporter 4), as well as others leading to protein synthesis, lipolysis, or transcription. In order to avoid hypoglycaemia the insulin signalling pathway has to be tightly regulated, which will be described in details further (de Luca and Olefsky 2008).

When secreted, insulin binds to the transmembrane insulin receptor (IR) composed of an α subunit and a β subunit. The binding of insulin on the α subunit of the insulin receptor leads to the tyrosine autophosphorylation of the tyrosine kinase domain of the receptor's β subunit. The tyrosine kinase domain then phosphorylates the insulin receptor substrate (IRS) proteins on tyrosine residue and therefore activates the protein. Tyrosine phosphorylated IRS then recruits the Phosphoinositide 3 kinase (PI3K), which catalyses the reaction transforming Phosphatidylinositol 4, 5-biphosphate (PIP2) into Phosphatidylinositol 3, 4, 5-triphosphate (PIP3). PIP3 then phosphorylates protein kinase B (PKB) also known as Akt (Lizcano and Alessi 2002).

Akt has 3 different isoforms. While Akt1 is implicated in protein synthesis and in

various cancers, Akt3 is only expressed in the brain. Akt2 is the isoform involved in the insulin signalling pathway. However, there are substantial evidences that Akt2 plays a role in colorectal cancer (Agarwal et al 2013).

One of the important function of Akt2 in the regulation of the blood glucose level is that it phosphorylates the protein phosphatase 2 (PP2A), which then represses the protein kinase C (PKC) λ/ζ and leads to the exocytosis of the glucose transporter 4 (GLUT4) from its vesicles and therefore its translocation to the plasma membrane. This translocation allows the transport of glucose from the extracellular compartment to the intracellular compartment and therefore the suppression on the decrease of blood glucose levels (Lizcano and Alessi 2002) (Figure 1.2).

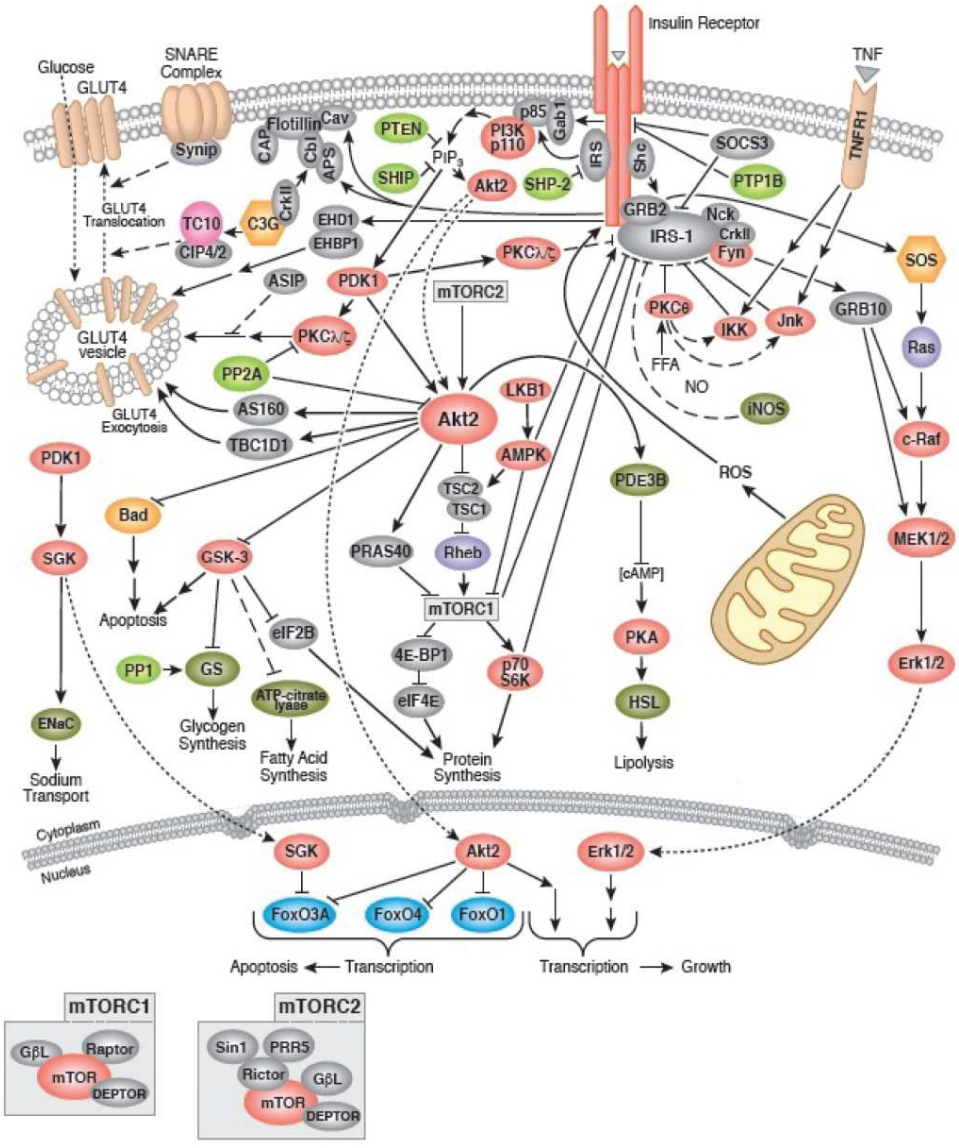

Figure 1.2: Insulin receptor signalling (modified from Cell Signaling®)

1.5.1 The glycogenesis and lipid metabolism pathways

After activation of Akt2 via the PI3K pathway, Akt2 phosphorylates glycogen synthase kinase 3 (GSK3), one of the major enzyme involved in the regulation of the glycogen synthesis. GSK3 is therefore inactivated and can no longer phosphorylate glycogen synthase (GS). GS is inactive when phosphorylated. Therefore, the inactivation of GSK3 ends up its activation. GS activation stimulates liver glycogenesis using blood glucose as a substrate and therefore results in the decrease of blood glucose level (Rowland et al 2011).

GSK3 phosphorylation also leads to the activation of ATP citrate lyase, an enzyme, which catalyses the reaction of conversion from citrate into oxaloacetate and acetyl CoA. Acetyl CoA is then used to synthesise fatty acids. Inactivation by phosphorylation of GSK3 therefore leads to an increase in fatty acid synthesis.

After activation, Akt2 can also phosphorylate the phosphodiesterase 3B (PDE3B). Phosphorylated PDE3B plays a role in the negative feedback of cAMP production by increasing its hydrolysis. The protein kinase A (PKA) is recruited and phosphorylates the hormone sensitive lipase (HSL), which leads to an inhibition of lipolysis (Carmen et al 2006) (Figure 1.2).

1.5.2 Regulation of the insulin signalling pathway

The insulin signalling pathway is regulated via phosphorylation/dephosphorylation processes. The protein tyrosine phosphatase dephosphorylates the insulin receptor leading to its inactivation.

Moreover, phosphatase and tensin homolog (PTEN) counteracts the PI3K pathway by hydrolysing phosphatidylinositol 3, 4, 5 tri-phosphate into PIP2 (Choi et al 2010).

The termination of the insulin signalling cascades can as well be done by modulation of the phosphorylation of IRS1. When IRS1 is phosphorylated on tyrosine residues it is active while when phosphorylated on serine or threonine residues this leads to its degradation (Pederson et al 2001).

Two main inflammatory pathways, activated by cytokines or free fatty acid (FFA), are involved in the regulation of the insulin signalling as well. The serine phosphorylation of IRS1 is mediated by IκB kinase β (IKKβ) and c-Jun N-terminal kinase (JNK). The FFA circulating in the blood can activate the protein kinase C θ (PKCθ) and can lead to

phosphorylation of JNK, which suppresses IRS-1/PI3K signalling via serine phosphorylation of IRS1 therefore leading to a decrease in glucose uptake. PKCθ can also activate IKKβ, which also phosphorylates IRS1 on serine residues leading to its degradation and termination of the insulin signalling cascade (Capurso et al 2012).

1.6 Diabetes and insulin resistance

1.6.1 Diabetes mellitus: definition

Diabetes mellitus is a disorder of glucose homoeostasis. Patients suffering from diabetes are unable to regulate their glycaemia without treatment since their blood glucose levels are chronically high. There are two main types of diabetes. The first one, the so-called type 1 diabetes, is insulin dependent. It has a genetically auto-immune aetiology, which leads to the destruction of the insulin secreting β-cells of the Langerhans' islets of the pancreas by the immune system. It is the most frequent type of diabetes seen in the youth. This diabetes is also referred to as “insulin-dependent diabetes” as insulin therapy and a particular diet can maintain normal glycaemia. The second type of diabetes is the type 2 diabetes, which is also called non-insulin-dependent diabetes. This type of diabetes has usually a late onset and is usually not commonly seen in the young people (OMIM Entry 125853).

The chronic hyperglycaemia in diabetic patients can lead to renal dysfunction, retinopathies as well as cardiac infarctus.

1.6.2 Pathogenesis of type 2 diabetes

Among the risk factors for the development of type 2 diabetes obesity appears to be very important. The aetiology of type 2 diabetes is quite complex. It is known since the beginning of the 1990's (Leahy 2005) that type 2 diabetes is characterised by three distinct features: insulin resistance, excessive production of glucose from the liver and dysfunction of β-cells. Even though a genetic predisposition has been highlighted, no gene has been pointed out as directly responsible for the development of type 2 diabetes so far. However, genetic deletion of leptin an anorexigenic hormone, leads to obesity and diabetes. Similarly, mutations in the leptin receptor gene provoke diabetes in mice (Chen et al 1996). The environment is playing an important role in the aetiology of this disease. Different studies have shown that the western life style is leading to obesity, which can cause type 2 diabetes. Diabetes is also

arising from acquired organ dysfunction, where defect occurs in glucose homoeostasis.

The chronology of development of type 2 diabetes has been proposed to be as follow (Leahy 2005). The first step is the acquirement of insulin resistance. Then the β-cell dysfunction occurs.

1.6.3 Insulin resistance

Different tissues are involved in the regulation of glucose homoeostasis. Therefore, insulin resistance can arise from different tissues or even from more than one at the same time.

1.6.3.1 Adipose tissue

The role of adipose tissue has been first thought to be only energy storage where lipolysis and fatty acid synthesis occurs. However, since few years, the role of adipose tissue has been enlarged to be an endocrine tissue synthesising hormones called adipokines and adipocytokines. Those hormones include leptin, adiponectin, and angiotensinogen (Antuna-Puente et al 2008).

The principal biological effect of leptin is in the central nervous system, more particularly in the hypothalamus and cerebellum, to regulate food intake and energy expenditure. It has some anorexic effects. Indeed, the deletion of the gene encoding for leptin (ob gene) in mice leads to obesity even without high fat diet (HFD) (Zhang et al 1994). Leptin has also some other effects in the regulation of body weight as it promotes weight loss by suppressing food intake and by stimulating metabolism (Klok et al 2006).

Leptinaemia also correlates well with the inflammatory status seen in obesity. Indeed, an increase in the pro-inflammatory response has been observed during hyperleptinæmia (Antuna-Puente et al 2008), which can be explained by the pro-inflammatory properties of leptin. Indeed, leptin controls TNFα production as well as macrophage activation (Loffreda et al 1998). Despite the increase of leptin expression in obese individuals, treatment with leptin does not lead to any weight loss. It has then been shown that obese individuals are leptin resistant (Klok et al 2006). Moreover, leptin might trigger MCP1 production leading to macrophage infiltration in the adipose tissue.

Contrary to those pro-insulin resistance effects, it has also been shown that leptin

improves insulin sensitivity through activation of AMP protein kinase (AMPK), which results in a decrease of lipogenesis and enhanced fatty acid beta oxidation leading to decreased free fatty acids (Antuna Puente et al 2008).

Adiponectin is highly expressed in the adipose tissue. Contrary to the other adipokines, adiponectin plasma concentration is decreased in obese patients suffering from insulin resistance or type 2 diabetes (Antuna Puente et al 2008). Adiponectin triggers the activation of AMPK like leptin and therefore improves insulin sensitivity. It has also been shown that adiponectin decreases liver gluconeogenesis by decreasing the mRNA expression of phosphoenolpyruvate carboxykinase (PEPCK) and glucose 6 phosphatase, the two key enzymes in gluconeogenesis. Moreover, adiponectin seems to have anti-inflammatory effects via reduction of TNFα-induced inflammation. (Ouchi et al 2001).

Fat tissue, as well as macrophage infiltrating adipose tissues secrete TNFα. TNFα knockout mice have an enhanced insulin sensitivity (Bastard et al 2006). Thus, it is likely that TNFα induced chronic inflammation plays an important role in fat tissue insulin resistance.

1.6.3.2 Skeletal muscle

The skeletal muscle is the major organ where glucose disposal takes place. During type 2 diabetes, insulin resistance in the skeletal muscle is an important contributing factor.

In skeletal muscle, the uptake of glucose is mainly done by GLUT4, which upon stimulation of the insulin pathway translocates from vesicles to the membrane. In skeletal muscle of type 2 diabetics patients, the expression of GLUT4 is normal. Actually, the insulin resistance seen in skeletal muscle might result from a deficiency of GLUT4 transport or an impaired function of this glucose transporter and not from a defect in GLUT4 expression (Garvey et al 1988, Dohm et al 1991).

Another possibility, which could explain the insulin resistance in skeletal muscle is an impaired insulin signalling via a reduced tyrosine phosphorylation of the IR or of IRS1 as well as a decrease in PI3K activation, which is the main pathway leading to glucose uptake (Abdul-Ghani et al 2010).

In type 2 diabetic patients, a decrease in PI3K activity has been shown (Kim et al 1999, Björnholm et al 1997). Since the PI3K pathway is the main pathway leading to GLUT4 translocation it further supports that insulin resistance in skeletal muscle might be due to an impaired transport of GLUT4.

Phosphorylation of glucose is the first step of glycogenesis as well as of glycolysis. Glycogen synthase (GS) is one of the main enzymes involved in glycogenesis. If there is a dysfunction of glucose phosphorylation or of glycogen synthase, the glucose cannot be used to produce glycogen. Therefore, it can lead to hyperglycaemia and then insulin resistance (Abdul-Ghani et al 2010).

It has been shown that insulin resistance in the skeletal muscle correlates well with increased BMI and that weight loss improves the skeletal muscle insulin resistance (Schenk et al 2009). Therefore, obesity *per se* can cause insulin resistance. This had been shown in studies that show accumulation of triglycerides in the skeletal muscle correlates inversely with insulin sensitivity (Pan et al 1997, Phillips et al 1996).

Moreover, in obese patients, fatty acid oxidation is decreased in comparison to lean persons (Kelley et al 1999). Fatty acid oxidation, also known as β-oxidation is used to produce energy from fatty acids. The complex responsible for the oxidative phosphorylation is located on the mitochondrial membrane. The decrease of oxidative phosphorylation found in obese patients is due to an impaired oxidative phosphorylation in the mitochondria (Abdul-Ghani et al 2010).

1.6.3.3 Liver

Insulin stimulates the transformation of glucose into glycogen in the liver, therefore, insulin resistance in liver provokes an increase in the glucose production. The mechanisms of hepatic insulin resistance are similar to that one in adipose tissue. During obesity, fatty acids can be found at ectopic location like liver. It results in liver inflammation with release of cytokines from the Kupffer cells, which are resident macrophages in liver. These cytokines can attract more macrophages and increase the inflammatory state leading to insulin resistance in the liver tissue (de Luca et al 2009).

1.6.4 β-cell dysfunction in type 2 diabetes

There are different causes of β-cell dysfunction in type 2 diabetes. Contrary to type 1 diabetes, the β-cells are not destroyed by the immune system but instead they show dysfunction.

Glucose toxicity, which is defined by high glucose levels leads to modification of β-cell physiology. Hyperglycaemia leads to the formation of advanced glycated end products

(AGEs), which activate JNK1 and IKKβ (Solinas and Karin 2010).

Oxidative stress, excessive production of electron flow from the mitochondria, is thought to be one possible cause of β-cell failure. As a matter of fact, oxidative stress causes impaired insulin secretion and activates JNK and NF-κB as well (Kamata et al 2005, Eriksson 2007, Kaneto et al 2007).

Lipotoxicity is defined by excess production of fatty acids. Indeed during adipose tissue expansion, lipids are found in ectopic locations like liver, muscle or pancreas. These fatty acids trigger activation of JNK, which constant activation is thought to cause β-cell dysfunction (Nguyen et al 2005, Malhi et al 2006, Solinas et al 2006).

The β-cell dysfunction provokes a decrease in insulin secretion and therefore causes glucose intolerance, which is the last step during development of type 2 diabetes (Leahy 2005). In conclusion, the JNK and NF-κB pathways seem to be at least partially responsible for the β-cell dysfunction.

1.7 Nuclear factor κB (NF-κB) pathway

1.7.1 NF-κB pathway is implicated in insulin resistance and diabetes

Insulin resistance is due to impaired glucose uptake in insulin sensitive tissues. Activation of IKKβ and therefore, NF-κB has been discovered to play a critical role in insulin sensitive tissues of obese and high fat-fed animals. A bulk of evidence points out the role of IKKβ in insulin resistance and diabetes. Indeed, heterozygous deletion of IKKβ or its pharmacological inhibition improves insulin sensitivity in rodents (Shoelson et al 2003). Moreover, IKKβ deletion in hepatocytes leads to fat and muscle insulin resistance while mice bearing IKKβ deletion in the myeloid cells remain insulin sensitive (Arkan et al 2005). Recently, another evidence linked IKKβ to insulin resistance. Indeed, the constitutive activation of IKKβ in fat tissue results in protection against diet-induced obesity and insulin resistance (Jiao et al 2012).

Loss of β-cells of the Langerhans islet in the pancreas is a key phenotype of type 1 diabetes. Eldor et al showed that the inhibition of NF-κB in the β-cells of the pancreas led to a protection of β-cells from apoptosis induced by diabetogenic agents. Additionally, an interference with TNFα, the major cytokine triggering the NF-κB classical pathway, protected from diet-induced insulin resistance (Solinas et al 2010, Eldor et al 2006).

In conclusion, substantial number of studies linked NF-κB, more precisely the

classical pathway via the IKKβ kinase, to insulin resistance. Nevertheless, to date there is no clear evidence that the alternative NF-κB pathway or IKKα plays a role in the development of insulin resistance and type 2 diabetes.

1.7.2 Proteins of the NF-κB pathway

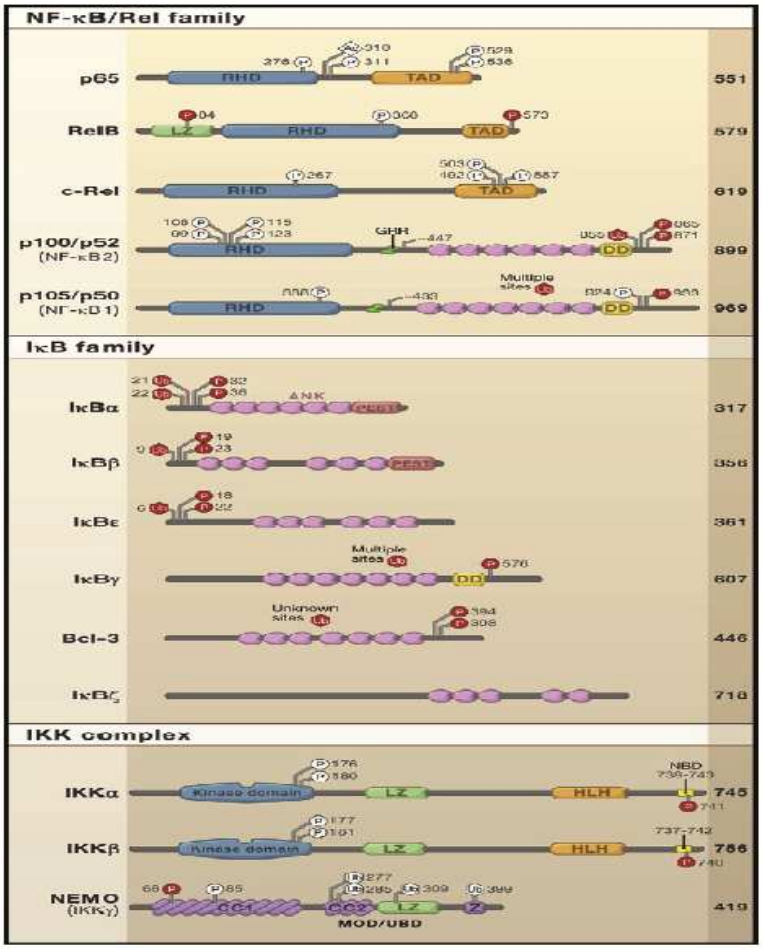

Figure 1.3: The proteins of the NF-κB pathway (from Hayden and Ghosh 2008)

NF-κB has first been discovered as a regulator of expression of the κB light chain in the B cells (Sen 1986). Since its discovery more than 25 years ago, much more is known about NF-κB now.

NF-κB is a family of transcription factors. In mammals, there are five members divided into two different subfamilies, the subfamily of the "NF-κB" protein and the subfamily of "Rel" protein (Gilmore 2006).

The proteins of the NF-κB family all contain a so-called Rel homology domain (RHD), which is a highly conserved DNA-binding/dimerization domain. This RHD contains a

nuclear localization sequence (NLS) and is involved in dimerization, DNA binding as well as interaction with the inhibitor of κB (IκB) proteins (Gilmore 2006).

c-Rel, Rel B and Rel A (also called p65) are the members of the Rel subfamily. They contain a C-terminal transactivation domain (Gilmore 2006).

The subfamily of NF-κB protein comprises the proteins NF-κB1 (p105) and NF-κB2 (p100). These proteins are processed via the proteasome upon activation of the pathway and results in cleaved called p50 and p52 proteins, respectively. The processing by the proteasome is vital for the activation of the NF-κB proteins (Gilmore 2006).

NF-κB proteins form homo or heterodimers. In a latent cell, the pathway is not activated and the NF-κB proteins are bound with IκB proteins, which are inhibitory proteins that interact with the nuclear localisation sequence (NLS) and the RHD to keep the NF-κB proteins in the cytoplasm (Gilmore 2006).

There are 5 different IκB proteins: IκBα, IκBβ, IκBγ, IκBε and Bcl-3. These proteins contain 5 to 7 ankyrin repeats, mediating protein-protein interaction, to bind the RHD of the NF-κB proteins.

The IκB kinases IKKα, also known as IKK1 or CHUK (conserved helix-loop-helix ubiquitous kinase) and IKKβ (IKK2) play a central role in the NF-κB pathway. These kinases are highly homologous and contain a kinase domain, a leucine zipper domain and a helix-loop-helix domain (Bonizzi 2004, Gilmore 2006).

The regulatory subunit IKKγ (also named NF-κB essential modulator NEMO), and NF-κB induced kinase (NIK) are also necessary for the NF-κB pathway. (Figure 1.3)

There are two major NF-κB pathways. The first one is called classical or canonical pathway and the second is called alternative or non-canonical pathway (Gilmore 2006).

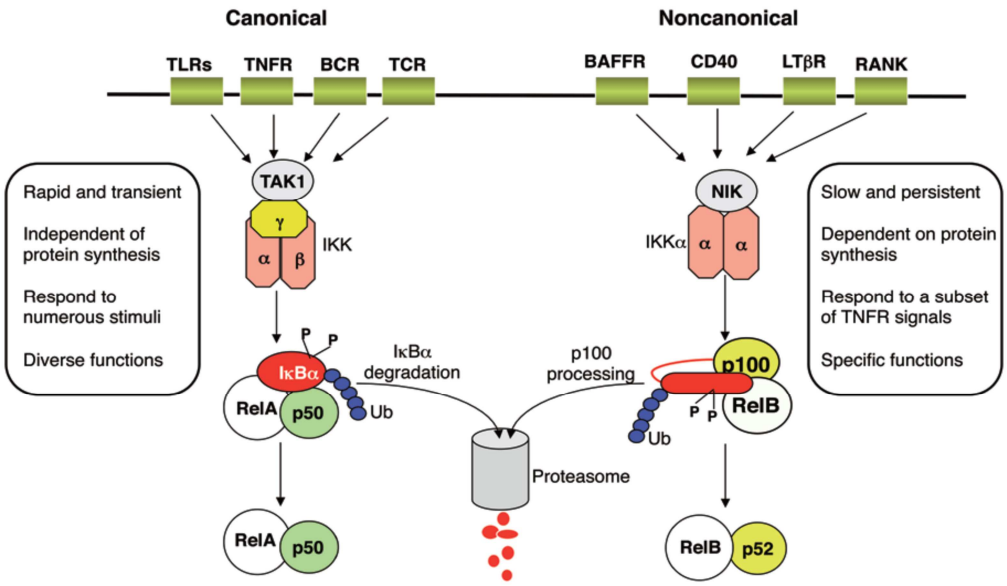

Figure 1.4 The classical and alternative NF-κB pathway (from Sun 2011)

1.7.3 Classical NF-κB Pathway

The canonical pathway is activated upon stimulation via various stimuli. Viruses or bacteria upon recognition by toll-like receptors (TLRs) can induce the activation of the NF-κB classical pathway. Activated macrophages produce the pro-inflammatory cytokines TNFα as well as interleukin 1 β (IL1β).Via binding to their receptors, tumour necrosis factor receptor (TNFR) and interleukin 1 receptor (IL1R) respectively, these cytokines can activate the NF-κB pathway (Hayden and Ghosh 2004).

Upon binding of the ligands on their respective receptors, the heterodimer IKKα/IKKβ bound to NEMO phosphorylates IκBα that is linked to the dimer p50/p65. This phosphorylation will lead to the ubiquitination of IκBα and its subsequent degradation by the proteasome. The degradation of IκBα releases the NLS and leads to the translocation of the p50/p65 dimer to the nucleus where it will transcribe genes encoding inflammatory proteins like cytokines, chemokines, adhesion molecules or inhibitors of apoptosis (Bonizzi and Karin 2004). Therefore, the classical pathway is important in inflammation, cell growth, differentiation and proliferation. It is as well essential for innate immunity as deficiencies in RelA or IKKβ leads to increased susceptibility to infection (Bonnizi and Karin 2004).

Regulation of the classical NF-κB pathway transcriptional activity has been shown to be at least partially dependent on the phosphorylation of p65. Indeed, when RelA is phosphorylated by protein kinase A (PKA), it enhances the DNA binding of NF-κB and

therefore facilitates transcription (Hayden and Ghosh 2004).

The mechanism of NF-κB pathway termination is poorly known. However, it is obvious that the resynthesis of the IκBs is important. Besides, a role of IKKα has been highlighted. It promotes p65 and c-rel degradation and therefore terminates inflammation driven NF-κB activation (Lawrence et al., 2005; Li et al., 2005). Besides the role of IKKα, Heat shock protein 70 (HSP70) interacts with NEMO to suppress NF-κB activation (Ran et al 2004, Weiss et al 2007) (Figure 1.4).

1.7.4 Alternative NF-κB pathway

The non-canonical NF-κB pathway has been discovered in 2001 (Senftleben et al 2001). This alternative pathway is independent of IKKβ and is activated by different stimuli like Lymphotoxin β (LTβ), B-cell activation factor (BAFF) or CD40 ligand (CD40L). The binding of ligands on the receptors will lead to an accumulation of NIK, which is going to phosphorylate the homodimer of IKKα. This results in the phosphorylation of the dimer p100/Rel B on the p100 subunit leading to the processing by the proteasome of p100 into p52. The processing of p100 releases the NLS of p100/p52 and therefore translocation of the resulting dimer p52/RelB to the nucleus occurs leading to transcription of genes encoding for proteins involved in development, function and organization of secondary lymphoid organs as well as B cell maturation and survival (Baud and Karin 2009).

The regulation of the NF-κB alternative pathway seems to be dependent on NIK (Razani et al 2010). When the pathway is not activated, NIK is degraded and cannot be detected unlike when the pathway is activated. The degradation of NIK is mediated by the TRAF-cIAP complex composed of TRAF2 (TNF receptor associated factor 2), 3, and cIAP (cellular inhibition of apoptosis). In unstimulated cells, this complex catalyses the ubiquitination of NIK leading to its degradation. However, in stimulated cells, the complex catalyses the ubiquitination of TRAF3 provoking destabilisation of the complex and NIK accumulation and activation of the NF-κB signalling cascade (Razani et al 2011). Yet, to avoid the constitutive activation of the NF-κB signalling, a negative feedback loop controlling NIK degradation must occur during activation. IKKα has been shown to exert a negative feedback on NIK after induction of the signalling cascade. IKKα destabilises NIK by phosphorylating it on its C-terminal part leading to its degradation (Razani et al 2010) (Figure 1.4).

1.8 IKKα

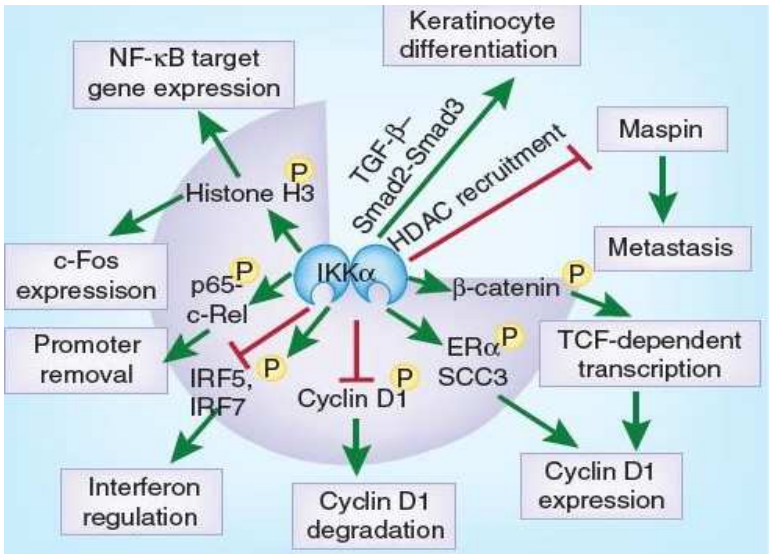

Figure 1.5: The NF-κB independent functions of IKKα (from Oeckinghaus et al 2011)

IKKα is an important kinase of the alternative NF-κB pathway as well as the classical pathway. Mice knocked out for IKKα in the whole body (Li et al 1999) present a wide range of developmental defects and are perinatally lethal. They lack whiskers and have a thicker epidermis, which can not differentiate. The limbs and tail do not expand out of the trunk. They also show some skeleton abnormalities.

Even though IKKα is an important kinase of the NF-κB pathway, it has some NF-κB independent functions, too. Kwak et al showed that IKKα deleted mouse embryonic fibroblasts (MEFs) are over-expressing cyclin D1 and that cyclin D1 is localised in the nucleus of the cells (Kwak et al 2005). When cyclin D1 is present, it leads to the entry in the S-phase of the cell cycle, therefore leading to proliferation. The presence of cyclin D1 in the nucleus of the cells is consequently implicated in tumour development. Kwak et al also showed that IKKα phosphorylates cyclin D1, which leads to the nuclear export of cyclin D1 and its degradation and subsequently to the exit of the cell cycle. NF-κB activation via TNFα and IL1 is decreased in these IKKα deficient MEFs. The increase in cyclin D1 transcription might be explained by the fact that IKKα seems to increase β-catenin protein levels as well as its downstream signals including cyclin D1 transcription (Oeckinghaus et al 2011).

When IKKα deficient MEFs are transplanted to nude mice, the animals develop tumour. Moreover, micro-array analysis showed a decrease in IKKα gene expression in human lung cancer cell lines. Taken together, these results characterise IKKα as a tumour suppressor (Kwak et al 2011). Indeed, IKKα has as well been implicated in skin carcinoma.

Indeed, some mutations in IKKα and a down-regulation of its gene have been found in human squamous cell carcinomas. The reduced IKKα expression leads to tumour promotion and progression to malignancy. Hence, IKKα appears to be a tumour suppressor (Liu et al 2012).

Contrary to its role as a tumour suppressor, IKKα has also been found to promote metastasis in prostate cancer but not tumour formation (Karin 2008).

Recently, (Shembade et al 2011) a role of IKKα in the regulation of the canonical NF-κB pathway has been highlighted. Indeed, a new substrate of IKKα has been discovered. The phosphorylation of TAX1BP1 (human T-cell leukaemia virus type I binding protein 1) by IKKα in response to pro-inflammatory stimuli leads to down-regulation of the canonical NF-κB signalling. Therefore, IKKα negatively regulates the classical NF-κB pathway by limiting inflammatory gene activation. IKKα also regulates the non-canonical pathway by phosphorylating NIK and therefore leads to its degradation and consequently the termination of the NF-κB signalling (Razani et al 2010).

Bakkar et al showed that IKKα KO mice have reduced mitochondrial content in the skeletal muscle and that over-expression of IKKα in the muscle leads to an increase in oxidative metabolism (Bakkar et al 2012).

IKKα has been shown to be able to shuttle from cytoplasm to nucleus to phosphorylate histone H3 under stimulation of TNFα. It can also directly regulate gene transcription by phosphorylating co-activators like CBP (Chariot 2009). The phosphorylation of CBP provokes a preference of CBP for NF-κB promoters versus p53 promoters therefore stimulating cell proliferation.

The phosphorylation of Steroid receptor co-activator SRC-3 by IKKα enhances SRC-3 translocation to the nucleus to transcribe pro-inflammatory NF-κB target genes (Chariot 2009).

In summary, in comparison to the other members of the NF-κB pathway, the role of IKKα is not fully known. It acts as a tumour suppressor and seems to have critical functions during development. It is a kinase involved in inflammation. Despite recent progress in unravelling its function, a lot remain to be discovered about IKKα (Figure 1.5).

1.9 Small bowel adenocarcinoma (SBA)

1.9.1 The hallmarks of cancer

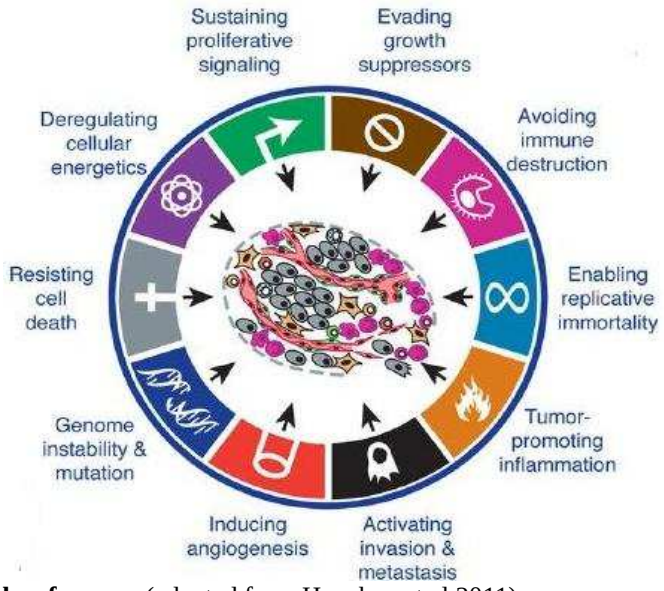

Figure 1.6: The hallmarks of cancer (adapted from Hanahan et al 2011)

The so-called “Hallmarks of cancer” have been suggested by Hanahan and Weinberg in 2000. These hallmarks represent the characteristics a cell needs to have in order to become malignant. The first one is that a tumour has the capacity of resisting cell death. Moreover, a tumour is capable of evading growth suppressors, sustain proliferation signalling, enabling replicative immortality. This leads to the development of the tumour. As tumours need a lot of energy to grow, it can also induce angiogenesis in order to increase nutrient supply. A malignant cell is also capable of invasion and metastasis. Since few years some other hallmarks have emerged. Inflammation has been shown to promote tumourigenesis. It has also been found that a tumour can escape destruction by the immune system, a process known as immune escape. Moreover, tumour cell have deregulated cellular energetics and genome instability and mutations (Hanahan and Weinberg 2000 and 2011) (Figure 1.6).

1.9.2 Epidemiology and aetiology

The small intestine is despite its length only rarely the site of neoplasms. Indeed, only 2% of the gastrointestinal cancers are located in the small intestine. Despite recent advances in diagnosis and treatment, the SBA remains as a poorly prognosed type of cancer. As a matter

of fact, only 30% of the patients diagnosed with SBA survive 5 years (Delaunoit et al 2005).

Histologically, there are around 40 different types of small intestinal neoplasms, among those the small bowel adenocarcinoma is the most common one. This type of adenocarcinoma arises from the mucosal glands of the intestine. Tumours are mostly found in the duodenum part of the small intestine while they are less common in the jejunum and ileum (Delaunoit et al 2005).

Some data suggest that SBA might arise from a sequence of mutations similar to the one found in colon cancer. Some key genes like *k-ras, p53* and the mismatch repair genes might be involved in this cascade of mutations. Moreover, clinical and pathological similarities are found between colorectal cancer and SBA. Therefore, the carcinogenesis model of colon cancer might apply to SBA (Delaunoit et al 2005).

Colorectal cancer (CRC) is due to two distinct cascades of mutations. The first one is involving mutations in APC (adenomatous polyposis coli), *k-Ras and p53* while the second one is due to mismatch repair defects. The most common mutation found in the *K-Ras* gene is a substitution mutation at the codon 12, which transforms glycine into aspartic acid (Delaunoit et al 2005).

The progression of SBA is similar to the one of colorectal cancer although some differences exist. The first mutation to appear in SBA is the *k-ras* mutation such in colorectal cancer. It has been shown that the down-regulation of p16 and p19 as well as an over-expression of cyclinD1 and p27 is an early event in SBA. (Arber et al 1999) Then mutations in p53, a gene involved in DNA repair during replication, occur commonly. In the colon this mutation seems to be rather late and defines the transition from adenoma to carcinoma. Mutations in the APC gene, although common in CRC, are rare in SBA. Nevertheless, a reduced expression of β catenin is frequently seen in SBA as well as in CRC, which suggest that β-catenin mutation is sufficient to induce SBA (Delaunoit et al 2005).

Mismatch repair genes might as well be responsible for SBA as patients with hereditary nonpolyposis colorectal cancer (HNPCC) have frequent mutations in these genes and that the HNPCC patients have a higher risk factor for developing SBA (Delaunoit et al 2005).

Risk factors for SBA are both genetic, as the incidence of SBA is higher in patients with a predisposition to gastrointestinal cancers like in familial adenomatous polyposis. Among the acquired predispositions, (obesity, Crohn's disease, coeliac disease) one can notice that inflammation is an important risk factor for carcinogenesis. Indeed, obesity is a state of low-grade chronic inflammation while Crohn's disease is an inflammatory bowel disease.

There is substantial evidence that inflammation is a risk factor for different cancers including colorectal cancer (Delaunoit et al 2005).

1.9.3 Ras pathway

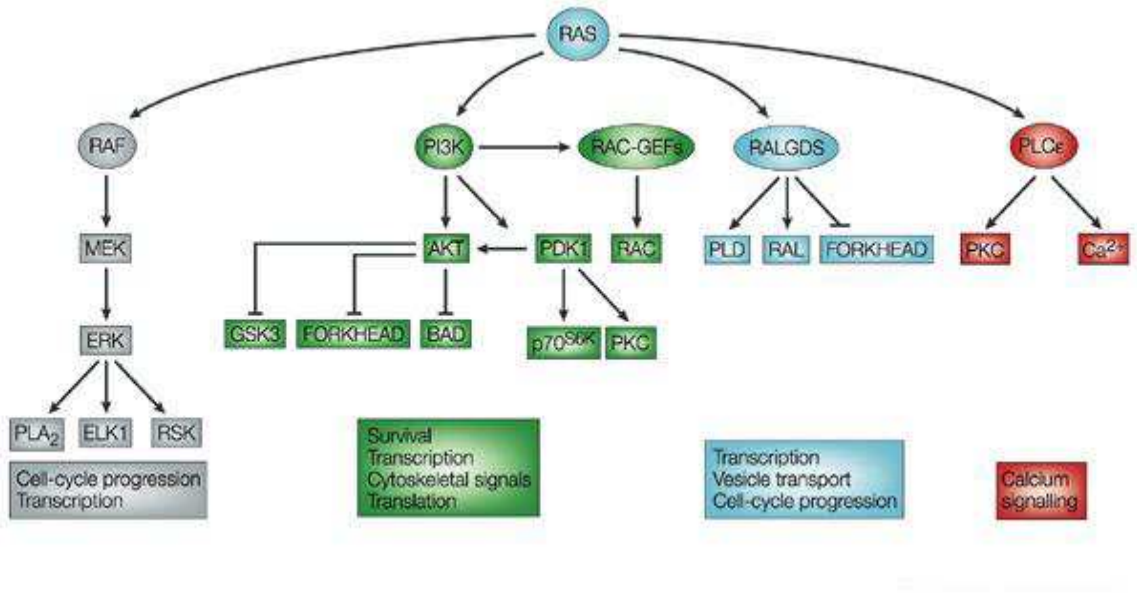

Figure 1.7: the Ras signalling pathway (adapted from Downward 2003)

Ras proteins (Rat sarcoma protein) are small guanosine triphosphate (GTP) binding proteins involved in signal transduction. Upon binding of growth factors on receptor tyrosine kinase (RTK) or antigen on T-cell receptor (TCR), the GEF (guanine nucleotide exchange factor) is activated and will replace the GDP (guanosine di-phosphate) coupled to Ras, which is therefore inactive, by a GTP (guanosine tri-phosphate) leading to the activation of Ras. Therefore, the Ras signalling cascade is activated and will, among others, activate the Raf pathway leading to cell-cycle progression. Ras can also activate Akt via the PI3K signalling, which is anti-apoptotic and therefore leads to survival, translation or transcription (Downward 2003). Mutations in Ras induce cells to have the characteristics of a malignant cell.

There are 3 different Ras proteins encoded by the genes *Hras*, *Kras* and *Nras*. *Kras* (V-Ki-ras2 Kirsten rat sarcoma viral oncogene homolog) mutations are often found in human cancers, among those colorectal, pancreatic and lung cancer. The *Kras* mutation leads to its activation and therefore to constitutive proliferation or transcription (Malumbres and Barbacid 2003) (Figure 1.7).

1.9.4 The villin-specific activation of *Kras* in a mouse model of intestinal cancer

As *Kras* mutation at codon 12 is the most commonly found mutation in colorectal cancer mice bearing a mutation in the *Kras* gene at the position 12 substituting glycine with aspartic acid (*Kras*^{G12D}) have been developed. Upstream of the first exon, flanking LoxP sites contain a STOP cassette (LSL *Kras* ^{G12D} mice), which allows upon crossing with a Cre expressing mouse line, the activation of the mutated *Kras* (Jackson et al 2001) in specific tissues or cells of interest.

The LSL *Kras* ^{G12D} mice have been crossed to a mouse strain expressing the gene of Cre recombinase under the promoter of Villin, a protein mostly expressed in the epithelial cells of the intestine (Bennecke et al 2010). Phenotypically, these mice show a significant increase in the intestine length. At 1 year of age, 25% of the LSL *Kras* ^{G12D} mice show spontaneous adenoma in the colon (Bennecke et al 2010). ViRas mice have longer and larger intestine than the control mice. This macroscopically observation is as well found at the microscopic level. Indeed, the villi of the ViRas mice are longer and serrated. Moreover, mice show hyperplastic colon (Bennecke et al 2010).

1.10 Protein glycosylation

1.10.1 Glycans

Saccharides are carbohydrates of different types. Among these, there are pentoses (ex: xylose), which contain 5 carbons, the hexoses (ex: glucose) that have 6 carbons, the hexosamines, which are hexoses with an amino-group that can be acylated (ex: N-acetyl-D-glucosamine (GlcNAc), as well as desoxyhexoses (ex: fucose), uronic acids (ex: glucuronic acid) and sialic acid that contains 9 carbon acidic sugars (Varki et al Essential of glycobiology Chapter 1).

Glycans are mono or polysaccharides covalently linked to cell or macromolecules like proteins. The glycocalix surrounding all the cells, as the name suggests, is composed of glycans linked to the membrane proteins. The mucus secreted by some cells is in majority composed of mucins, which are heavily glycosylated proteins (Varki et al Essential of glycobiology Chapter 9).

The attachment of the glycan to the protein may be done via a α or β linkage on the anomeric carbon of one sugar. Then, the second sugar can be linked at diverse positions

generating variable glycans with different three dimensional structures and biological roles. These different ways that covalently link saccharides result in a huge diversity of glycans. Moreover, small changes in the environment may lead to changes in the glycans (Varki et al Essential of glycobiology Chapter 1).

There are two main types of protein glycosylation. The N-glycosylation consists of linking a glycan to the nitrogen of an asparagine residue of the protein. The O-glycosylation is linking a glycan to an oxygen atom of the side chain from a serine or a threonine residue. The glycosylation takes place in the Golgi apparatus.

1.10.2 Biological roles of protein glycosylation

Glycosylation is a post translational modification. The genome contains only few genes encoding for glycosyltransferases responsible for the glycosylation of the proteins (Varki et al Essentials of glycobiology Chapter 1).

Protein glycosylation is a very important mechanism in the organism discovered a long time ago. Some much known antigens like blood group antigens are glycosylated proteins. In medicine, glycans are already used for treatment. Indeed, heparin, one of the most common anti-coagulant drugs is a glycoprotein. Protein glycosylation is not only a feature of eukaryotes. Indeed, the bacterial cell wall is composed of glycan and viruses have hemagglutinine on their surface (Varki et al Essential of glycobiology Chapter 6).

Glycans have a lot of biological roles. They are crucial for development, growth, function and survival (Varki et al Essentials of glycobiology chapter 1). The glycoproteins, which are in the glycocalix, are a physical barrier against pathogens for the cells. Moreover, glycans are important for tissue structure and protect the proteins against proteases or antibodies. Glycans are important for the proper folding of the proteins in the endoplasmic reticulum. The interaction between proteins is facilitated by their glycosylation pattern. The selectins, one type of glycoprotein, are adhesion molecules important for the interaction between blood cells and matrix cells.

Glycosylation is a reversible post translational modification and can therefore be used as a regulatory mechanism.

1.10.3 Glycosylation and immune system

Glycosylation is very important in the immune system. Indeed, almost all membrane immune receptors are glycoproteins. Moreover, pathogens contain membrane glycans used by the immune system to recognise them. Therefore, the immune system uses the glycans to recognise viruses, bacteria or parasites. Glycosylation is present at every step of the development of an infection, from the recognition to the spreading and inflammation (Rabinovich et al 2012).

The glycosylation of pathogens can be a barrier to the immune system recognition. In fact, as an example the Human Immunodeficiency Virus has its main antigen protein completely glycosylated that makes it almost inaccessible to the antibodies (Rabinovich et al 2012). The gram negative bacteria, which have lipopolysaccharide (LPS) in their outer membrane are recognised by the TLR4 receptor which then trigger inflammation and NF-κB pathway activation. However, bacteria modify their LPS to escape the TLR4 recognition (Varki et al Essential of glycobiology chapter 39). In order to escape the immune system, some pathogens developed the capacity to mimic the glycosylation pattern of the host and therefore use it as a decoy for the immune system, which no longer recognises them as “non-self” (Varki et al Essentials of glycobiology chapter 6).

Glycoproteins are as well important for the invasion step of infection. The interaction between lectin and glycan is useful for the epithelial barrier invasion. Some pathogens are totally dependent on some glycoprotein to be able to infect human. For example, the human malaria parasite needs an interaction with a blood group antigen in order to invade erythrocytes (Varki et al Essentials of glycobiology chapter 39).

Moreover, it has been shown that bacteria influence the glycosylation pattern of the intestinal mucosa. Indeed, conventional raised mice have more glycosylation in the mucosa than germ-free raised mice (Freitas et al 2002).

1.10.4 ST3 Beta-Galactoside Alpha-2,3-Sialyltransferase 4 (St3Gal IV) and Sialyl Lewis X antigen

St3GalIV is a sialyltransferase, which transfers sialic acid residue on galactose. It has been shown to be important for leukocytes recruitment in the epithelium. Mice deficient for St3GalIV show reduced leukocyte extravasation and adhesion (Sperandio 2012). St3GalIV is as well essential for chemokine receptor function. St3GalIV is not present in CD4 naive T-

cells but its expression is up-regulated upon stimulation. (Blander et al 1999) Moreover, TNFα up-regulates Sialyl Lewis X via the up-regulation of St3GalIV (Colomb et al 2012) suggesting a role for St3galIV in Sialyl Lewis X synthesis. This implication is additionally shown by studies, which showed that St3GalIV is implicated in selectins ligands formation (Ellies et al 2002, Sperandio et al 2006, Frommhold et al 2008).

Mice deficient for St3GalIV (Ellies et al 2002b) present a complete loss of L-selectin ligand function. Further sialylation done by St3GalIV is necessary for leukocyte arrest under inflammatory conditions (Frommhold et al 2008).

The Sialyl Lewis X antigen (sLe^x Sia α 2, 3 Gal β 1, 4 (Fucα 1, 3) GlcNAc) is a blood antigen. It is synthesised by the β4GalNAcT-II and fucosyltransferase IV and VII (Malagolini et al 2007) as well as from the α2, 3 sialyltransferases III, IV and VI (Lühn and Wild 2012). The first step of synthesis of sialyl lewis X is adding a sialic acid to a galactose residue of a lactosamine and then a fucose residue is added (Lün and Wild 2012). Sialyl Lewis X is found at the surface of leukocytes and tumours cells (Barthel et al 2007). Therefore, Sialyl Lewis X has an important role for selectin mediated interactions between leukocytes and endothelial cells. It is as well important in tumour cell adhesion processes. Moreover, Sialyl Lewis X is found on numerous cancer cells (Portela et al 2011). The ectopic expression of Sialyl Lewis X antigen favours metastasis (Malagolini et al 2007). Therefore, sialyl Lewis X antigen is important in carcinogenesis and its synthesis might be a good target for cancer treatment.

Furthermore, Lewis X antigen is thought to have an important role in the pathogenesis linked to H.*pylori*, however, its exact role is not yet known (Varki et al Essentials of Glycobiology chapter 13).

80% of the gastro-duodenal ulcers are due to the infection by the bacteria H.*pylori*. The presence of H.*pylori* correlates with pre-cancerous gastric lesion and its role in gastric cancer is recognised (Sauerbaum and Michetti 2002).

1.10.5 O-GlcNacylation

Among the different types of glycosylation, O-GlcNacylation (glycosylation of nuclear or cytoplasmic proteins with β-linked N-Acetylglucosamine) is the most abundant one. It has been shown that O-GlcNAc modification is important for cell-cycle progression. The transferase responsible for O-GlcNacylation (O-GlcNAc transferase, OGT) is required for embryonic stem cell survival. O-GlcNacylated proteins are transcription factors, among

those NF-κB or p53, translation regulatory factors as well as proteins involved in signalling, stress responses and energy metabolism. O-GlcNAc glycosylation is as well required for the trafficking of β-catenin and E-cadherin to the cell surface of epithelial cells. When they are O-GlcNAcylated, they are blocked on the cytoskeleton. E-cadherin is an important adhesion molecule and therefore its sequestration in the cytoplasm could impair the metastatic process. O-GlcNacylation has also an impact on diabetes. It is known that O-GlcNacylation of GLUT4, an important glucose transporter in the muscle and adipose tissue, inhibits the transport of glucose (Park et al 2005).

O-GlcNAcylation has been shown to enhance the metastasis of breast and lung cancer (Gu et al 2011). In the same study they also showed that breast cancer cells are more glycosylated than the normal tissue.

1.10.6 Glycan binding proteins

Glycans are recognised by two major types of glycan binding proteins. The first class is the lectins while the second one is glycosaminoglycan binding proteins. Lectins are subdivided into four different groups. The C-type lectins need calcium for the recognition of the glycan, the galectins need free thiols, the I-type lectin is from the immunoglobulin superfamily and the last group is the P-type lectins (Varki et al Essentials of Glycobiology chapter 45);

1.10.7 Glycosylation changes in cancer

Different changes in the glycosylation pattern of proteins have been found in tumour cells. Since years, over or down-expression of mucins, which are heavily glycosylated proteins, has been found in carcinomas. For instance, MUC2 expression is down-regulated in colorectal, gastric and ovarian cancers. Similarly, MUC5AC is abnormally expressed in colorectal and pancreatic cancers (Rachagani et al 2009). Glycosylation of carcinomas is often incomplete and loss of certain structures or over-expression of others is a common feature of tumours (Varki et al Essentials of glycobiology chapter 44). As there is a difference of glycosylation between cancer tissue and normal tissue, there are attempts to use the serum glycoproteins as a cancer biomarker in order to diagnose cancer by non-invasive and reliable methods (Adamczyk et al 2011).

Cancer cells might also change their glycosylation pattern in order to escape the immune system, which will not recognise their tumour antigens. Sialyl Lewis X antigen is frequently over-expressed in carcinomas and its expression correlates with tumour progression, metastatic potential and metastatic spread.

Tumour cells can escape the immune system such that they are not recognised and therefore not eliminated. The mechanism of immune escape is not well defined. However, evidence points out to an important role for regulatory T-cells (T_{reg}) in immune escape (Oleinika et al 2013). Indeed, T_{reg} are responsible for tolerance to self-antigens. T_{reg} accumulate in tumours and it has been shown that the T_{reg} suppression is concentration dependent (Oleinika et al 2013). van Gisbergen et al showed that dendritic cells recognise colorectal tumour cells via a C-type lectin (DC-SIGN) and a tumour-specific glycosylation. They also suggest that the tumour cells might use this interaction with DC-SIGN to suppress dendritic cell function and therefore escape the immune system (van Gisbergen et al 2005). The changes of glycosylation during carcinogenesis are thought to provoke the immune escape of the tumours cells (AnandKumar and Devaraj 2013). Therefore, inhibition of glycosylation, and more particularly inhibition of the “tumour antigens” might be an effective tool against cancer.

2. AIM OF THE STUDY

2.1 The role of IKKα in diet-induced diabetes

Since a few decades, a change in diet habits happened. A switch from a vegetable rich, meat poor diet to a vegetable poor, meat rich diet increased the daily calories uptake and therefore the percentage of overweight and obese people worldwide. At the same time, a decrease in energy expenditure took place. As obesity has a lot of medical complications like type 2 diabetes and gastrointestinal cancers, the increased incidence of obesity correlates with an increase of those pathologies, which reached epidemical levels. The increased incidence of chronic disease increased the health costs. To fight the obesity pandemic is not only a matter of public health but as well a matter of economy.

Glucose homoeostasis is a tightly regulated process, which involves pancreas, adipose tissue, liver and skeletal muscle. Therefore, a dysfunction of one of those tissues can lead to glucose intolerance, insulin resistance and finally to diabetes. The molecular mechanisms leading to type 2 diabetes are only partially understood, therefore, to elucidate the complete mechanisms is important to develop treatments.

Obesity is characterised by a state of low chronic inflammation arising from the hypertrophic adipocytes, which secrete adipokines. Inflammation has been shown to be a cause of cancer and diabetes development. NF-κB pathway, a well-known inflammatory pathway, has been shown to be involved in inflammation related cancers. Moreover, there are some evidences that NF-κB pathway is as well involved in diabetes. However, while the role of the canonical NF-κB pathway in diabetes and more especially IKKβ is known, there is currently no clue about the role of the non-canonical pathway in diabetes. As IKKα, a kinase homologous to IKKβ is a key kinase of the non-canonical pathway, we thought that it might have a role to play in diet-induced diabetes. To verify this hypothesis, mice with a deletion of IKKα in the insulin sensitive tissues; endocrine and exocrine pancreas, fat tissue and skeletal muscle were used. In order to trigger obesity and chronic inflammation, the mice were fed a HFD. To separate the effects due to IKKα deletion and the obesity *per se* effects, some mice were kept on ND to compare them to the HFD fed animals. The animals have been analysed at the physiological (GTT, weight monitoring) as well as at the cellular (IHC, histology) and molecular (real-time PCR, western blot) levels.

2.2 Glycosylation changes in intestinal cancer

Obesity is a risk factor for cancer and especially gastrointestinal cancers. The oncogene *Kras* has been shown to be important in the onset of gastrointestinal cancers. Therefore, mice bearing an oncogenic activation of *Kras* specifically in the intestinal epithelial cells were used for the study (ViRas mice). The carcinogenesis of the ViRas mice is faster when fed a HFD than when fed a ND showing that obesity *per se* triggers cancer.

Moreover, intestine is the host of millions of bacteria from different species. Their role is to mature the immune system as well as to help digestion. It has been shown that a switch in the populations of commensal bacteria is found in obese patients. The shift in the bacterial populations has as well been found in the ViRas mice fed a HFD reproducing the results found in obese patients. The switch of bacterial population led to the hypothesis that the bacteria might somehow be responsible for the carcinogenesis. Furthermore, bacteria are heavily glycosylated organisms. The glycosylation serves as a bacterial identity card for the immune system and influences the host own glycosylation pattern. During cancer, a modification of the host glycosylation has been found. Therefore, the shift in microbiota during obesity coupled to the glycosylation changes found in cancer lead us to study the glycosylation changes in the ViRas mouse model fed a HFD.

As the ViRas mice presented glycosylation changes as well as differences in glycosyltransferase gene expression, we crossed the ViRas mice with a mouse line bearing a whole body deletion of the glycosyltransferase St3GalIV and checked the glycosylation changes and the carcinogenesis development. Moreover, we wanted to know if the pharmacological inhibition of glycosyltransferase has the same effect as the genetic deletion. We therefore treated the ViRas mice fed a HFD with two different glycosyltransferase inhibitors and studied the effect of the treatment on carcinogenesis, glycosylation pattern. As it was shown that ViRas mice present a decreased activation of the immune system we as well checked if the same effect is seen in the mice treated with a glycosyltransferase inhibitor.

3. MATERIALS AND METHODS

3.1 Mice models

The mice used in this study were kept in pathogen-free facility under a 12h/12h light/dark cycle and fed a normal diet (Rodent Standard Diet, Altromin #1314) or when specified a high fat diet (Research Diets, #D12492).

IKKα fl/fl mice (Liu 2008)

A neomycin cassette surrounded by LoxP site has been inserted in intron 6 of the IKKα gene. A supplementary LoxP site has been created in intron 9. The neomycin cassette has been removed using a Cre vector. The Cre recombination leads to a deletion of exon 6 to 8 leading to a frameshift.

Ins-Cre mice (Postic et al 1999)

Those mice bear the gene of the Cre recombinase under the promoter of the rat insulin II and a fragment of the human growth hormone leading to the specific expression in the β-cells of the pancreas.

Fabp4-Cre mice (He et al 2003)

This mouse line has the Cre recombinase gene under the promoter of mouse Fabp4 a promoter mainly expressed in the adipose tissue.

Ckmm-Cre mice (Brüning et al 1998)

This strain carries the Cre recombinase gene under the Ckmm promoter leading, when breed with a floxed strain to a deletion in skeletal and cardiac muscle

p48 (Ptf1a)-Cre mice (Kawagushi et al 2002)

The coding region of p48 has been replaced by the Cre recombinase gene, leading to the expression of the recombinase in the acinar cells of the pancreas.

Villin-Cre mice (Madison et al 2002)

This mouse strain carries the Cre recombinase under the promoter of the villin protein, therefore expressed only in the intestinal epithelial cells.

K-ras^{G12D} mice (Johnson et al 2001)

A floxed stop cassette has been inserted upstream of an exon 1 modified with a mutation at codon 12. Upon Cre recombinase activation, the stop cassette is deleted and the exon with the mutation is transcribed.

St3GalIV $^{\Delta/wt}$ mice (Ellies et al.2002)

Mice bearing a deletion of the St3GalIV gene were purchased from Jackson laboratory.

3.1.1 Genotyping of mice

The mice are anaesthetized via inhalation of Isofluran^{TM} and a piece of tail is cut with a scalpel.

The tail biopsy is lysed in 190 µL of tail lysis buffer and 10 µL of proteinase K (Qiagen®) at least 2 h at 60°C. The proteinase K is then inactivated by heating at 95°C during 10 min. The tails are centrifuged 10 min at 4°C at 13200 rpm. 10 µL of the supernatant is diluted into 90 µL of dH_2O. This dilution is used as a template for the PCR reaction.

Tail lysis buffer:
1.5 M Tris (pH 8.5) (Roth®)
200 mM NaCl (Sigma®)
0.2% sodium dodecyl sulfate (SDS) (Fluka®)
5 mM Ethylenediaminetetraacetic acid (EDTA) (Fluka®)

PCR mix:
12,5 µL Taq PCR master mix (Qiagen®)
0,5 µL 10 pmol forward primer
0,5 µL 10 pmol reverse primer
9,5 µL RNase free water (Qiagen®)
DNA 2µL

PCR conditions

Cre/αLox PCR

94°C 5 min
94°C 30 s
58°C 30 s
72°C 30 s
} 35 cycles
72°C 7 min
4°C ∞

kRas PCR

94°C 5 min
94°C 30 s
60°C 1 min
72°C 1 min
} 35 cycles
72°C 7 min
4°C ∞

St3GalIV PCR

94°C 3 min
94°C 30 s
65°C 1 min
72°C 1 min
} 35 cycles
72°C 2 min
10°C ∞

3.1.2 Primers

All primers used in this study have been manufactured by Eurofins MWG.

Primer name	Primer	Primer sequence
kRas	Forward	CCATGGCTTGAGTAAGTCTGCG
	Reverse	CGCAGACTGTAGAGCAGCG
Cre	Forward	ACCTGAAGATGTTCGCGATTATCT
	Reverse	ACCGTCAGTACGTGAGATATCTT
αlox	Forward	GGAATTAGTTCTCCTCTTCTCATATGG
	Reverse	TTAAATTGTTGAAATATCTGTAAAGGAAGG
St3	Forward	GGCTGCTCCCATTCCACT
	Reverse	GGCTCTTTGTGGGACCATCAG

Table 3.1: list of primers used for genotyping

3.1.3 Mouse Sacrifice and tissue processing

Prior to sacrifice mice were fasted overnight and 2h prior to sacrifice, an intraperitoneally injection of 5'-Bromo 2' deoxyuridine (BrdU). Mice were sacrificed by cervical dislocation after inhalation of Isofluran in order to anaesthetize them. Organs: liver, spleen, stomach, pancreas, fat, muscle and intestine were collected and put overnight in 4% para-formaldehyde (Electron microscopy science). On the next day, tissues were processed in a dehydration machine (Leica ASP300S) and embedded in paraffin.

For RNA and protein isolation, a part of each tissue was snap frozen in liquid nitrogen and stored at -80°C.

3.1.4 Blood count

About 40 µL of blood is collected from the tail vein and put in 10 µL EDTA 0.5M. The samples are then diluted at a 1 to 3 dilution in dilution buffer from the machine Sysmex xt 2000i and analysed on that same machine.

3.2 Histology

Paraffin blocks were cut in 2 µm section using a microtome (Leica RM2235) and put in a water bath at 45°C and afterwards on glass slides (Thermo scientific®). The slides are dried at room temperature until processing.

3.2.1 Haematoxylin and eosin staining (H&E)

2 µm sections were cleared from paraffin by immersing in xylol during 10 min. The sections were then dehydrated using decreasing concentrations of ethanol (100% 96% 80% 70% 50%) each time 2 min.

The slides were then counter-stained in haematoxylin (Vector laboratories®) during 1 min and rinsed with dH_2O. Afterwards, the sections are stained with a solution of 1% eosin Y and rinsed twice with dH_2O

They were then dehydrated using increasing concentration of ethanol (50% 70% 80% 96% 100%) each time 2 min. A final step of cleaning is performed by immersion in xylol during 10 min.

After drying at room temperature the sections were covered with mounting medium (Vecta Mount from Vector Laboratories®) and cover-slides.

3.2.2 Immunohistochemistry (IHC)

The sections were cleared from paraffin and dehydrated the same way as for H&E staining. The slides were then washed during 5 min with PBS.

After washing the sections were circled using an ImmEdge pen™ (Vector laboratories®) and incubated in 3% H_2O_2 diluted in PBS during 10 min to mask endogenous peroxidase activity. Three steps of 5 min washing are then performed in PBS.
*For nuclear proteins, the sections were boiled in the microwave submerged with Antigen masking solution (Vector Laboratories®) during 20 min.
The slides were then cooled down during 20 min.
*For cytoplasmic or membrane proteins the section were incubated 10 min in 0.03% triton in PBS at room temperature

The slides were then washed 5 min in PBS. The unspecific antigens were blocked

in blocking solution (3% BSA (Sigma®) /PBS+ 4 drops of streptavidin (Vector laboratories ®)) during 30 min at room temperature.

The first antibody was diluted in 3% BSA/PBS with 4 drops of streptavidin and 4 drops of biotin. (Blocking kit Vector laboratories®) (For the dilutions and the conditions of the different antibodies used *cf* table 2)

The sections are incubated in primary antibody solution either overnight at 4°C or 2 hours at room temperature. Three steps of 5 min washing are then performed in PBS. Slides are then incubated during 30 min with secondary antibody solution (Second antibody 1/200 in 3%BSA/PBS with 4 drops of streptavidin per mL) at room temperature. The sections are then washed 3 times 5 min with PBS and then incubated with ABC solution from Vector Laboratories® (5 mL PBS+ 2 drops of solution A+ 2 drops of solution B) during 30 min at room temperature. The slides were then washed 3 times 5 min in PBS and then transferred in dH_2O.

To reveal the IHC DAB solution is used: 5 mL dH_2O+ 2 drops buffer+ 4 drops DAB stock+ 2 drops of H_2O_2. (Vector laboratories®) The slides are checked for colour reaction under the microscope. When the colour reaction appeared the slides are transferred in clean dH_2O. The nuclei are stained during 1 min in haematoxylin (Vector Laboratories®) and then washed with dH_2O.afterwards the slides are re-hydrated and mounted the same way than in H&E staining.

3.2.3 Immunofluorescence

The deparaffinisation and re-hydration is done as in H&E staining. The sections are then washed 3 times with PBS for 5 min each.

For antigen retrieval the slides are incubated during 10 min at room temperature in 0.03% Triton in PBS. Then 3 steps of 5 min washing in PBS are performed. To block nonspecific antigens the slides are incubated 30 min at room temperature in 3% BSA/PBS with Fc Block (antibody anti CD16/32) at a dilution of 1/1000.

The following steps have to be performed in the dark.

The sections are incubated 1 hour at room temperature in the antibody solution: 3% BSA/PBS+ fluorescently labelled antibody. 3 washing steps are performed and the slides are covered with Anti Fade Prolong Medium (Invitrogen®) which contains DAPI to stain the nuclei.

Antibody	Labeling	Dilution	Secondary antibody	Incubation	Company
BrDU	X	1:200	Rat	2h room temperature	Amersham bioscience
IKKα	X	1:1000	Mouse	Overnight 4°C	IMGENEX
Insulin	X	1:1000	Guinea pig	Overnight 4°C	
Glucagon	X	1:1000	Mouse	Overnight 4°C	R&D systems
Ki67	X	1:1000	Rabbit	Overnight 4°C	SantaCruz
F4/80	FITC	1:200	X	1h room temperature	No secondary antibody
B220	FITC	1:200	X	1h room temperature	No secondary antibody
GR1	FITC	1:200	X	1h room temperature	No secondary antibody

Table 3.2 : Antibodies used in immunohistochemistry and immunofluorescence

3.2.4 Periodic acid Schiff staining

The periodic acid Schiff (PAS) staining is used to determine glycogen amount in liver, heart or muscle.

The sections are deparaffinised and rehydrated as for the H&E staining. They are then stain in 0.5% of periodic acid solution (Sigma®) for 5 min and afterwards rinsed in dH_2O. The slides are then incubated in Schiff reagent (Sigma®) for 15 min and washed in lukewarm tap water for 5 min. Sections are counter-stained with haematoxylin during 1 min, washed in tap water. Dehydration and clearing is done as for H&E staining.

3.2.5 Alcian blue staining

The sections are cleared from paraffin and rehydrated as previously described in H&E staining section.

The sections are then stained 30 min at room temperature with Alcian blue solution (1g Alcian Blue+ 100 mL 3% Acetic acid, pH 2.5). Afterwards, the slides are washed with tap water until colour is gone and counter-stained in Nuclear Fast red solution (Vector laboratories) for 5 min. Sections are then washed with tap water for 1 min and dehydrated with ethanol and cleaned with xylol as previously described.

Sections are then mounted with mounting medium.

3.3 RNA extraction

RNA extraction was done using Trizol™. (Ambion®). 30 to 50 mg of tissue was homogenized in 1 mL of Trizol™ using a Polytron PT 1200E™. Between each sample the polytron is washed with 10% SDS (Fluka®) in DEPC water and 2 times DEPC water. Samples are then centrifuged 10 min at 12000 rpm at 4°C. The supernatant is collected and transferred in another tube. Samples are incubated 5 min at room temperature and 200 µL of chloroform is added. The samples are mixed vigorously by hand and incubated 2 to 3 min at room temperature. A centrifugation step 15 min 4°C 12800 rpm is performed. The upper aqueous part is collected and 400 µL of isopropyl alcohol and 400 µL of high salt solution™ (MRC®) is added. Samples are incubated 15 min at room temperature and then centrifuged 10 min at 4°C 12800 rpm. The supernatant is removed with pipette and the pellet washed with 400 µL of 70% ethanol in DEPC water.
Samples are vortexed and centrifuged 5 min at 4°C 10100 rpm. The supernatant is removed and the RNA pellet is dried at room temperature cap open. RNAs are dissolved in 50 µL of DEPC water and the quality is checked with a Nano drop™.

3.4 cDNA synthesis

The cDNA synthesis was realized using the Invitrogen® Superscript II™ kit. 1 µg of RNA was used for the synthesis. 1 µL of dNTP (10 nM each) from Invitrogen® was mixed with 1 µL Oligo (dT) 12-18 (500 µg/mL) from Invitrogen®, 1 µg of RNA and RNase free water up to 12 µL. The mix was heated at 65°C during 5 min in a thermomixer compact (Eppendorf®) then removed and quickly put on ice. After a quick centrifugation, 4 µL of the 5x first strand buffer, 2 µL of 0.1M of DTT (dithiothréitol) from the Superscript II™ kit was added as well as 1 µL of RNase out (40 units/µL from Invitrogen®) and 1 µL of Superscript II™ enzyme. The samples were heated at 42°C during 50 min. They were then removed and put at 70°C during 15 min. 80 µL of water (Aqua ad injectabilia Braun®) was added to the samples.

The cDNA were stored at -80°C.

3.5 Real time PCR

To performed real time PCR, 5 µL of RNAse free water is mixed with 2 µL of primer mix and 10 µL of SYBR green. 3 µL of cDNA is added. The program used is as followed:

Denaturation

50°C 2 min

95°C 10 min

*Cycling stage *40*

95°C 15 s

60°C 1 min

Melting curve

95°C 15 s

60°C 1 min

95°C 15s

Target	Primer	Primer sequence
Mttp	Forward	CAAGCTCACGTACTCCACTGAAG
	Reverse	TCATCATCACCATCAGGATTCTC
SteCoA	Forward	GAGGCCTGTACGGGATCATA
	Reverse	CCGAGCCTTGTAAGTTCTGTG
AOX	Forward	CGCCTATGCCTTCCACTTTCTC
	Reverse	CGCAAGCCATCCGACATTCTT
Mcad	Forward	GCAGCCAATGATGTGTGCTTA
	Reverse	CACCCTTCTTCTCTGCTTTGGT
ACC	Forward	GCCATTGGTATTGGGGCTTAC
	Reverse	CCCGACCAAGGACTTTGTTG
LPL	Forward	AAGGTCAGAGCCAAGAGAAGCA
	Reverse	CCAGAAAAGTGAATCTTGACTTGGT
Fas	Forward	GGCATCATTGGGCACTCCTT
	Reverse	GCTGCAAGCACAGCCTCTCT
Cpt1α	Forward	CTCAGTGGGAGCGACTCTTCA
	Reverse	GGCCTCTGTGGTACACGACAA
IL1β	Forward	GTGGCTTGAGAAGCTGTG
	Reverse	GAAGGTCCACGGGAAAGACAC

IL6	Forward	ATGGTACTCCAGAAGACCAGAGGA
	Reverse	GTATGAACAACGATGATGCACTTG
TNFα	Forward	ACTCCAGGCGGTGCCTATG
	Reverse	GAGCGTGGTGGCCCCT
Cyclophilin	Forward	ATGGTCAACCCCACCGTGT
	Reverse	TTCTGCTGTCTTTGGAACTTTGTC
IL18	Forward	CAAAAGAAACCCGCCTGTGT
	Reverse	TCACAGCCAGTCCTCTTACTTCAC
F4/80	Forward	CTTTGGCTATGGGCTTCCAGTC
	Reverse	GCAAGGAGGACAGAGTTTATCGTG
CD4	Forward	GAGGCTCAGATTCCCAACCA
	Reverse	GCAGCAAGCGCCTAAGAGAG
CD8	Forward	CGTGGTGGTGCATGCCT
	Reverse	CGTGGTGGTGCATGCCT
CD11c	Forward	AACAGAGGTGCTGTCTACATATTTCATG
	Reverse	TGCTGAAATCCTCTGGCTGG
Glucagon	Forward	GGCACATTCACCAGCGACTAC
	Reverse	GTTCCGGTTCCTCTTGGTGTT
Insulin	Forward	GGACCTTCAGACCTTGGCGTT
	Reverse	GTTGCAGTAGTTCTCCAGCTGGTAG
PP	Forward	CTCTCCCTGTTTCTCGTATCCACTT
	Reverse	TATCTGCGGAGCTGAGTTTCATATT
GLUT1	Forward	ATCGTCGTTGGCATCCT
	Reverse	CAAGTCTGCATTGCCCA
GLUT2	Forward	GGTGTGATCAATGCACCTC
	Reverse	GTATCTGGGGCTTTCTGGAC
PEPCK	Forward	CCCAGGAAGTGAGGAAGTTTGT
	Reverse	CTTTCTCCGAAGCCTCATTAGC
FBPase	Forward	CCATCATAATAGAGCCCGAGAAGA
	Reverse	CTTTCTCCGAAGCCTCATTAGC
Leptin	Forward	GAGACCTCCTCCATGTGCTG
	Reverse	CATTCAGGGCTAAGGTCCAA
Ghrelin	Forward	GTCAGGAGCTCAGTATCAGC
	Reverse	TTCTTGCTCAGGAGAAGGAAAG
VIP	Forward	TTCACCAGCGATTACAGCAG
	Reverse	TCACAGCCATTTGCTTTCCTG

GIP	Forward	CAGGTAGGAGAGAAGACCTCCA
	Reverse	CCTAGATTGTGTCCCCTAGCC
G6Pase	Forward	GAAGGCCAAGAGATGGTGTGA
	Reverse	TGCAGCTCTTGCGGTACATG
GLUT4	Forward	CACAGAAGGTGATTGAACAGAGC
	Reverse	TCCGGTCCCCCAGGA
IRS1	Forward	GGCTGGCAATACGGT
	Reverse	GCCAAATCCAGGTCTATGTA
IR	Forward	TGAGTCAGCCAGTCTTCGAA
	Reverse	ACTACCAGCATTGGCTGTCCT
Dgat1	Forward	GGTGCCGTGACAGAGCAGGAT
	Reverse	CAGTAAGGCCACAGCTGCTG
CCK	Forward	TGATTTCCCCATCCAAAGC
	Reverse	GCTTCTGCAGGGACTACCG
GAPDH	Forward	TGAAGCAGGCATCTGAGGG
	Reverse	CGAAGGTGGAAGAGTGGGAG
Mgat4c	Forward	TCCCACGTCTGGCCCA
	Reverse	AGAGAGAAGGTTTAAATCGAATCACAT
St3GalIV	Forward	AGCCTCGAGTGTCGTCGCT
	Reverse	TCAATCTGATGACCACGTCGTACT
Reg3a	Forward	GGTGAGGCTTCCTTTGTGTCC
	Reverse	CTCCATTGGGTTGTTGACCC
B4galt6	Forward	AAGCCCAGATGGAAGGTGG
	Reverse	GTTTCTGGAGCATCGGAATCA
Gcnt3	Forward	CCTTTGGGCCACCCTCC
	Reverse	CAAATTTTCGATGCAAGGGATC
Fut4	Forward	AGAACGCACGGATAAGGCG
	Reverse	GCGATTCGAAGTTCAATCCACA
Tm4sf4	Forward	GGAGGAATATTGGGAAGTGGAGT
	Reverse	TCGTTGTTCTGCAGGCCC

Table 3.3: List of the primers used for RT-qPCR

3.6 Protein extraction

Protein lysis buffer

50 mM tris-HCl pH 7.5

25 mM Sodium Pyrophosphate decahydrate (Sigma®)

250 mM Sodium chloride (Sigma®)

3 mM EDTA (Fluka®)

3 mM EGTA 1% Triton X (Sigma®)

0.5% NP-40

10% glycerol

dH_2O to 1L

A tablet of Roche® complete phosphatase inhibitor cocktail is dissolved in 50 mL of protein lysis buffer. 8 mL of this protein lysis buffer + phosphatase inhibitor cocktail is mixed with 100 µL of PMSF and 500 µL of each of the phosphatase inhibitor (Sodium pyrophosphate decahydrate, sodium orthovanadate (Sigma®), glycerol 2 phosphate disodium salt pentahydrate (Sigma®), sodium fluoride (Sigma®).

The tissues are crushed on liquid nitrogen using a mortar and a pestle and then homogenized in complete protein lysis buffer. Samples are then centrifuged 20 min at 4°C 13200 rpm. The supernatant is collected and stored at -80°C.

3.7 Bradford assay

10 mL of the stock solution is diluted with 40 mL of dH_2O. 1 mL of this dilution is used per sample. 2 µL of protein sample is added, mixed and incubated 5 min at room temperature. Absorbance is read at 595 nm using the Nanodrop™.

3.8 Western blot

Separation gel solution:

181.65 g of Tris in 400 mL of dH_2O. pH is set to 8.8. 20 mL of 20% SDS is added and the volume adjusted to 500 mL

Stacking gel solution:

12.11g Tris in dH_2O, pH 7.0

5 mL of 20% SDS

Adjust volume to 100 mL

10X transfer buffer

144g glycine

30g Tris

1L dH_2O

1X transfer buffer

100 mL 10X transfer buffer

200 mL methanol

700 mL dH_2O

Separation gel

<u>10%</u>

7.5 mL dH_2O

3.75 mL running gel buffer

3.75 mL acrylamide/bisacrylamide 40%

112.5 µL APS 10%

11.25 µL TEMED

<u>7%</u>

8.62 mL dH_2O

3.75 mL running gel buffer

2.63 mL A/B 40%

112.5 µL APS10%

11.25 µL TEMED

<u>12%</u>

6.75 mL dH_2O

3.75 mL running gel buffer

4.5 mL A/B

112.5 µL APS 10%

11.25 µL TEMED

Stacking gel
4.6 mL dH_2O
950 µL stacking gel buffer
950 µL A/B
62.5 µL APS 10%
12.5 µL TEMED

Laemmli buffer
3.55 mL dH_2O
1.25 mL Tris-HCl 0.5 M pH 6.8
2.5 mL Glycerol
1 mL 20% SDS
0.2 mL of 0.5% bromophenol blue (Sigma®)

The gel is run at 120V in running buffer. Transfer is realized on a PVDF membrane after activation with methanol during 15 seconds for 2 hours at 250 mA in transfer buffer. After the transfer the membrane is incubated 30 min at room temperature in 5% milk (Sigma/®) in PBS-T to block unspecific binding. The membrane is then incubated in first antibody solution overnight at 4°C (for dilutions of the antibodies *cf* Table 3.4). The next day the membrane is washed 3 times 5 min with PBS-T and incubated with the secondary antibody solution at a concentration of 1/3000 in 5% Milk/PBS-T. The membrane is afterwards washed 3 times 5 min with PBS-T then incubated 5 min with a mix 1:1 of ECL solution (Super Signal WEST Pico Thermo Scientific®) and put in contact with X-Ray films (Thermo Scientific®) between 1s to 40 min. The film was developed using the Hyperprocessor (Amersham Bioscience®).

3.9 Western-blot O-GlcNAc

In order to detect the glycosylation pattern, the O-GlcNAc detection kit from Thermo Scientific®. The protocol of the manufacturer is followed.

Antibody	Dilution	2nd antibody	Dilution 2nd antibody	Company
O-GlcNAc	1:5000 in blocking buffer	goat@mouse	1:5000 in blocking buffer	Thermo Scientific
IKKα	1:1000 in 5% Milk/PBS-T	@mouse	1:3000 in5% Milk/PBS-T	IMGENEX
β-actin	1:2000 in 5% Milk /PBS-T	@Mouse	1:3000 in5% Milk/PBS-T	Sigma
Akt	1:1000 in 5% Milk/PBS-T	@rabbit	1:3000 in5% Milk/PBS-T	Cell signaling
P-Akt	1:1000 in 3% BSA/PBS-T	@rabbit	1:3000 in5% Milk/PBS-T	Cell signaling
GAPDH	1:1000 in 5% Milk/PBS-T	@rabbit	1:3000 in5% Milk/PBS-T	Cell signaling
@mouse	1:3000 in 5% milk/PBS-T	X	X	GE Healthcare
@rabbit	1:3000 in5% Milk/PBS-T	X	X	GE Healthcare
goat@mouse	1:5000 in blocking buffer	X	X	Thermo Scientific

Table 3.4 : Antibodies used in western-blot

3.10 Glucose tolerance test

In the morning mice are fasted and housed in separate cages. After 9 hours of fasting, mice are injected intraperitonealy with 1.5 g/kg body weight of glucose (Glucosteril®, BadHomburg, Germany). Blood glucose concentration is measured at 0, 15, 30, 60, 90 and 120 min after injection using a glucometer (Bayer® Ascensia Elite XL, Leverkusen, Germany). Blood samples were collected at 0, 15, 30, 60 and 90 min after injection. Blood was centrifuged during 10 min and the plasma was collected and stored at -20°C until analysis.

3.11 Enzyme linked immunosorbent assay (ELISA)

The kit “Ultra sensitive Rat insulin ELISA kit” (Crystal Chem Inc®) was used with the “mouse insulin standard” (Crystal Chem Inc®).

The standard is first dissolved in sample diluent to reach a concentration of 12.8

ng/ml. Then serial dilutions are made to have standard concentrations of 0.1; 0.2, 0.4, 0.8, 1.6, 3.2 and 6.4 ng/ml

95 µL of sample diluent is dispensed in every well and 5 µL of sample/standard is added. The plate is then incubated 2 hours at 4°C.

The wells are washed 5 times with 300 µL of wash buffer and 100 µL of ant-insulin enzyme conjugated is added. The plate is incubated 30 min at room temperature.

The wells are washed 7 times with 300 µL of wash buffer and 100 µL of enzyme substrate solution is added. The plate is incubated 40 min at room temperature in the dark.

The reaction is stopped by adding 100 µL of enzyme reaction stop solution. Absorbance is measured using an ELISA plate reader (Versa Max multiplate reader, Molecular devices) at 450 nm and 630 nm.

3.12 Cell extraction from Peyer's patches

The mouse is sacrificed and the intestine is removed. The intestine is flushed with PBS to remove all faeces.

The Peyer's patches are cut out of the small intestine and put in 3 mL RPMI (Gibco®)+ collagenase D (Roche®) (100 mg/mL)+ DNaseI (Roche®) (20 mg/mL) into a 6 wells plate. The plate is incubated at 37°C with agitation during 20 min. The Peyer's patches are pressed through a 70 µm cell strainer and 2 mL of RPMI medium is added then incubated 10 min at 37°C with agitation. The reaction is stopped by adding EDTA at a final concentration of 1 mM and the sample is transferred to a 15 mL falcon tube. The volume is completed to 10 mL with RPMI and the samples are centrifuged at 1700 rpm during 5 min The pellet is re-suspended in 500 µL of FACS buffer (PBS+2% FCS)

3.13 Cell extraction from lamina propria

The mouse is sacrificed and the intestine is removed. The intestine is flushed with PBS to remove all faeces. The intestine is then cut longitudinally. The intestine is cut in 3 mm pieces in 25 mL of RPMI and shacked vigorously.

After settle down, the supernatant is removed and the samples are washed 3 times with PBS by shaking vigorously. The falcon containing the tissues samples is filled up with 50 mL PBS with 2 mM DTT and 5 mM EDTA and transferred to a 100 mL glass

beaker. The samples are agitating during 20 min at 37°C. The tissue samples are passed through a 70 µm cell strainer. The intestine pieces are put in a falcon filled with RPMI 10 mL+ 50 µL DNAse+ 50 µL collagenase and incubated 25 min at 37°C with shaking. The solution is pressed through a strainer and washed with RPMI. The samples are centrifuged 5 min at 1500 rpm. The pellet is re-suspended in 500 µL FACS buffer then filtered with glass wool.

3.14 Cell isolation from mesenteric lymph nods

All steps are performed on ice or at 4°C.

The mesenteric lymph nodes are removed from the mouse and smashed between 2 glass slides in sterile PBS. The samples are then filtered with a 70 µm cell strainer. The samples are spinned down 5 min at 1500 rpm and the supernatant is aspirated. 1 mL of red blood cell lysis buffer is added and incubated 5 min at room temperature. 10 mL of PBS is added and the samples are centrifuged 5 min at 1500 rpm. The pellet is re-suspended in 150 µL of FACS buffer.

3.15 Flow cytometry analysis

The cells are stained as followed:

100 µL of cells are put in a 96 wells plate with U bottom and the plate is centrifuge during 5 min at 1500 rpm. The supernatant is removed by inverting the plate on absorbent paper. The cells are then stained with EMA: per well 1.5 µL Etidium monoazide (EMA) in 100 µL PBS/FCS 2% and incubated 15 min on ice under a lamp. The plate is then washed with 100 µL PBS/FCS 2% and centrifuged at 2000 rpm during 5 min. The supernatant is then removed by inverting the plate. In order to block the unspecific antigens the cells are incubated during 10 min on ice with CD16/32 antibody at a dilution of 1:100 in PBS/FCS 2%. The plate is then washed once as previously.

The first antibodies cocktail is prepared as followed: 100 µL of PBS/FCS 2% per well + each antibody at a dilution of 1:200. The plate is incubated on ice 20 min covered with aluminium. The cells are washed once as previously.

The second antibody is added at a dilution of 1:200 in PBS/FCS 2% and incubated 20 min on ice covered with aluminium. One wash is performed and the cells are fixed

with 100 µL of fixation buffer during 25 min on ice. One last wash is performed and the cells are re-suspended in 2% FCS/PBS and transferred to FACS tubes.
Two sets of first antibodies have been used in this study.

Set 1:

Antibody	Labeling	company	Dilution
CD3	FITC	BD Pharmingen®	1:200
CD4	PB/405	eBiosciences®	1:200
CD8a	APC	eBiosciences®	1:200
CD25	PE	eBiosciences®	1:200
CD45	Alexa 700	eBiosciences®	1:200
CD16/32	X	BD Pharmingen	1:100

Set 2:

Antibody	Labeling	company	Dilution
F4/80	FITC	eBiosciences®	1:200
CD86	PE	BD Pharmingen	1:200
MHCII	APC	eBiosciences®	1:200
CD11c	Biotin	BD Pharmingen	1:200
Streptavidin	PE-Cy7	eBiosciences®	1:200
CD16/32	X	BD Pharmingen	1:100

Table 3.5 : List of antibodies used for Flow cytometry

The samples are then analysed with the FACS Gallios from Beckmann coulter.

3.16 Stool sample analysis

Fresh stool samples are collected from the mice and put in 200 µL sterile PBS. 1mg of stool is weighed and homogenised with a homogeniser. 800 mL of sterile PBS is added and cascade dilutions are performed in sterile PBS until $10^{\wedge -5}$ dilution.

100 µL of $10^{\wedge -4}$ is plated on Columbia agar (Biomerieux) (COS) and Schaedler-KV agar (SNVS) (Biomerieux) plates. 100 µL of $10^{\wedge -2}$ dilution is plated on MacConkey

(MCK) agar plate (Biomerieux) and 100 µL of the $10^{\wedge-5}$ dilution is plated on Schaedler agar (SCS) plate (Biomerieux®).

The SCS and SNVS plates are then incubated at 37°C during 48 h under anaerobic conditions using Anaerogen (Oxoid) and the COS and MCK plates are incubated in aerobic conditions during 24 h at 37°C.

The colonies on each plate are count and Gram coloration is performed to identify bacteria. For anaerobic conditions, a Rapid ID is done.

3.16.1 Gram coloration

Some bacteria are put in dH_2O on a microscope glass slide and dried then fixed by flaming. Gram crystal violet is added during 1 min and then washed with tap water. Gram iodine is put on it during 1 min then washed with tap water. The slide is then flushed with gram decolouriser and washed with tap water. The slide is then incubated in gram safranin during 30 s to 1 min and washed with tap water. The bacteria are identified using a microscope with a 100X objective.

3.16.2 Rapid ID

Each bacterium to identify is suspended in 2 mL water until an OD of MacFarland 4 is reached. 55 µL of bacteria suspension is added in each well of the Rapid ID 32A. 2 drops of paraffin oil is added in the first well and the ID is incubated 4 h at 37°C.

Reagents are added like said in the protocol of the manufacturer and the result is read after 5 min. Identification is done using the Apiweb website.

3.17 Statistical analysis

Significances analysis has been done using a Student t-test. P-values ≤ 0.05 are considered as significant.

*≤ 0.05; **≤ 0.01; ***≤ 0.001. Graphics show mean and standard error to the mean (SEM).

3.18 Mice treatment

3.18.1 Gallic acid treatment

Mice were treated 3 times per week with 4 µL/g of a solution of Gallic acid at 5mg/mL diluted in water.

3.18.2 ZP103 treatment

Acetylated Galβ1→4GlcNAcβ-O-naphthalenmethanol (ZP103) was purchased from Jeffrey Esko laboratory and injected with 70 µL of 5 mg/mL ZP103 diluted in 10% DMSO/water.

3.19 Bomb calorimetry preparation of samples

To perform bomb calorimetry measurement stool samples from single housed mice are collected in order to get at least 3 g of stool.
3g of dried stool are homogenised in a coffee grinder. 1 g of homogenised material is filled into the tablet press and a tablet is extruded. This tablet is weighed.

4. RESULTS

4.1 The role of IKKα in the exocrine pancreas

4.1.1 IKKα deletion in the exocrine pancreas does not alter body weight gain under HFD regimen

In order to define the role of IKKα during diet-induced obesity and type 2 diabetes, floxed IKKα mice were bred to tissue specific Cre lines. As IKKα whole body KO mice are perinatally lethal, we used mice with tissue specific IKKα deletion in order to perform the study.

To delete IKKα specifically in the exocrine pancreas floxed IKKα mice were crossed to Ptf1a-p48 Cre (IKKα$^{fl/fl}$ p48-Cre) (Kawagushi *et al* 2002). Starting at 6 weeks of age, the mice were fed either with a normal diet (ND) containing 5% of calories from the fat or with a high fat diet (HFD) containing 60% of calories from the fat. The weight was monitored every two weeks for over 20 to 24 weeks on the diet.

IKKα$^{fl/fl}$ p48-Cre animals continued to gain regular weight over the weeks when fed a HFD. At no point, the weight difference between IKKα$^{fl/fl}$ (controls) and IKKα$^{fl/fl}$ p48-Cre was significantly different. (Figure 4.1) Therefore, deletion of IKKα in the exocrine pancreas did not have any impact on the weight of the animals.

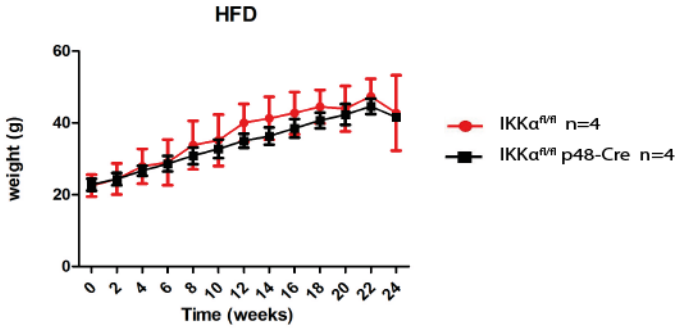

Figure 4.1: Mice having a deletion of IKKα in the exocrine pancreas did not show any body weight difference. Weight curve over the course of HFD feeding from female IKKα$^{fl/fl}$ p48-Cre and controls mice. n.s: non significant

Complete blood cell count is a routine diagnostic tool in medicine. It allows to detect signs of inflammation, anaemia or any change in its normal composition that can be a symptom of a dysfunction in the organism. In order to determine if the deletion of IKKα in

the exocrine pancreas has any consequence blood samples from IKKα$^{fl/fl}$ p48-Cre mice and controls were analysed.

The red blood cells were significantly decreased in the IKKα$^{fl/fl}$ p48-Cre animals. However, both groups were still in the normal range of erythrocytes count (7*10^6 to 13*10^6/µL) suggesting none of the mice were anaemic. Consistently with this result, the haematocrit, which is the percentage of red blood cell in the blood, was as well significantly lower in IKKα$^{fl/fl}$ p48-Cre mice than that of the controls. Haemoglobin levels also showed a tendency towards a decrease in the IKKα$^{fl/fl}$ p48-Cre mice, which correlated with the decreased red blood cell count and haematocrit (Figure 4.2) suggesting IKKα deletion in the exocrine pancreas led to a slight decrease in erythrocytes amount.

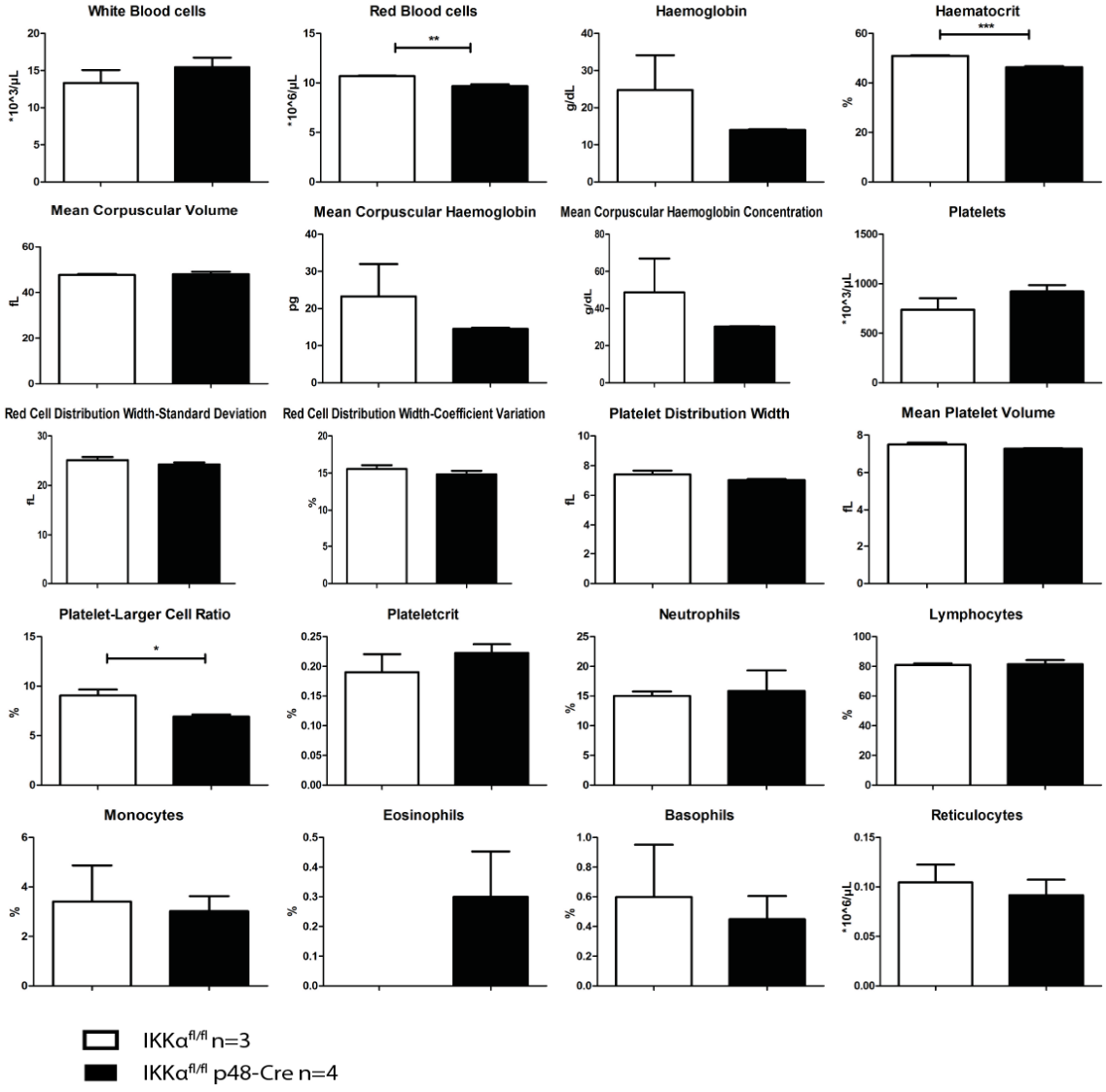

Figure 4.2: Exocrine pancreas specific deletion of IKKα leads to a decrease in erythrocyte count. Blood cell count from IKKα$^{fl/fl}$ p48-Cre mice after 13 weeks under HFD. Student t-test: **: p<0.01; ***: p<0.001

4.1.2 IKKα$^{fl/fl}$ p48-Cre animals did not show a difference in inflammatory cell infiltration and cytokine production in pancreas or liver

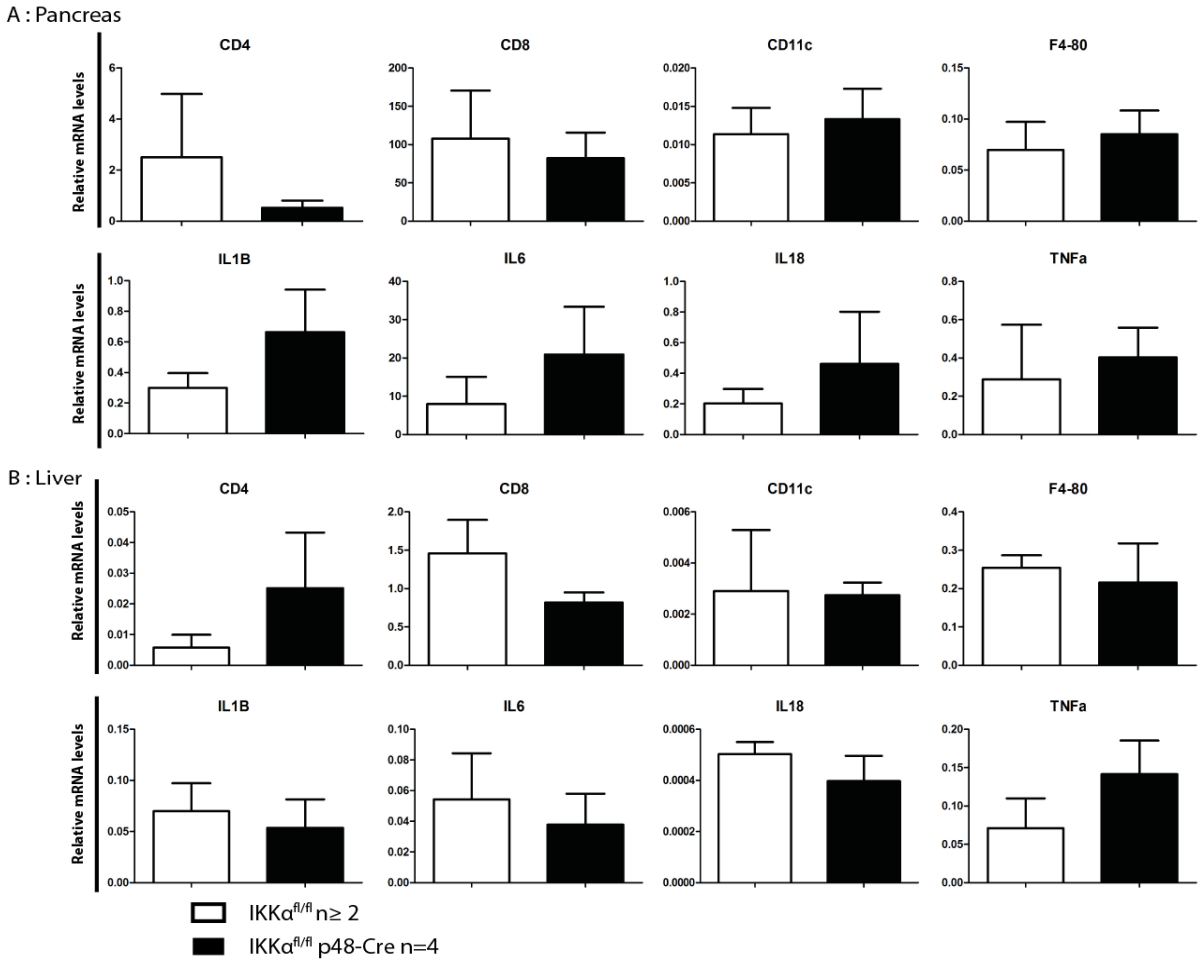

Figure 4.3: IKKα deletion in the exocrine pancreas does not trigger inflammation. Relative mRNA levels of cytokines and inflammatory cells markers in **A**: Pancreas and **B**: Liver of IKKα$^{fl/fl}$ p48-Cre mice. Relative levels were assessed by real-time PCR. Student t-test n.s: not significant

Inflammation plays an important role in the onset of obesity and type 2 diabetes. Therefore, we checked inflammatory markers in the pancreas and liver of IKKα$^{fl/fl}$ p48-Cre mice. However, neither infiltration of inflammatory cells nor associated proinflammatory cytokine production was significantly affected in both pancreas and liver from IKKα$^{fl/fl}$ p48-Cre animals. (Figure 4.3 A and B)

4.1.3 IKKα deletion in exocrine pancreas did not affect the glucose tolerance and insulin sensitivity

Impaired glucose tolerance is a pre-diabetic stage characterised by hyperglycaemia. It correlates well with insulin resistance, which is the inability of the cells to respond correctly to insulin. To assess glucose clearance, GTT was performed.

There was no difference in glucose tolerance between the IKKα$^{fl/fl}$ and the IKKα$^{fl/fl}$ p48-Cre mice. Both groups had an increase in their glucose levels after 15 min, which then declined until 90 min post glucose injection. The IKKα$^{fl/fl}$ p48-Cre mice reached their basal glycaemia after 2 h while the IKKα$^{fl/fl}$ had a slight increase between 90 min and 120 min after injection. Even though HFD induced hyperglycaemia (fasting glucose levels ≥150 mg/dL at time 0), all mice were still able to lower their blood glucose levels suggesting they are glucose tolerant. (Figure 4.4A)

The insulin secretion during the GTT correlated well with glucose clearance. Both IKKα$^{fl/fl}$ p48-Cre and IKKα$^{fl/fl}$ mice had an increase in insulin secretion after 15 min that declined at 60 min, and increased again at 90 min. Therefore, as the insulin concentration raised in parallel with the glucose levels, both groups of mice were able to clear glucose from their circulation within 2 hours. (Figure 4.4B)

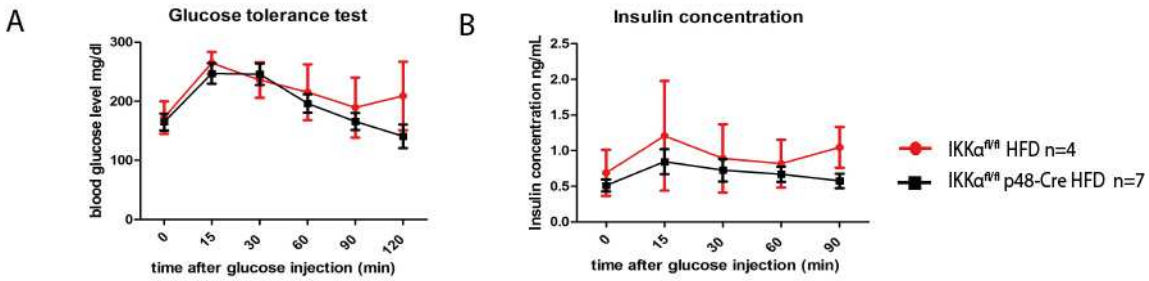

Figure 4.4: IKKα deletion in exocrine pancreas did not affect glucose tolerance and insulin sensitivity. **A:** Glucose and **B:** Insulin levels during glucose tolerance test of IKKα$^{fl/fl}$ p48-Cre and control mice (male) after 11 weeks under HFD.

4.1.4 IKKα deletion in exocrine pancreas slightly alters expression of genes involved in lipid metabolism both in pancreas and liver

Pancreas is an important organ for glucose homoeostasis. Although none of the genes tested showed a significant difference, however, a slight increase in the expression of gene involved in lipid metabolism was observed in the pancreas and more pronouncedly in the liver

of IKKα$^{fl/fl}$ p48-Cre animals. Beta oxidation seemed to be decreased in the pancreas while fatty acid synthesis was upregulated. (Figure 4.5A and B)

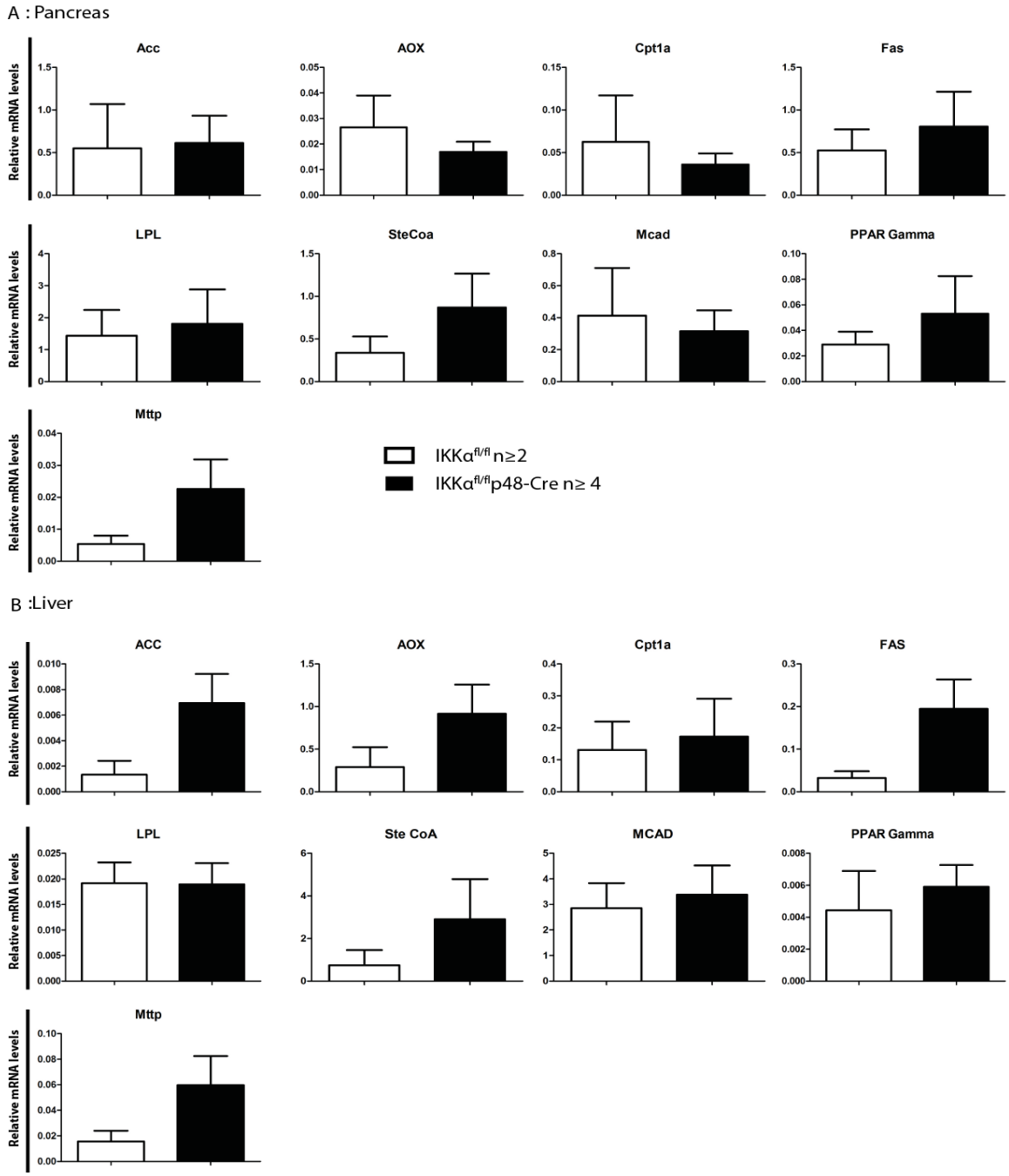

Figure 4.5: Lipid metabolism was slightly affected in the pancreas and liver of IKKα$^{fl/fl}$ p48-Cre mice. Relative mRNA levels of genes involved in of lipid metabolism's genes determined by real-time PCR in **A**: Pancreas and **B**: Liver of IKKα$^{fl/fl}$ p48-Cre and control mice.

4.1.5 Deletion of IKKα in the exocrine pancreas led to lipomatosis in the pancreas but reduced steatosis in the liver

Along with gene expression analysis, pathological evaluation of the pancreata revealed lipomatosis in the pancreas of IKKα$^{fl/fl}$ p48-Cre mice (4 out of 9) and abscesses in others (2 out of 9) (Figure 4.6 A and B). Haematoxylin and eosin (H&E) stained sections from pancreas showed increased accumulation of fat in IKKα$^{fl/fl}$ p48-Cre mice (Figure 4.6 C and D), whereas HFD-induced steatosis was significantly reduced suggesting possible crosstalk between pancreas and liver in HFD-associated alterations in lipid metabolism.

Taken together, exocrine specific deletion of IKKα leads to differential regulation of lipid metabolism in pancreas with compensatory responses in liver with intact IKKα.

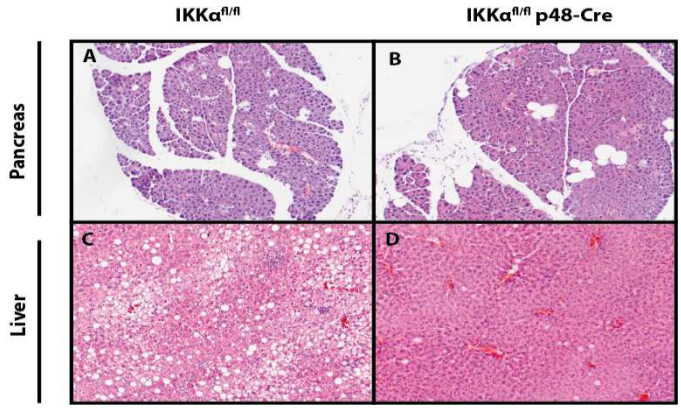

Figure 4.6: IKKα deletion in the exocrine pancreas promoted lipid accumulation in the pancreas but improved steatosis in the liver. H&E staining of pancreas (**A and B**) and liver (**C and D**) from controls and IKKα$^{fl/fl}$ p48-Cre mice. Magnification 10X. The mice were 24 weeks on HFD.

4.2 Deletion of IKKα in the endocrine pancreas

4.2.1 Mice with IKKα deletion in endocrine pancreas remained resistant to HFD-induced obesity

The deletion of IKKα in the exocrine pancreas did not lead to significant differences in glucose tolerance. To check whether the endocrine compartment might have an effect, we crossed IKKα floxed mice to an Ins2-Cre line (IKKα$^{fl/fl}$ Ins2-Cre).

Starting from six weeks of age, IKKα$^{fl/fl}$ Ins2-Cre mice were kept either on a ND or a HFD and the weight gain was monitored every 2 weeks. There was no significant difference between the IKKα$^{fl/fl}$ and the IKKα$^{fl/fl}$ Ins2-Cre mice under ND regimen (Figure 4.7A). However, IKKα$^{fl/fl}$ Ins2-Cre mice remained significantly leaner than their littermate controls

under HFD. Although IKKα$^{fl/fl}$ Ins2-Cre mice almost did not gain any weight during the 18 weeks of HFD regimen, IKKα$^{fl/fl}$ controls nearly doubled their initial weight and became obese as expected. (Figure 4.7 B)

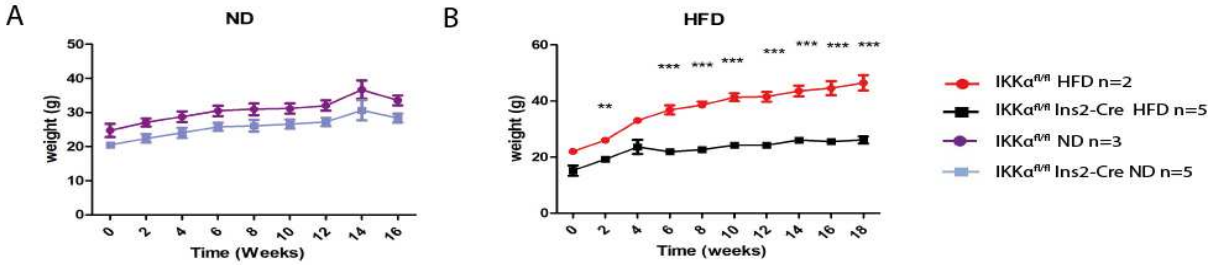

Figure 4.7: Deletion of IKKα in the endocrine pancreas protected mice from diet induced obesity. Weight curves of male IKKα$^{fl/fl}$ Ins2-Cre mice under **A**: ND and **B**: HFD. Student's t-test: *: p<0.05, **: p<0.01, ***: p<0.001

4.2.2 IKKα deletion in endocrine pancreas improved glucose tolerance

To check whether diet-induced obesity leads to type 2 diabetes in IKKα$^{fl/fl}$ Ins2-Cre mice, we performed GTT and checked insulin secretion.

No differences were detected in the different mice groups under ND and all mice were glucose tolerant. (Figure 4.8 A) However, in accordance with resistance to weight gain IKKα$^{fl/fl}$ Ins2-Cre mice remained much more glucose tolerant than their littermate controls under HFD. Indeed, while the blood glucose level of the IKKα$^{fl/fl}$ animals increased during the first 30 min of the test and then decreased gradually during the next 90 min, they still did not reach their initial glucose levels, suggesting glucose intolerance in these mice. On the contrary, IKKα$^{fl/fl}$ Ins2-Cre increased only during the initial 15 min of glucose injection, and then decreased finally reaching their initial blood glucose level suggesting they remained glucose tolerant in agreement with decreased weight gain and increased glucose tolerance. (Figure 4.8 B)

Furthermore, IKKα$^{fl/fl}$ Ins2-Cre mice under HFD were secreting significantly less insulin than the IKKα$^{fl/fl}$ animals suggesting that they needed less insulin to regulate their blood glucose levels implicating insulin sensitivity in these animals. When insulin secretion was compared between ND and HFD conditions, the IKKα$^{fl/fl}$ mice under HFD secreted much more insulin than under ND suggesting that HFD induced insulin resistance. On the contrary, insulin secretion in IKKα$^{fl/fl}$ Ins2-Cre mice under HFD was similar to the one under ND condition providing further evidence for resistance against HFD-induced obesity, glucose

intolerance and insulin resistance. (Figure 4.8 A and B)

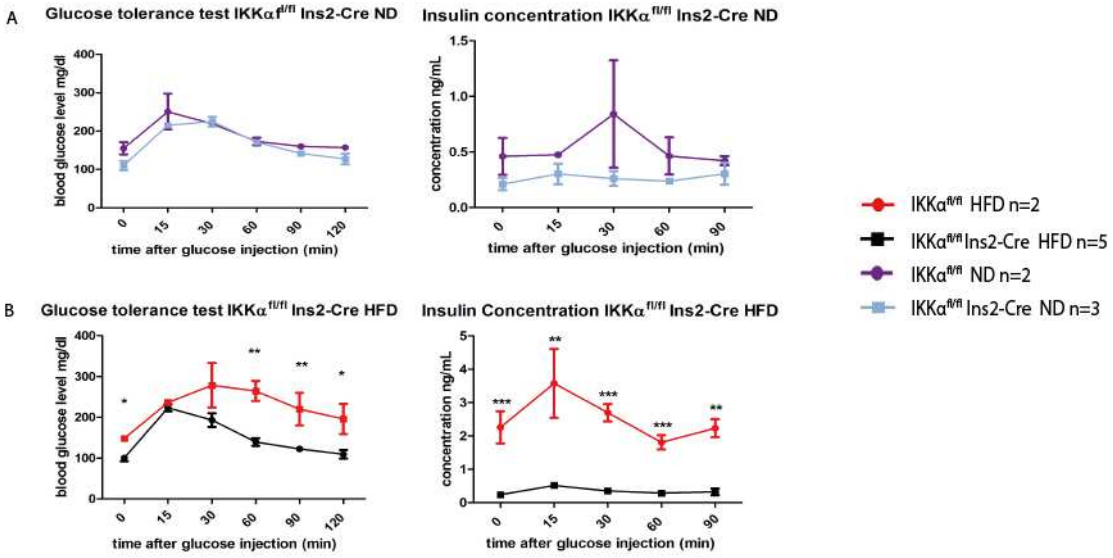

Figure 4.8: Deletion of IKKα in endocrine pancreas protected the mice from HFD-induced glucose intolerance and hyperinsulinaemia. Blood glucose and plasma insulin levels of IKKα$^{fl/fl}$ Ins2-Cre mice during glucose tolerance test**, A**: performed at 18 weeks on ND (males) and **B:** 11 weeks on HFD (males). Student's t-test: *: p<0.05, **: p<0.01, ***: p<0.001.

As the IKKα$^{fl/fl}$ Ins2-Cre mice showed improved insulin sensitivity in response to glucose overload during GTT, we checked whether insulin concentration increased at all during HFD regimen. Therefore, we performed ELISA to detect insulin levels in the blood during the time of HFD feeding.

Consistent with the GTT results, IKKα$^{fl/fl}$ Ins2-Cre mice had significantly less insulin secretion along 16 weeks on HFD. This suggested that the IKKα$^{fl/fl}$ animals became hyperglycaemic and needed more insulin than the IKKα$^{fl/fl}$ Ins2-Cre mice in order to regulate their glucose levels. This is due to a dysfunction of the insulin receptor or in the insulin signalling cascade leading to insulin resistance. (Figure 4.9)

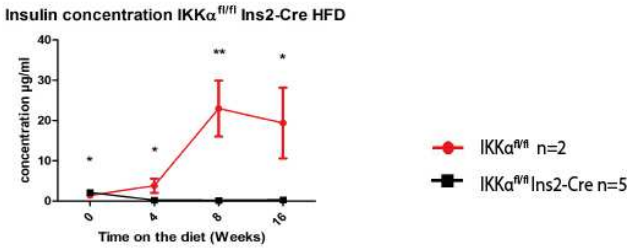

Figure 4.9: Mice bearing a deletion of IKKα in the endocrine pancreas did not become hyperinulinaemic under HFD condition. Plasma insulin concentration over the time of the HFD feeding from Ins2-IKKα and control mice. Student's t-test: *: $p<0.05$, **: $p<0.01$.

4.2.3 IKKα deletion in endocrine pancreas did not alter blood cell count

A weight loss often correlates with anaemia. To exclude that the weight difference between the IKKα$^{fl/fl}$ Ins2-Cre and the IKKα$^{fl/fl}$ mice was due to anaemia, blood cell count were checked.

Blood parameters from IKKα$^{fl/fl}$ Ins2-Cre mice and their controls littermate were not changing significantly. (Figure 4.10)

The white blood cell count was slightly decreased in the IKKα$^{fl/fl}$ Ins2-Cre mice than that of the IKKα$^{fl/fl}$ animals. The decrease in lymphocytes numbers in the IKKα$^{fl/fl}$ Ins2-Cre mice correlates well with the fact that they are leaner than the IKKα$^{fl/fl}$ animals. Indeed, obesity is a low-grade inflammatory state. As the IKKα$^{fl/fl}$ mice had more fat tissue than the IKKα$^{fl/fl}$ Ins2-Cre animals then it is expected that they also should have more inflammation. (Figure 4.10)

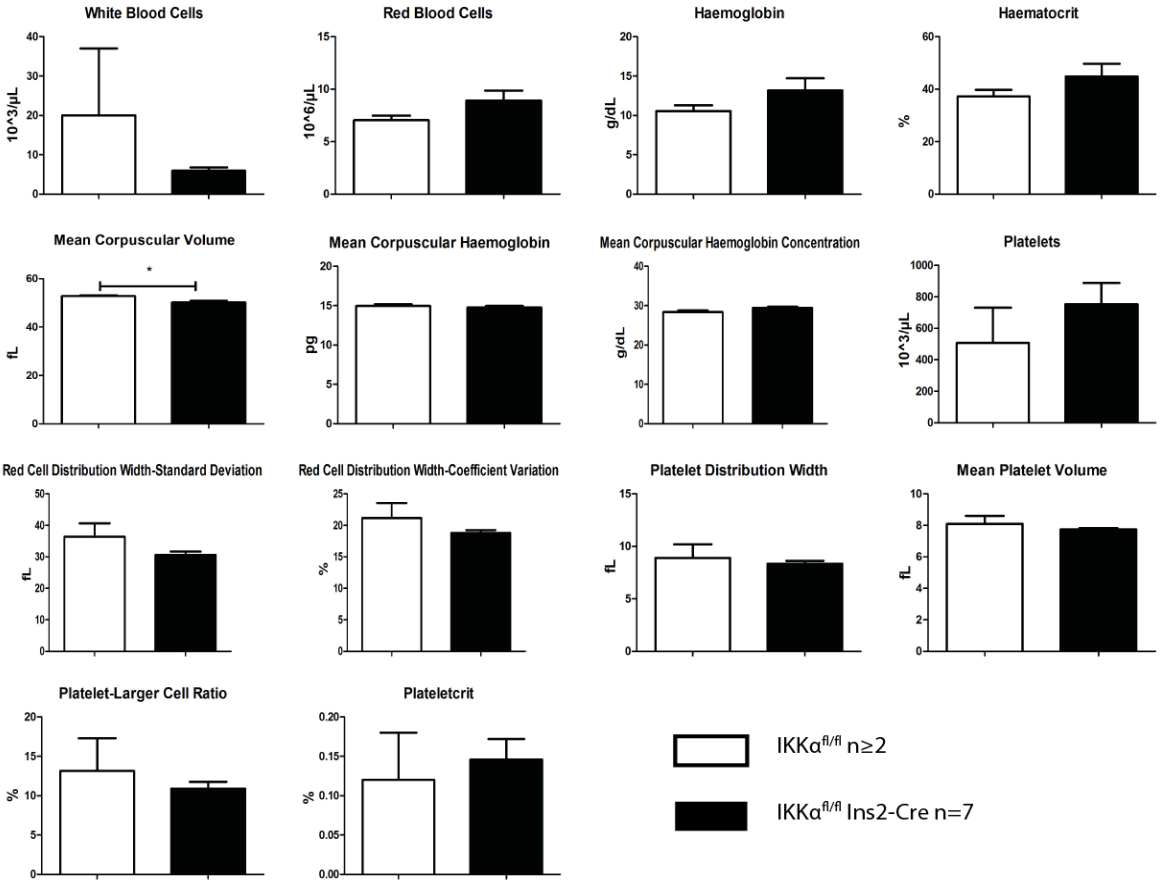

Figure 4.10: Endocrine pancreas deletion of IKKα did not affect cell count. Blood cell counts for IKKα$^{fl/fl}$ Ins2-Cre and control mice after 17 weeks under HFD. Student's t-test: *: $p<0.05$

4.2.4 IKKα deletion in endocrine pancreas did not lead to any histological changes in pancreas, but in fat and liver under HFD condition

Pancreas, liver and fat tissue are organs important for the regulation of glucose and lipid metabolism.

There was no difference in the histology of pancreas between IKKα$^{fl/fl}$ Ins2-Cre mice and IKKα$^{fl/fl}$ animals under both HFD and ND. However, when comparing HFD to ND one could notice that the HFD mice had hypertrophic Langerhans' islets as expected. Under ND, no difference was found in liver and adipose tissue. However, HFD led to increase accumulation of fat in liver of the IKKα$^{fl/fl}$ mice but not in IKKα$^{fl/fl}$ Ins2-Cre animals, which is in accordance with the fact that those mice did not become obese under HFD regimen. (Figure 4.11)

Similarly, the fat tissue of the IKKα$^{fl/fl}$ mice showed hypertrophic adipocytes under

HFD, which is explained by the increased obesity state of these animals. (Figure 4.11) The adipocytes from IKKα$^{fl/fl}$ Ins2-Cre mice remained small as there was no demand to store excess energy.

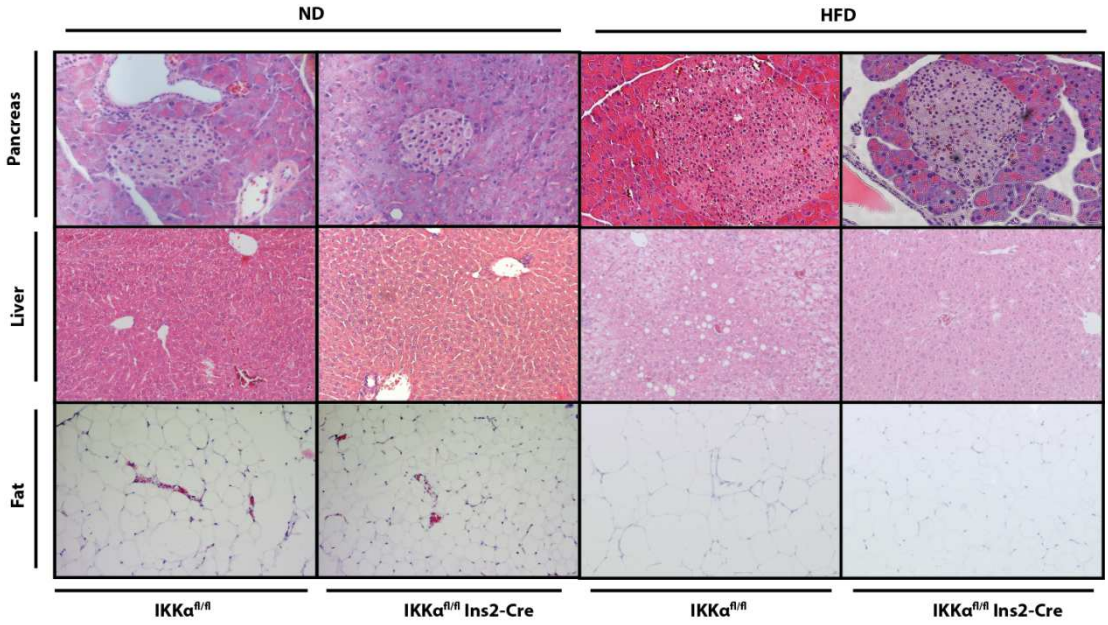

Figure 4.11: IKKα deletion in endocrine pancreas reduces liver steatosis and adipocytes size. H&E staining of pancreas, liver and fat tissue from IKKα$^{fl/fl}$ and IKKα$^{fl/fl}$ Ins2-Cre mice, under ND and HFD. Mice were kept 20 weeks on the respective diet.

4.2.5 IKKα$^{fl/fl}$ Ins2-Cre mice showed altered α-cell to β-cell ratio in the Langerhans' islets of the pancreas

As IKKα$^{fl/fl}$ Ins2-Cre mice were leaner and secreted less insulin than the controls, we checked the number of α and β-cells that secrete glucagon and insulin, respectively.

In a normal tissue, the insulin secreting β-cell are found in the whole Langerhans' islet while the glucagon secreting α-cells, are not that abundant and are found at the periphery of the islet.

As expected, Langerhans' islets of the pancreas from IKKα$^{fl/fl}$ Ins2-Cre mice had increased ratio of β-cells to α-cells. Regarding the number of cells of each type, no differences could be seen between the IKKα$^{fl/fl}$ and the IKKα$^{fl/fl}$ Ins2-Cre mice for insulin producing cells. (Figure 4.12 D, F) However, the IKKα$^{fl/fl}$ Ins2-Cre mice seemed to have more glucagon producing cells than the controls. (Figure 4.12 C, E)

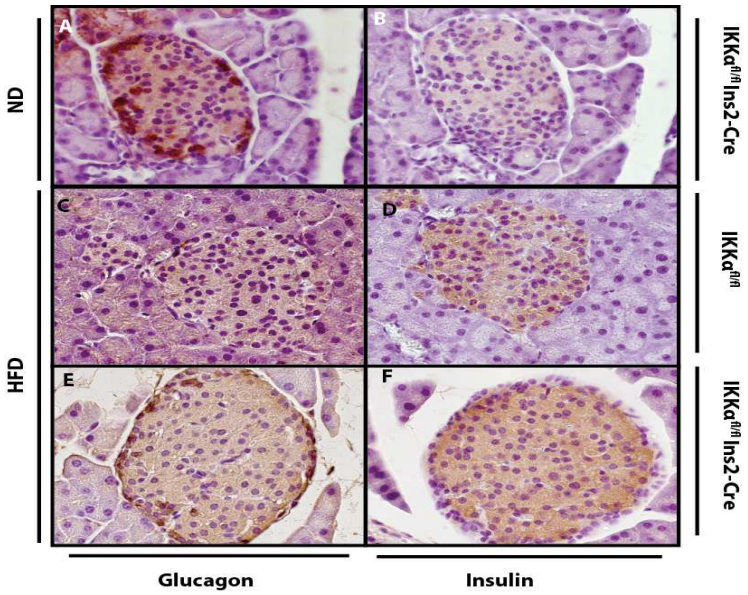

Figure 4.12: Deletion of IKKα in the endocrine pancreas increases α-cell to β-cell ratio. IHC of pancreas from IKKα$^{fl/fl}$ Ins2-Cre mice and controls for insulin and glucagon. **A:** Glucagon staining from IKKα$^{fl/fl}$ Ins2-Cre ND. **B**: Insulin staining from a serial section. **C**: Glucagon staining of IKKα$^{fl/fl}$ HFD. **D**: Insulin staining of the same islet than C. **E:** Glucagon staining of IKKα$^{fl/fl}$ Ins2-Cre HFD. **F:** Insulin staining from a serial section. Mice were kept 20 weeks under the diet. Magnification 40X.

4.2.6 IKKα deletion in endocrine pancreas led to an increased mitochondrial β-oxidation

IKKα$^{fl/fl}$ Ins2-Cre animals remained leaner than their littermate controls on HFD. Alteration in glucose and lipid metabolism might be a reason which explains the weight difference. To assess the genes involved in glucose and lipid metabolism pathway, we performed RT-PCR from pancreas and liver, to check relative mRNA levels.

Genes encoding proteins for the mitochondria oxidation showed an increased expression indicating enhanced mitochondrial metabolism. As the IKKα$^{fl/fl}$ Ins2-Cre mice seemed to have increased oxidative phosphorylation, it may suggest that they use more energy via this pathway than the IKKα$^{fl/fl}$ mice. Indeed, this up-regulated metabolism might explain the weight difference seen in these animals. (Figure 4.13)

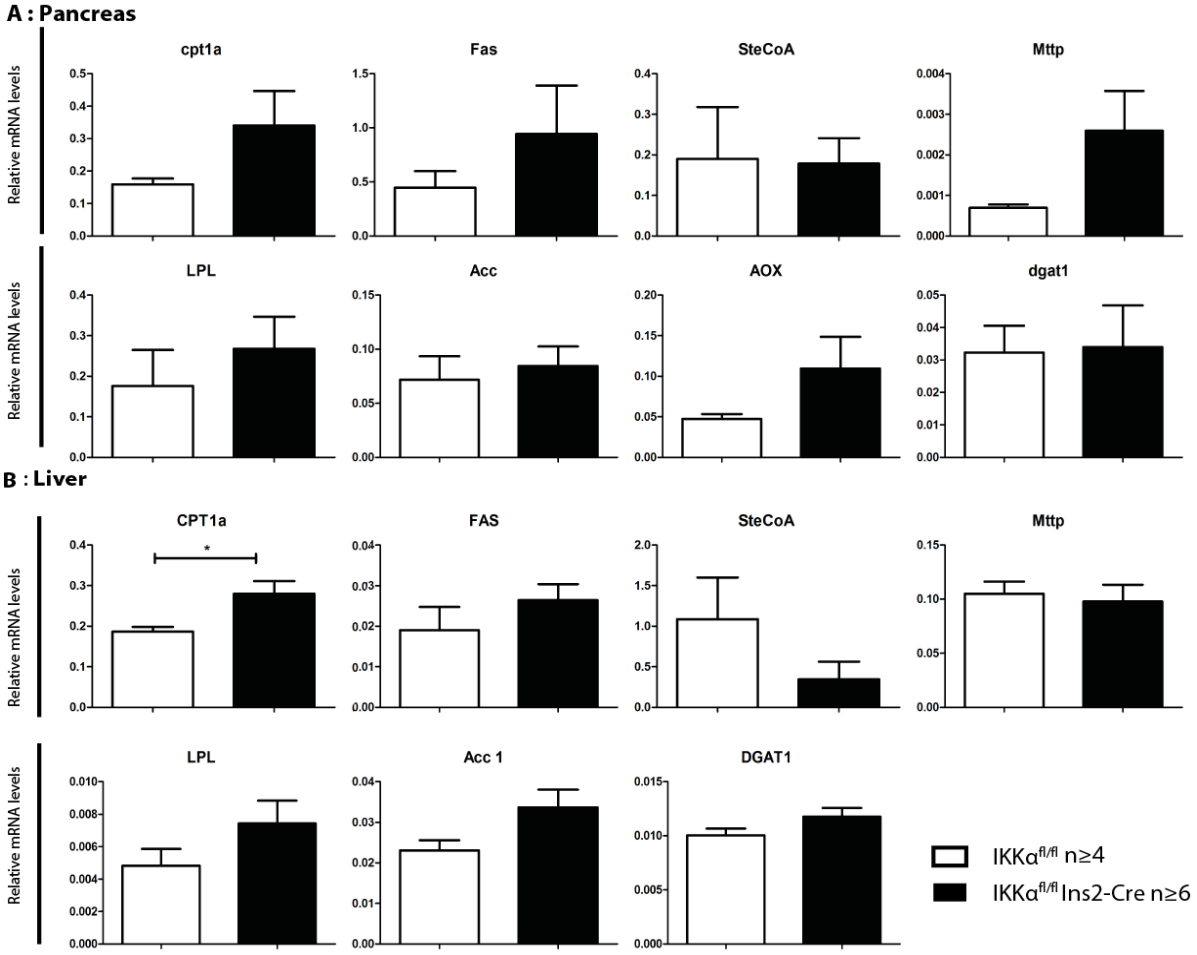

Figure 4.13: Deletion of IKKα in the endocrine pancreas increases expression of genes involved in oxidative phosphorylation. Relative mRNA levels of genes involved in lipid metabolism in **A**: pancreas and **B:** liver of IKKα$^{fl/fl}$ Ins2-Cre mice. Mice were kept 20 weeks under HFD. Student's t-test: *: $p<0.05$

Deregulation in glucose metabolism is an important hallmark of diabetes. Therefore we checked the expression of genes involved in glucose metabolism in the pancreas and liver from IKKα$^{fl/fl}$ Ins2-Cre mice and their littermate controls.

Glucose 6 phosphatase (G6Pase) was significantly decreased in the pancreas of IKKα$^{fl/fl}$ Ins2-Cre mice suggesting a decrease in gluconeogenesis, while PEPCK (Phosphoenol pyruvate carboxykinase) and FBPase (1, 6 Fructose biphosphatase) had a tendency towards an increase. (Figure 4.13 A) In the liver, the expression of some genes involved in gluconeogenesis was decreased. FBPase and G6Pase were both decreased suggesting decreased gluconeogenesis which correlates with the tendency towards increased glycolysis seen in the liver. (Figure 4.13 B) Indeed, both hexokinase 1 and 2, which are the first enzymes of the glycolysis converting glucose to Glucose-6-phosphate, had a tendency

towards an increase, suggesting enhanced glycolytic pathway in the liver. This enhanced glycolysis might lead to increased ATP production and therefore more availability to energy. The enhanced glycolysis could as well explain the improved glucose tolerance seen in these animals, the IKKα$^{fl/fl}$ Ins2-Cre mice might use more of the glucose available in the blood stream to produce energy. (Figure 4.14)

In the liver, the glucose transporter GLUT2 was significantly increased suggesting an increase in glucose uptake, which can at least partially explain the increased glycolysis. (Figure 4.14)

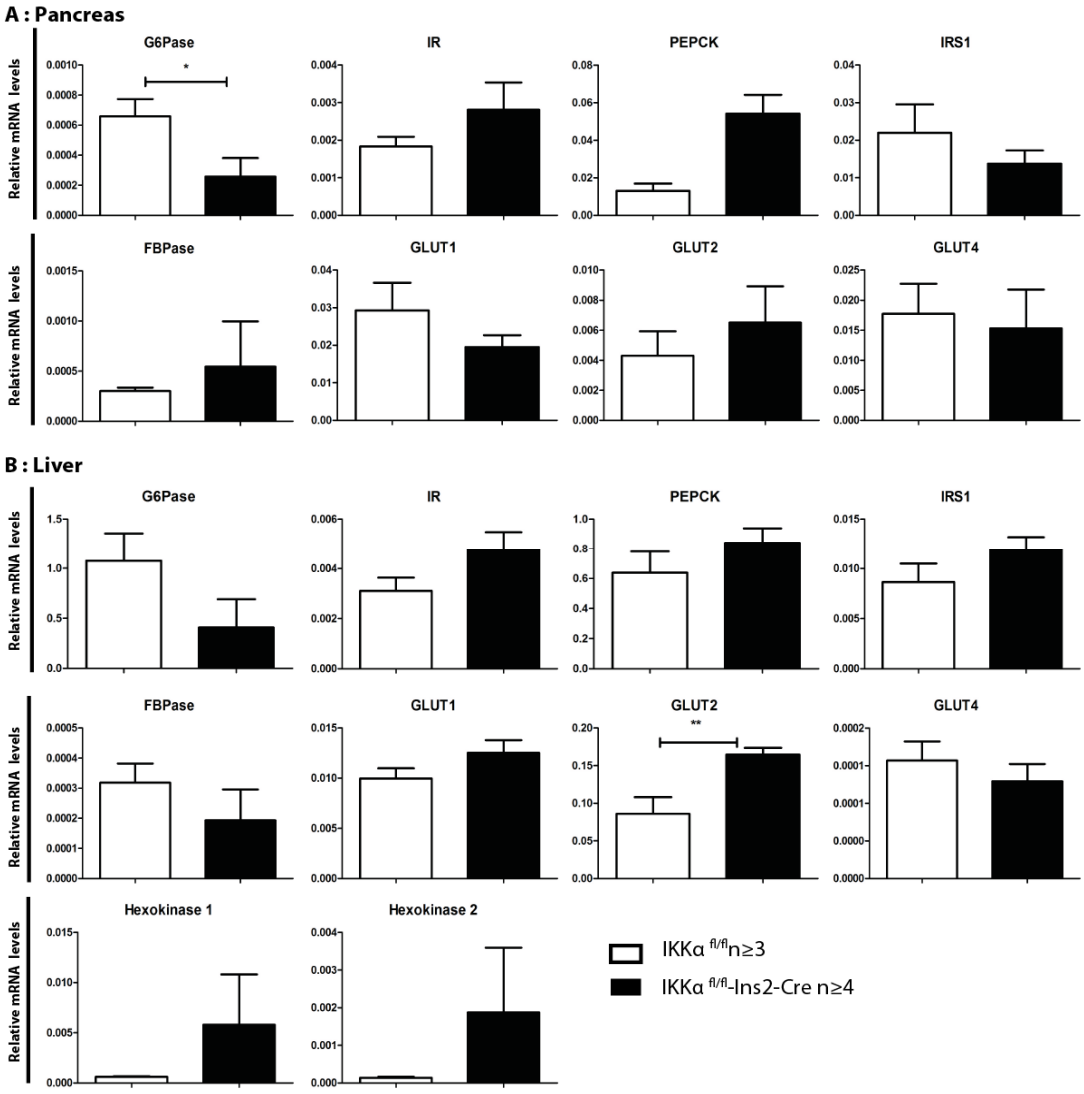

Figure 4.14: IKKα deletion in the endocrine pancreas promotes slight changes in glucose metabolism. Relative mRNA levels of genes involved in glucose metabolism in **A**: pancreas and **B**: liver from IKKα$^{fl/fl}$ Ins2-Cre and controls mice. Mice were 20 weeks under HFD. Student's t-test, *: $p<0.05$, **: $p<0.01$

4.2.7 Endocrine pancreas specific deletion of IKKα provokes an increase in inflammatory cell infiltration and cytokine production in the pancreas and the fat tissue

As IKKα is a protein of the NF-κB pathway, which is well defined for its role during inflammatory responses, we wanted to know if the IKKα$^{fl/fl}$ Ins2-Cre mice showed a difference in HFD-induced inflammation. We performed real-time PCR in the pancreas, fat tissue and brain for inflammatory cytokines and for markers of inflammatory cells.

Inflammation was overall increased in the pancreas of the IKKα$^{fl/fl}$ Ins2-Cre mice. Both macrophage (F4-80) and T cell (CD4 and CD8) populations were more present in the pancreas of the IKKα$^{fl/fl}$ Ins2-Cre mice than their controls. The cytokines TNFα and IL1β, produced by the macrophages, and IL6, produced by both macrophages and T-cells were increased in the IKKα$^{fl/fl}$ Ins2-Cre mice, which correlated well with the increased T-cells and macrophages. (Figure 4.15 A)

However, the picture was less clear in the fat tissue. While IL6, MCP1 and IL1β were increased in the IKKα$^{fl/fl}$ Ins2-Cre, F4-80, the marker of macrophages was significantly decreased in the IKKα$^{fl/fl}$ Ins2-Cre. (Figure 4.15 B) suggesting adipocytes to be the major source for chemokine and cytokine production. Indeed, this also correlates well with the decreased weight gain on HFD, small adipocytes as well as their secretive properties.

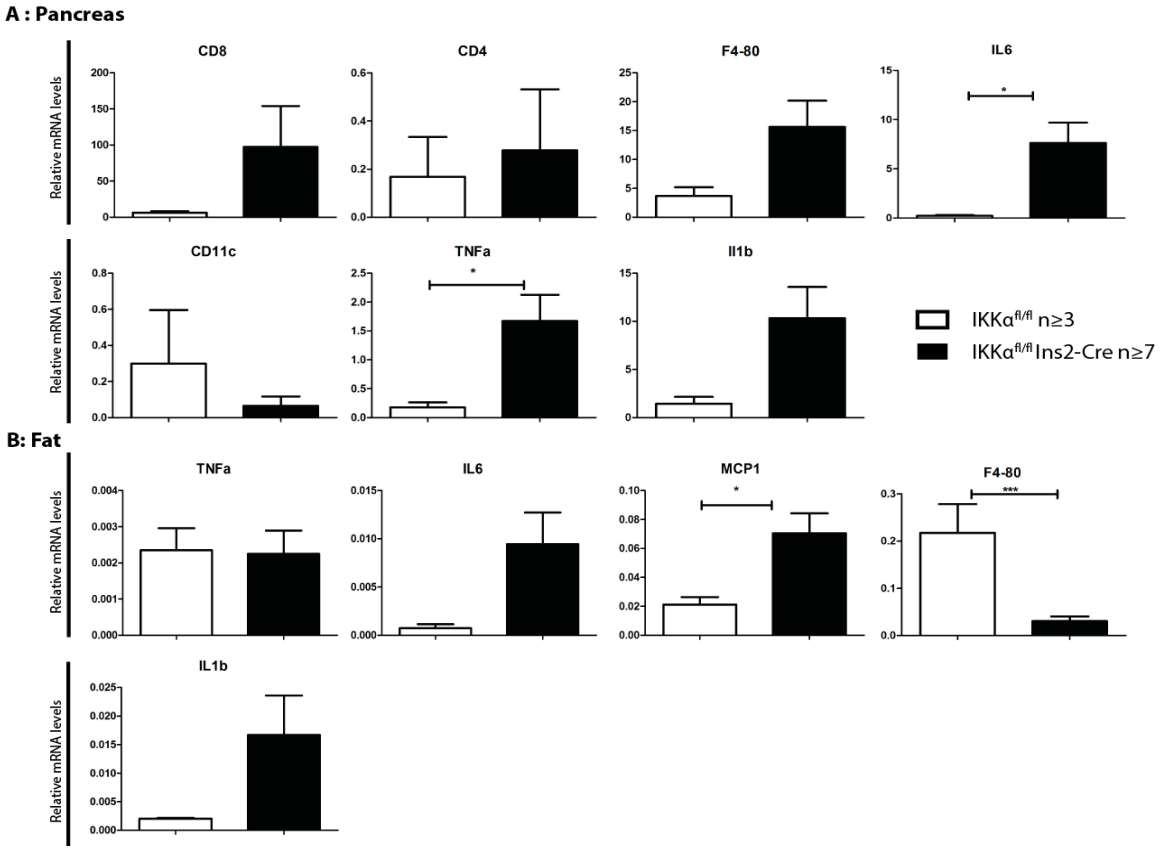

Figure 4.15: IKKα deletion in the endocrine pancreas triggers the expression of inflammatory genes. Real-time PCR of inflammatory cells markers and cytokines in **A:** the pancreas and **B**: the fat tissue of IKKα$^{fl/fl}$ Ins2-Cre mice. Mice were 20 weeks under HFD at the time of sacrifice. Student's t-test: *: p<0.05, ***: p<0.001

4.2.8 IKKα$^{fl/fl}$ Ins2-Cre mice mRNA expression show a decrease in appetite

IKKα$^{fl/fl}$ Ins2-Cre mice were leaner than the controls. The appetite is regulated partially by hormones like ghrelin or leptin acting in the brain. Moreover, some peptides are important for proper digestion and are responsible for the motility of the intestine. (Moody *et al* 2011)

Leptin is an anorectic hormone synthesised in the fat tissue, which has an effect on the brain. In our mice, there was a decrease in leptin mRNA in the brain and the fat tissue. (Figure 4.16 B and C) As leptin decreases appetite, this correlates well with the leaner phenotype observed in the IKKα$^{fl/fl}$ Ins2-Cre mice. Similar to leptin, ghrelin, an appetite stimulating hormone was decreased in the pancreas.

GCG (glucagon gene) is a gene encoding for 4 different mature peptides. The first one is glucagon, which stimulates release of glucose in the blood stream. In the pancreas of our mice, glucagon and GCG were both decreased. GCG encodes as well for GLP-1, which

stimulates glucose dependent insulin release. We already showed via ELISA on blood samples that the IKKα$^{fl/fl}$ Ins2-Cre mice had less insulin than the IKKα$^{fl/fl}$ animals. This result was confirmed by the RT-PCR, which showed a decrease in the mRNA levels of insulin and GCG. The 3rd peptide encoded by GCG is GLP-2, which stimulates the nutrient uptake in the small intestine. The 4th peptide, glicentin, has a less clear role yet. (Figure 4.16 A) (Irwin and Prentice 2011)

Cholecystokinin (CCK) is a protein, which diminishes hunger and stimulates the release of digestive enzymes by the pancreas. (Smitka *et al* 2013) CCK was increased in the pancreas of the IKKα$^{fl/fl}$ Ins2-Cre mice correlating with the leptin and ghrelin levels. VIP, a peptide important for intestinal motility, was increased.

Adiponectin is a hormone secreted by the adipose tissue, which inversely correlates with the percentage of body fat. In our IKKα$^{fl/fl}$ Ins2-Cre mice, it was increased correlating with the fact that they remained leaner than their controls after HFD feeding. (Figure 4.16C)

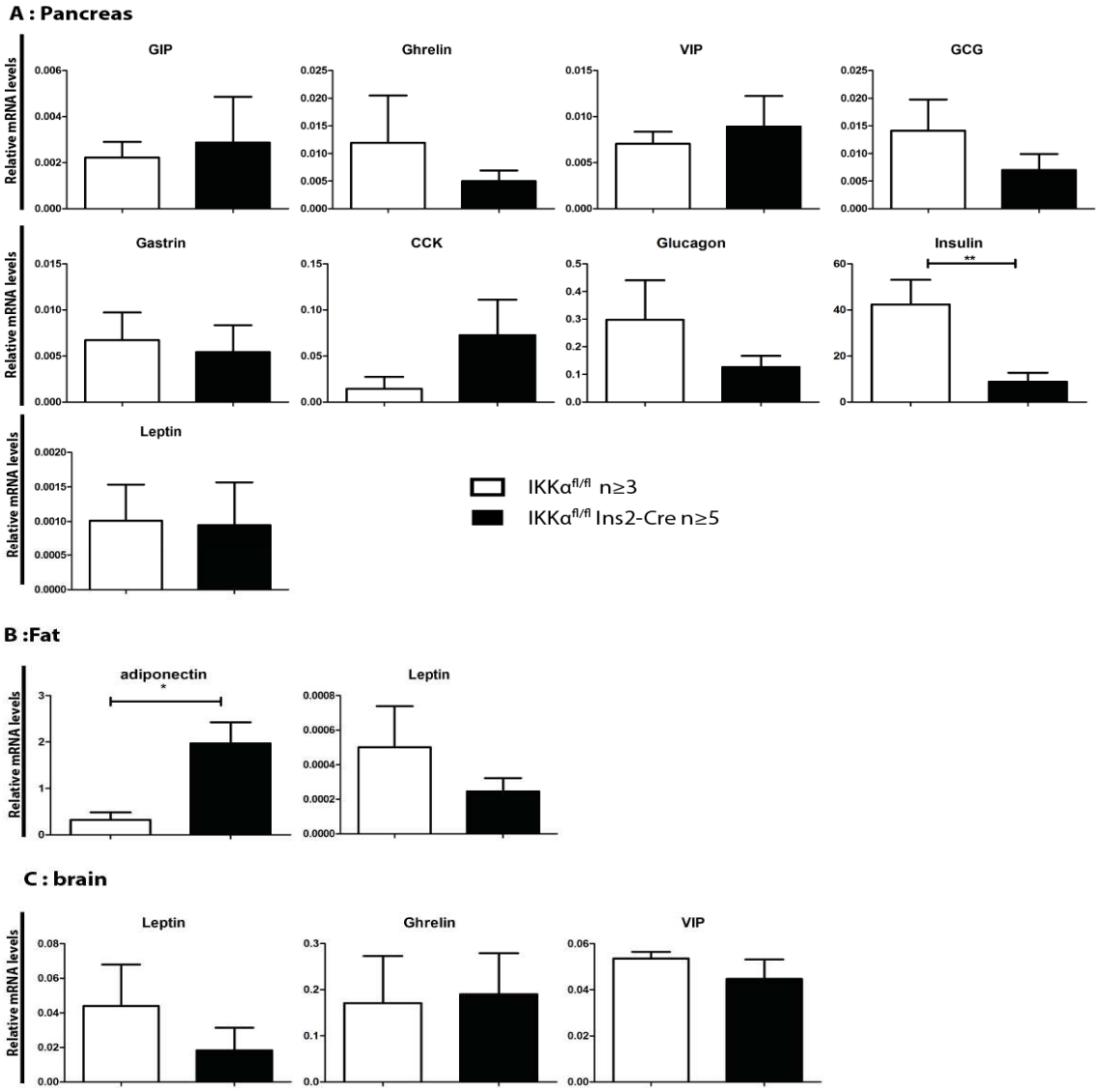

Figure 4.16: Appetite hormones show reduced expression in the IKKαfl/fl Ins2-Cre mice. Real-time PCR in **A**: the pancreas, **B**: the fat tissue and **C**: the brain of digestive peptides and appetite regulating hormones from IKKα$^{fl/fl}$ Ins2-Cre animals and controls. Animals were kept 20 weeks under HFD. Student t-test: *: $p<0.05$, **: $p<0.01$

4.2.9 IKKα$^{fl/fl}$ Ins2-Cre mice do not excrete more energy than the IKKα$^{fl/fl}$ controls

Real-time PCR results suggested that IKKα$^{fl/fl}$ Ins2-Cre had a decreased appetite and spent more energy than IKKα$^{fl/fl}$ animals. In order to confirm those results we collected stool samples and performed bomb calorimetry to measure the energy content excreted in the faeces.

The results showed that there was no difference in the energy content of the faeces

between IKKα$^{fl/fl}$ Ins2-Cre and IKKα$^{fl/fl}$ under both ND and HFD. However, faeces from HFD fed control mice contained more energy than the one from ND fed animals.

Therefore, the leaner phenotype of the KO mice was not due to an increased energy excretion but rather to a decreased appetite or increased energy expenditure in these animals. (Figure 4.17)

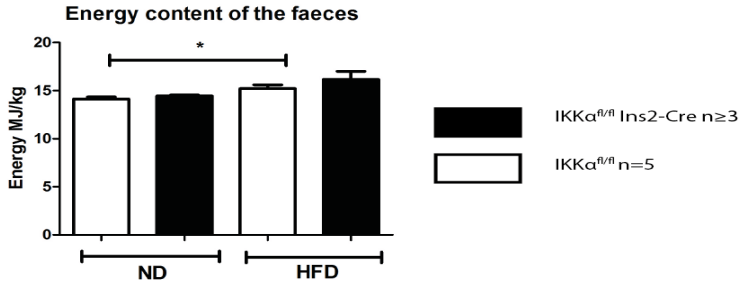

Figure 4.17: Energy excretion depends on the diet but not on IKKα deletion in the endocrine pancreas. Faecal energy content of IKKα$^{fl/fl}$ Ins2-Cre and control animals assessed by bomb calorimetry. Student t-test *: $p<0.05$

4.3 Deletion of IKKα in the fat tissue

4.3.1 Mice bearing a deletion of IKKα in the fat tissue have a significant weight difference under HFD condition

Adipose tissue is where energy is stored as lipids. However, it is also a key player in glycaemia regulation by up-taking glucose and transforming it through fatty acid synthesis into lipids. When need for energy, the adipose tissue transforms the fatty acids into glucose via the lipolysis.

We wanted to see if a specific deletion of IKKα in the adipose tissue might have any effect on glucose metabolism in mice. We therefore crossed IKKα floxed mice with a Fabp4-Cre line specific for the fat tissue (IKKα$^{fl/fl}$-Cre mice).

When fed a ND, IKKα$^{fl/fl}$ animals and IKKα$^{fl/fl}$ Fabp4-Cre mice did not show any weight difference overtime. (Figure 4.18 A) Both groups of mice gained little weight over time. However, when fed a HFD, IKKα$^{fl/fl}$ Fabp4-Cre mice were significantly bigger than the controls even if both groups gained weight regularly. (Figure 4.18 B)

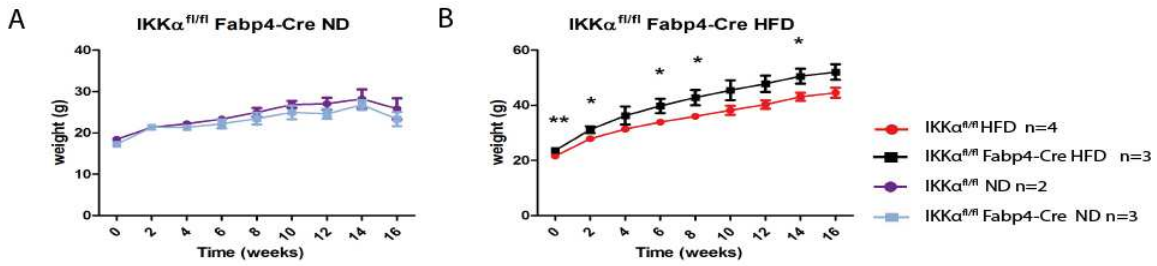

Figure 4.18: IKKα deletion in the adipose tissue promotes increased weight gain under HFD but not under ND. A: Weight curves of IKKα$^{fl/fl}$ Fabp4-Cre and control mice under ND. **B**: Weight curves of IKKα$^{fl/fl}$ Fabp4-Cre and control mice under HFD. Student t-test: *: p<0.05, **: p<0.01

4.3.2 No difference in glucose tolerance or insulin secretion is found in IKKα$^{fl/fl}$ Fabp4-Cre mice compared to IKKα$^{fl/fl}$ controls

To determine if IKKα deletion in fat tissue leads to any change in glucose clearance, GTT was performed with IKKα$^{fl/fl}$ Fabp4-Cre mice and controls on both ND and HFD conditions.

No differences were seen in the IKKα$^{fl/fl}$ Fabp4-Cre animals when compared to the IKKα$^{fl/fl}$ mice. Under ND, the mice were glucose tolerant (Figure 4.19 A). Similarly, the mice were glucose tolerant and reached their basal glycaemia after 2h under HFD. The secretion of insulin followed the same trend both on ND and HFD. (Figure 4.19 A, B) Interestingly, although both groups gained significant weight on HFD, they still remained insulin sensitive suggestive of resistance against diet-induced glucose intolerance at around 11 weeks on HFD.

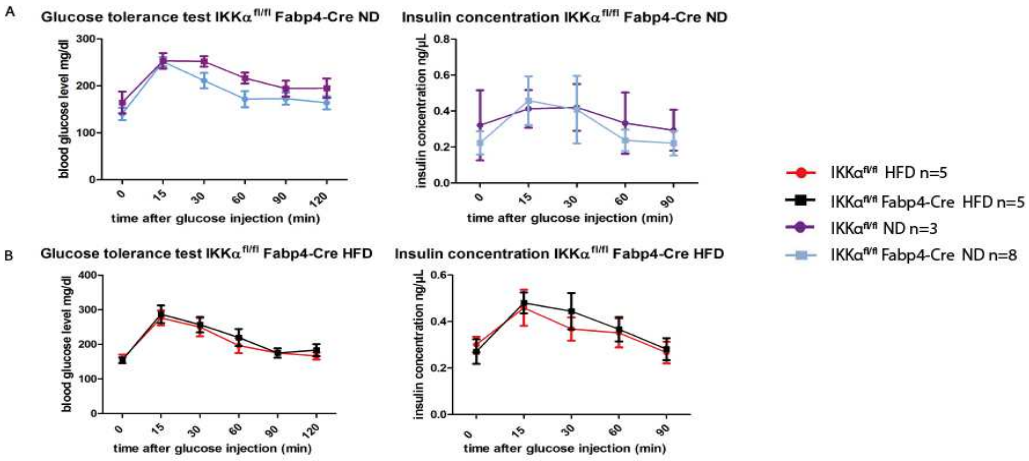

Figure 4.19: Deletion of IKKα in the adipose tissue does not induce changes in glucose tolerance and insulin sensitivity under ND or HFD. A: Blood glucose and plasma insulin levels during GTT from male IKKα$^{fl/fl}$ Fabp4-Cre mice at 11 weeks under ND. **B**: Blood glucose levels and plasma insulin levels during GTT after 13 weeks under HFD. Student t-test was not significant**.**

4.3.3 Mice bearing a deletion of IKKα in the fat tissue secrete less insulin in the course of the HFD feeding

We wanted to see if the insulin concentration overtime was different in the IKKα$^{fl/fl}$ Fabp4-Cre mice. We measured insulin levels using blood samples collected during the course of the diet.

The insulin concentration at the beginning of the diet was not different between IKKα$^{fl/fl}$ and IKKα$^{fl/fl}$ Fabp4-Cre animals. However, at 16 weeks under HFD, the IKKα$^{fl/fl}$ Fabp4-Cre had significantly lower insulin concentration than the IKKα$^{fl/fl}$ mice. At 20 weeks on HFD, the difference was not significant but there was still a tendency towards a lower concentration in the IKKα$^{fl/fl}$ Fabp4-Cre mice. (Figure 4.20)

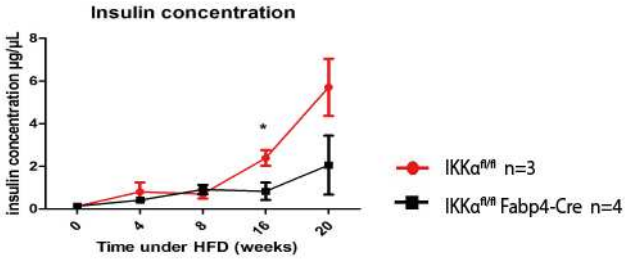

Figure 4.20: IKKα$^{fl/fl}$ Fabp4-Cre mice secrete less insulin under HFD than the controls: Insulin concentration in the blood of IKKα$^{fl/fl}$ Fabp4-Cre mice over the time of HFD feeding. Student's t-test, *: $p<0.05$

4.3.4 IKKα$^{fl/fl}$ Fabp4-Cre mice show a decrease in CD11c dendritic cell marker in the colon

As Fabp4 is as well slightly expressed in the intestine, we checked the markers for inflammatory cells in this tissue via real-time PCR.

IKKα$^{fl/fl}$ Fabp4-Cre mice had a decrease in CD11c expression which is a marker for dendritic cells. The others markers checked did not show a difference between IKKα$^{fl/fl}$ Fabp4-Cre and IKKα$^{fl/fl}$ mice. (Figure 4.21)

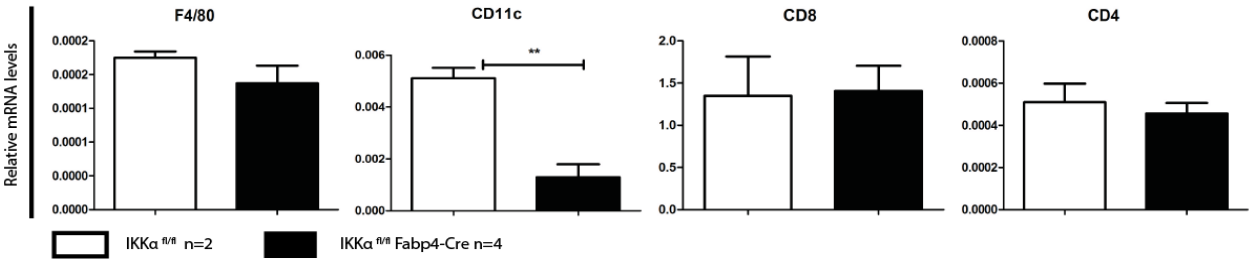

Figure 4.21: IKKα deletion in the fat tissue leads to a decrease in the dendritic cell number in the colon: Relative mRNA expression in the colon of IKKα$^{fl/fl}$ Fabp4-Cre mice for inflammatory cells markers after 20 weeks under HFD. Student's t-test, **: $p<0.01$

4.3.5 IKKα deletion in the adipose tissue leads to kidney disease

The mice bearing a deletion of IKKα in the fat tissue developed unilateral kidneys problems. Their kidney appeared huge and cystic. In some cases, the ureter was completely blocked with kidney stones. Moreover, this phenotype was only found in older mice. Young mice of 4-5 weeks of age never showed kidneys problems.

Interestingly not all the IKKα$^{fl/fl}$ Fabp4-Cre mice developed kidney problems. However, the incidence of kidney problems was almost twice as much in the mice fed a ND than in the mice fed a HFD. (Figure 4.22)

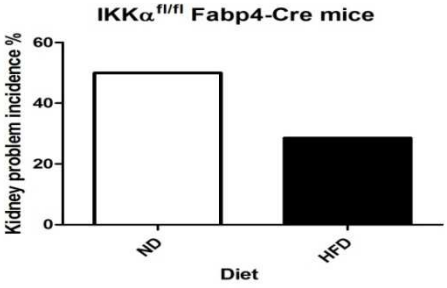

Figure 4.22: IKKα deletion in the adipose tissue leads to kidneys problems. The percentage incidence of kidneys problems in IKKα$^{fl/fl}$ Fabp4-Cre mice after 20 weeks under ND and HFD, ND: 7/14 IKKα$^{fl/fl}$ Fabp4-Cre animals presented kidneys problems; HFD: 2/7 IKKα$^{fl/fl}$ Fabp4-Cre mice had kidney problems.

4.3.6 IKKα deletion in the adipose tissue leads to increased proliferation and increased IKKα expression in the abnormal kidneys

As the IKKα$^{fl/fl}$ Fabp4-Cre animals developed kidney problems, we performed histological analysis on kidney sections from these mice.

Figure 4.23. A and B show an overview of the kidney histology. The figure 4.23 A shows the capsule of the kidney, the cortex and the medulla were completely disappeared. In Figure 4.23 B, we can as well see a kidney with only the capsule remaining. The ureter is also present but completely blocked. IKKα deletion in fat tissue was associated with the disappearance of the cortex and medulla from the kidneys.

As Fabp4-Cre is slightly expressed in the kidney, we thought that a deletion of IKKα in the kidneys might be the reason for kidneys disorders. In order to show if IKKα protein was still present in the kidneys, we performed western-blot. As seen in Figure 4.23 C, IKKα was still present in the kidneys, therefore the cause of this abnormality was not directly associated with IKKα deletion in the kidney. However, since the whole tissue was used for protein extraction, one cannot exclude the contribution of cells that do not express Fabp4-cre and have intact IKKα expression.

To confirm the IKKα expression in the kidneys, immunohistochemistry was performed (fig 4.23 H and I). The western blot results were confirmed and moreover, IHC revealed increased expression of IKKα in the abnormal kidneys, perhaps due to infiltrating inflammatory cells.

Fig D is an H&E staining of an abnormal kidney that shows crystals in the ureter and the disruption of the normal structure of the kidney. Fig E is an H&E staining of a normal kidney from the $IKK\alpha^{fl/fl}$ Fabp4-Cre mice. Fig F and G are BrdU (Bromodeoxyuridine) staining from abnormal and normal kidneys respectively. It shows an increased proliferation in the abnormal kidneys compared to the normal one.

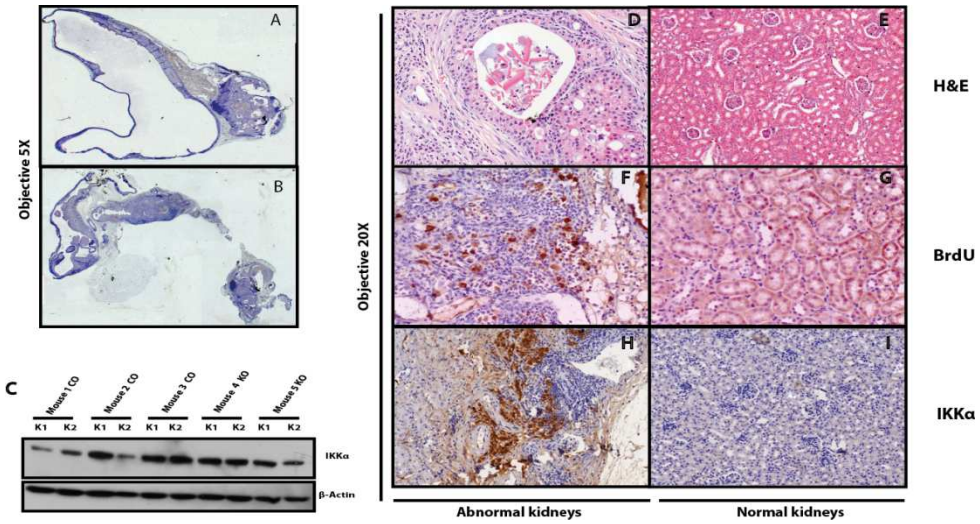

Figure 4.23: Abnormal kidneys from IKKαfl/fl Fabp4-Cre mice present more IKKα expression and more proliferation. A, B, D and E: H&E staining from kidney of IKKα$^{fl/fl}$ Fabp4-Cre mice**, C:** detection of IKKα in kidneys of IKKα$^{fl/fl}$ Fabp4-Cre mice by WB**, F and G:** IHC for BrdU in the kidney of IKKα$^{fl/fl}$ Fabp4-Cre mice, **H and I**: IHC for IKKα in the kidney of IKKα$^{fl/fl}$ Fabp4-Cre mice 20 weeks under ND. 5X magnification

4.3.7 Deletion of IKKα in the fat tissue is associated with macrophage infiltration in the abnormal kidneys

IKKα is implicated in inflammation. To check if inflammation was triggered in the kidney we performed immunofluorescence staining for markers of inflammatory cells: B220 for differentiated hematopoietic cells, GR1 for neutrophils and F4-80 for macrophages.

In the abnormal kidneys, there was more F4-80 positive cells than in the normal kidneys suggesting an increased macrophage infiltration. (Figure 4.24 E, F) No differences could be seen between abnormal kidneys and normal kidneys for GR1+ and B220+ cells. (Figure 4.24 A to D)

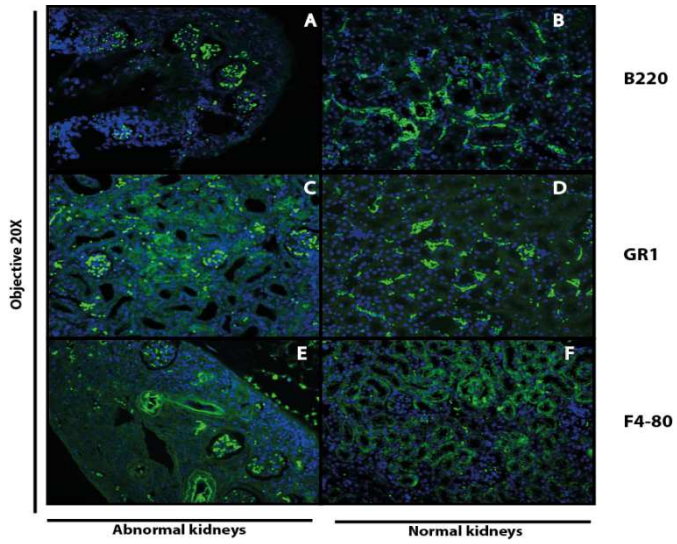

Figure 4.24: Deletion of IKKα in the adipose tissue leads to macrophage infiltration in the abnormal kidneys: Immunofluorescence staining for inflammatory cells markers in the kidneys of IKKα$^{fl/fl}$ Fabp4-Cre mice: **A and B**: B220**, C and D**: GR1 and **E and F**: F4-80 20 weeks under ND.

4.3.8 Blood counts slightly differ between IKKα$^{fl/fl}$ Fabp4-Cre and IKKα$^{fl/fl}$ mice under ND and HFD

Blood analysis has been performed for IKKα$^{fl/fl}$ Fabp4-Cre and control mice under ND and HFD condition.

The IKKα$^{fl/fl}$ animals under HFD had significantly less haemoglobin per cell than the IKKα$^{fl/fl}$ mice under ND. Under HFD, the red cell distribution width was increased showing that the red blood cells have more differences in size when fed a HFD than a ND. (Figure 4.25)

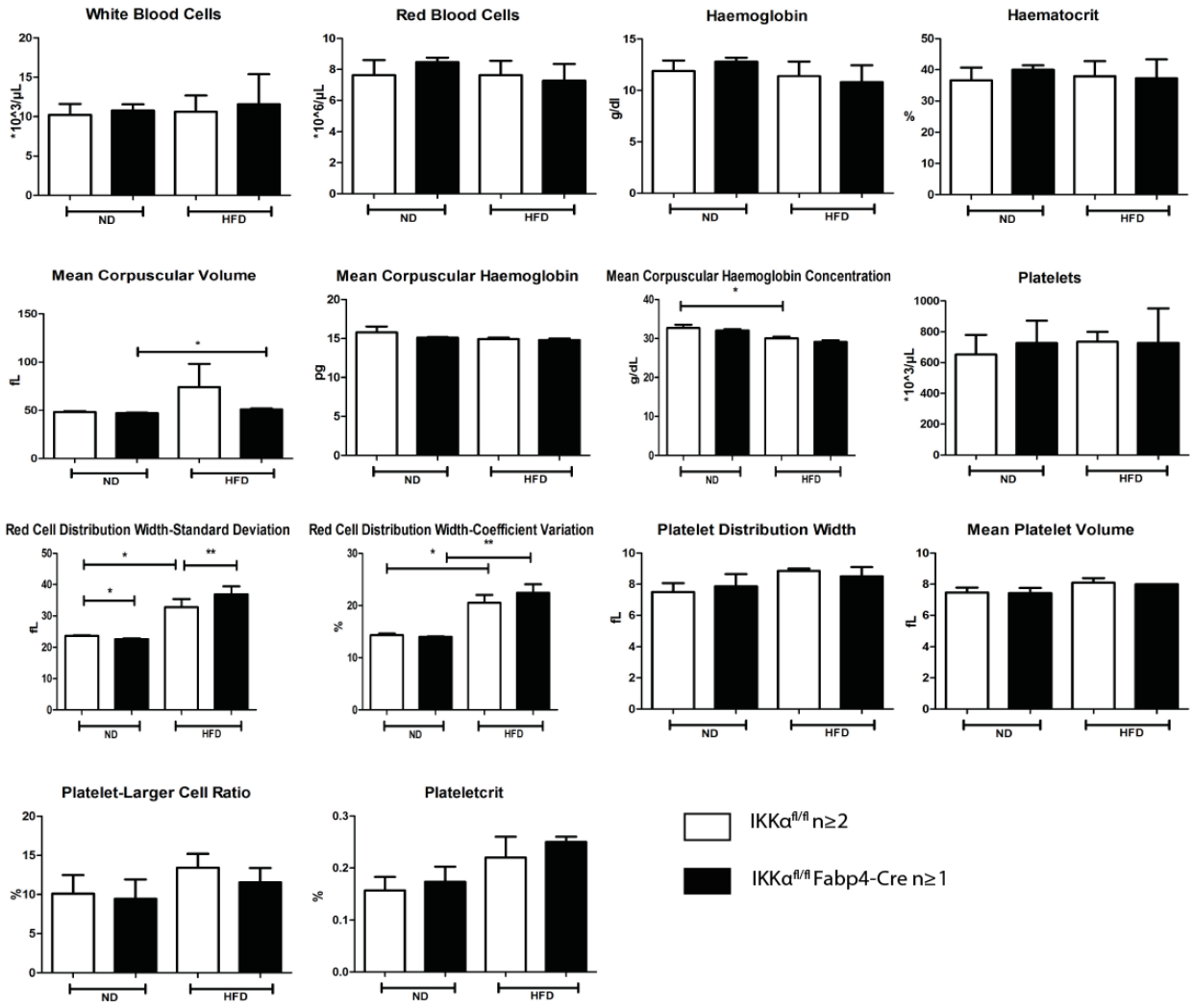

Figure 4.25: IKKαfl/fl Fabp4-Cre mice have blood cell counts slightly different than the controls. Whole blood cell count for IKKα$^{fl/fl}$ Fabp4-Cre and control mice 11 weeks under ND and 16 weeks on HFD. Student's t-test, *: p<0.05, **: p<0.01

4.4 Deletion of IKKα in the muscle

4.4.1 Deletion of IKKα in the muscle does not significantly lead to difference in weight gain

The muscle is the major organ where glucose uptake takes place. The glucose is used in the muscle to produce energy for the contraction of the muscle fibres. Therefore, it has an important role to play in the glucose homoeostasis. To see if IKKα in the muscle is important for glycaemia regulation, we crossed the IKKα floxed mice with a Ckmm-Cre line muscle specific (IKKα$^{fl/fl}$ Ckmm-Cre mice). We fed the mice with a ND or with a HFD during several weeks.

The IKKα$^{fl/fl}$ Ckmm-Cre animals and controls did not show any weight difference under ND or HFD. Both IKKα$^{fl/fl}$ and IKKα$^{fl/fl}$ Ckmm-Cre animals gained regularly weight on both diets. (Figure 4.26 A, B)

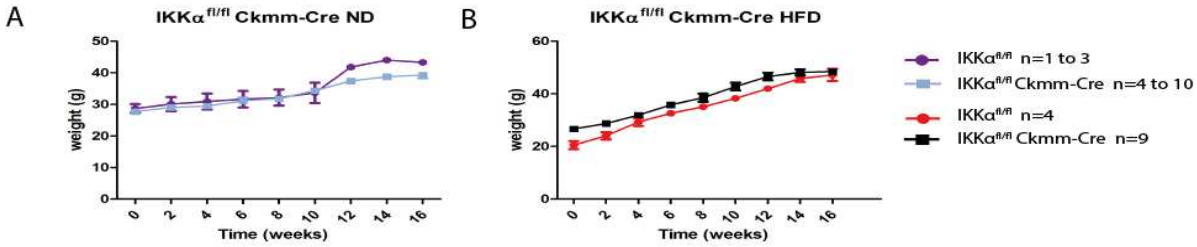

Figure 4.26: Deletion of IKKα in the muscle does not lead to weight differences between IKKα$^{fl/fl}$ Ckmm-Cre and IKKα$^{fl/fl}$ controls mice, males. **A:** Weight curves of IKKα$^{fl/fl}$ Ckmm-Cre and control mice under ND and **B**: under HFD**.**

4.4.2 Deletion of IKKα in the muscle does not affect the glucose tolerance and the insulin secretion at early time points but leads to diabetes at late time points

As the muscle is the main organ for glucose uptake and therefore plays a critical role in glucose tolerance, we performed GTT with the IKKα$^{fl/fl}$ Ckmm-Cre and control mice to check if there was a difference when IKKα was deleted in the muscle.

The deletion of IKKα in the muscle did not affect the glucose tolerance of the mice when fed a ND or a HFD until 10 weeks. Both IKKα$^{fl/fl}$ Ckmm-Cre and IKKα$^{fl/fl}$ were glucose tolerant and secreted insulin at the same concentration. They both were able to lower their glucose therefore were insulin sensitive and glucose tolerant. (Figure 4.27 A)

However, after 16 weeks under HFD, the IKKα$^{fl/fl}$ Ckmm-Cre mice became diabetic while the IKKα$^{fl/fl}$ animals remained glucose tolerant. Indeed, the KO mice had very high fasting glucose levels that were around 180 mg/dL. Following glucose load, it increased further to 300 mg/dL and stayed at this level during the rest of the GTT. Indeed, IKKα$^{fl/fl}$ Ckmm-Cre mice were unable to clear glucose from their bloodstream suggesting they became significantly glucose intolerant. (Figure 4.27 B)

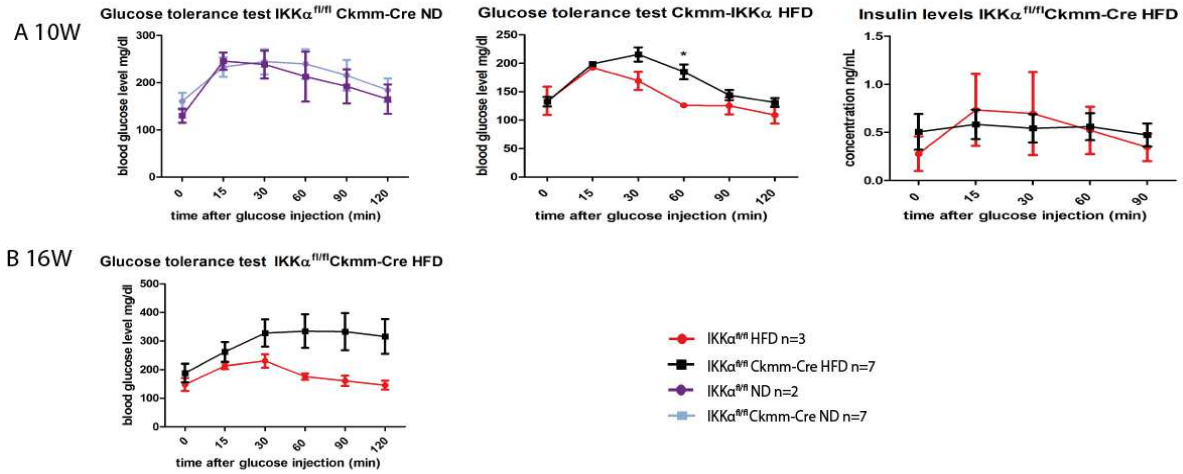

Figure 4.27: Deletion of IKK*α* in the muscle leads to diabetes at the late time point of the HFD feeding. GTT results and Insulin concentration during GTT from male IKKα$^{fl/fl}$ Ckmm-Cre mice and controls. **A**: at 10weeks under the ND**. B**: at 16 weeks under HFD.

4.4.3 IKKα deletion in muscle does not lead to any histological changes in skeletal and heart muscle.

To see if the deletion of IKKα in the muscle led to differences in the skeletal muscle and the heart muscle, we performed H&E staining and PAS staining.

No difference could be seen between IKKα$^{fl/fl}$ Ckmm-Cre and IKKα$^{fl/fl}$ mice under HFD or ND in the skeletal muscle or in the heart muscle. (Figure 4.28 A to H)

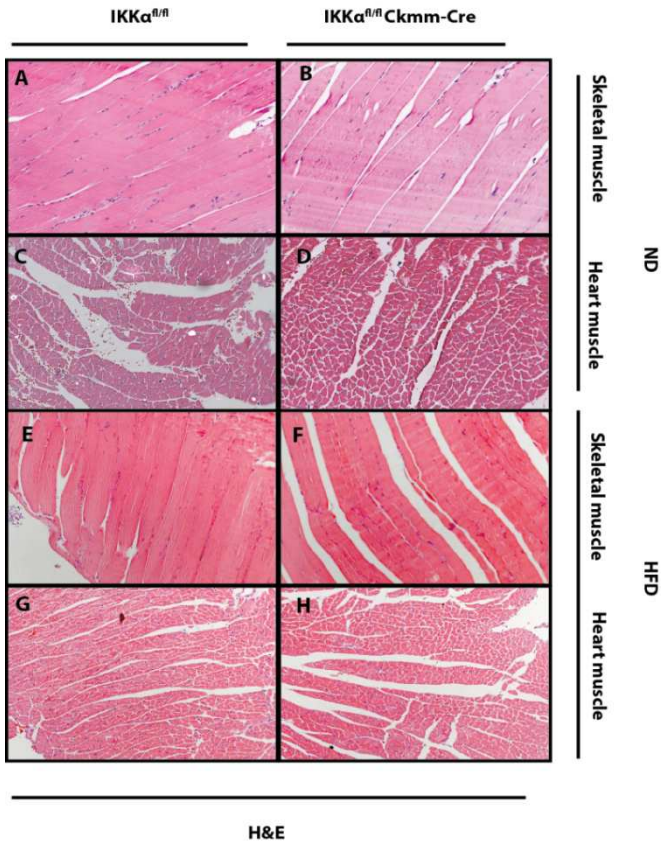

Figure 4.28: IKKα deletion in the muscle does not lead to any histological change in skeletal muscle and heart. H&E staining from muscle and heart of IKKα$^{fl/fl}$ Ckmm-Cre mice, **A to D**: under ND **E to H**: under HFD. 20 weeks on the respective diets.

4.4.4 IKKα deletion in the muscle does not affect the glycogen storage capacity of the cells

In order to see if the glycogen content of the skeletal and heart muscle from IKKα$^{fl/fl}$ Ckmm-Cre differs from that of IKKα$^{fl/fl}$ animals we performed Periodic acid Schiff (PAS) staining on skeletal and heart muscle sections from non-fasting mice. Both groups sowed similar glycogen in skeletal and heart muscle suggesting the deletion of IKKα did not affect the capacity of the muscle cells to store glycogen. (Figure 4.29 A to D) However, on has to bear in mind that PAS staining is more of a qualitative method than a quantitative one. Additionally, one cannot tell slow-switching fibres from the fast ones by only H&E and PAS staining.

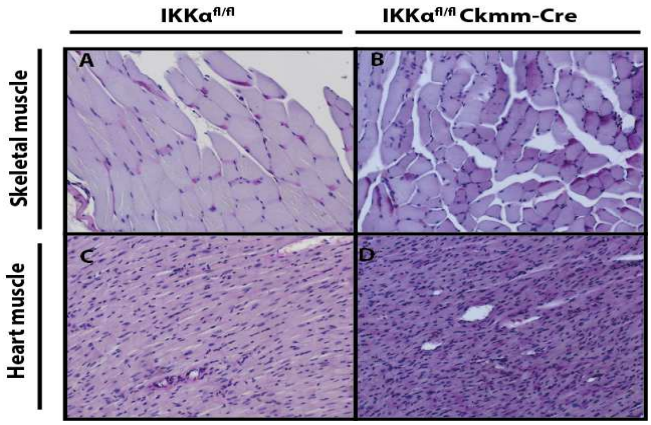

Figure 4.29: Glycogen storage is not affected by the deletion of IKKα in the muscle. PAS staining from **A and B:** skeletal muscle and **C and D**: heart muscle from IKKα$^{fl/fl}$ Ckmm-Cre and controls under non-fasting conditions.

4.4.5 Deletion of IKKα in the muscle provokes a slight increase of red blood cells and platelet number and a decrease in white blood cells

We additionally performed blood cell counts on IKKα$^{fl/fl}$ Ckmm-Cre and controls under HFD.

The IKKα$^{fl/fl}$ Ckmm-Cre mice had a slight increase in red blood cell numbers. Consistent with it, haemoglobin, haematocrit and haemoglobin concentration per cell were as well increased.

The mean corpuscular volume was significantly decreased in the IKKα$^{fl/fl}$ Ckmm-Cre animals. This result correlated with the increased number of red blood cells, which are smaller cells.

IKKα$^{fl/fl}$ Ckmm-Cre mice had also increased number of platelets and an increased plateletcrit. (Figure 4.30)

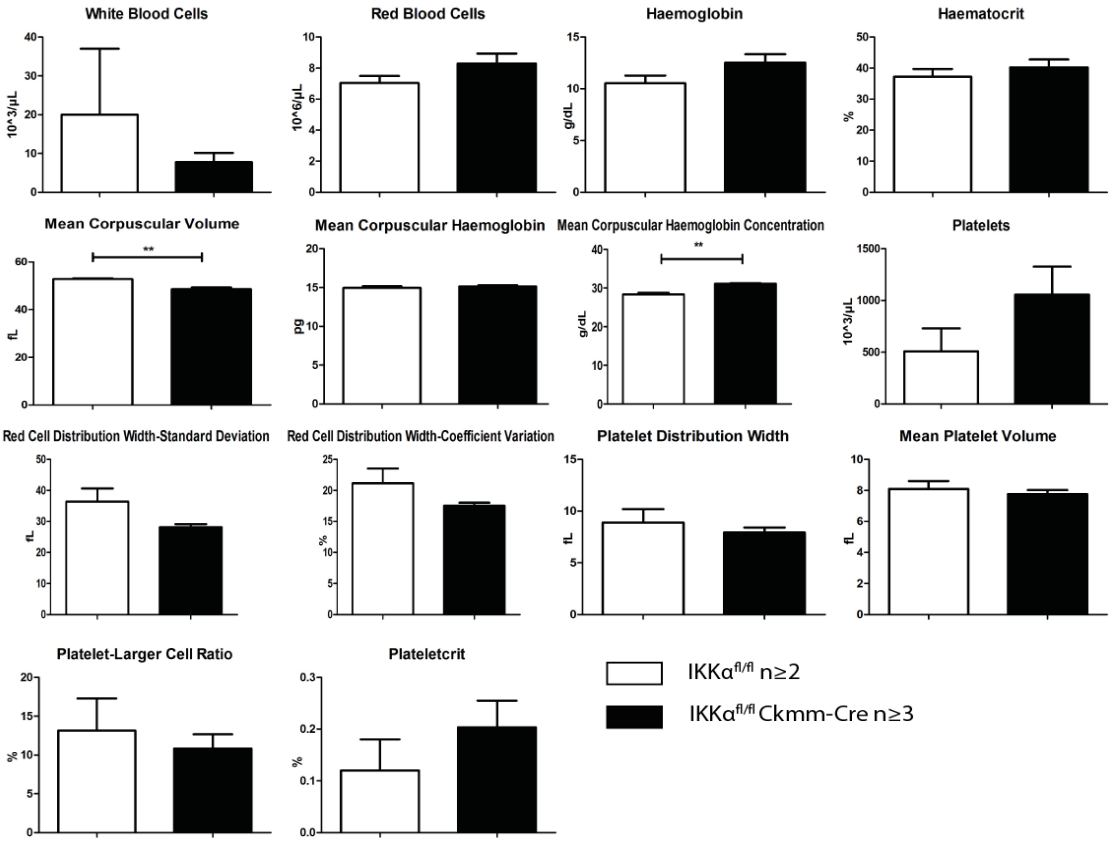

Figure 4.30: Deletion of IKKα in the muscle slightly changes the blood cell counts. Whole blood counts of IKKα$^{fl/fl}$ Ckmm-Cre and controls mice after 17 weeks under HFD. Student's t-test, **: p<0.01

4.4.6 IKKα deletion in the muscle does not change the insulin signalling in the pancreas

As IKKα$^{fl/fl}$ Ckmm-Cre mice developed diabetes at later time points during HFD, we wanted to know if there was a decreased activation of the insulin signalling cascade. We therefore injected mice either with saline as a control or with insulin to activate receptor-mediated insulin signalling and downstream activator Akt, which, then signals to glucose transporters for the proper clearance of glucose from bloodstream.

There were no differences in the activation of the signalling cascade between IKKα$^{fl/fl}$ Ckmm-Cre and IKKα$^{fl/fl}$ mice under ND and HFD. (Figure 4.31)

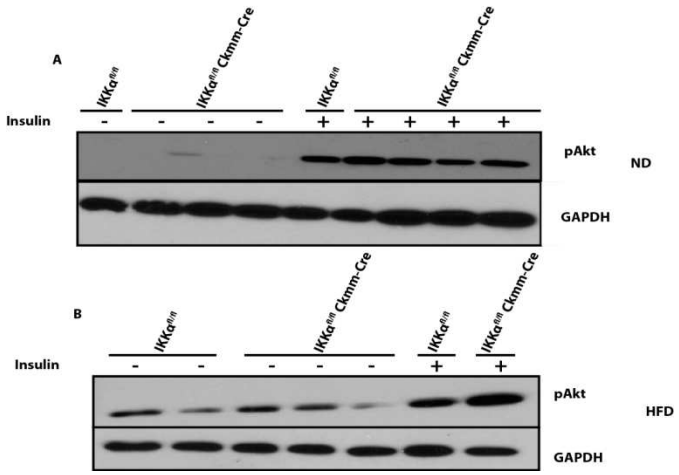

Figure 4.31: Insulin signalling is still functional in IKKα$^{fl/fl}$ Ckmm-Cre mice. Western blot analysis of pAkt in IKKα$^{fl/fl}$ Ckmm-Cre mice, **A**: under ND**, B:** under HFD. Mice were 20 weeks on the diet.

4.5 Role of glycosylation in intestinal cancer

Obesity is a well-known predisposition for cancer and especially colorectal cancer. Intestinal and colon cancer, although different, share common features like the sequence of mutations leading to carcinogenesis.

4.5.1 Diet and intestinal cancer

In order to study the mechanisms underlying the early onset of cancer in obese patients, a mouse model of intestinal cancer has been used. The mice have a constitutional activation of the oncogene *Kras* under the promoter of Villin, a protein specific for the intestinal epithelial cells (termed ViRas mice). Therefore, the activation of *Kras* is only present in the intestinal epithelial cells.

Previous results showed that when fed a ND, ViRas mice did not show any weight differences in comparison to the controls while under HFD, ViRas mice remained significantly leaner than the controls. The ViRas mice started losing weight after around 10 weeks under the diet and weight loss correlated with the development of tumours. Moreover, Viras mice became anaemic under HFD, another sign of development of cancer in these animals. (Schulz *et al* in revision)

ViRas mice under HFD develop adenocarcinoma especially in the duodenum (Figure 4.32B) and rarely in the jejunum. When fed for over 47 weeks with HFD, the mice showed metastasis in the liver, pancreas and spleen. At the contrary, after 6 to 7 months under ND the ViRas mice did not display tumours but only hyperplastic polyps. (Figure 4.32A) Therefore, HFD enhanced the onset of carcinogenesis significantly.

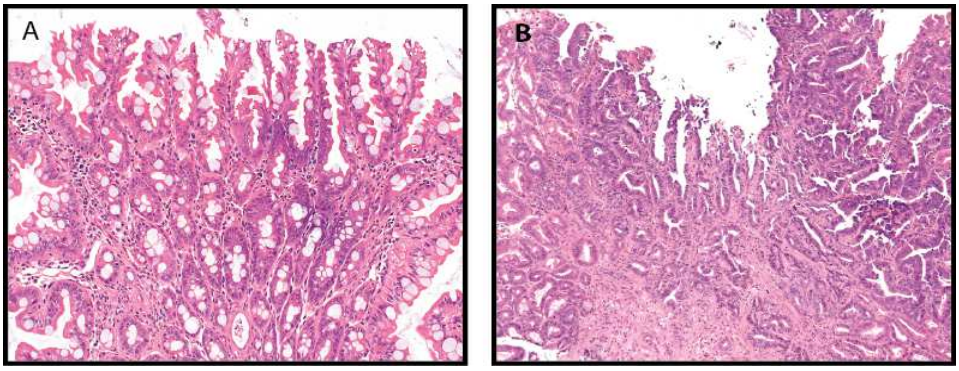

Figure 4.32: Hyperplastic polyp (A) and serrated adenocarcinoma (B) in mouse

Macroscopically, ViRas mice displayed an enlarged and longer intestine (Bennecke *et al* 2010) while microscopically, the villi of the intestine were longer and serrated. As for the colon, non-malignant hyperplastic polyps were detected. (Figure 4.33)

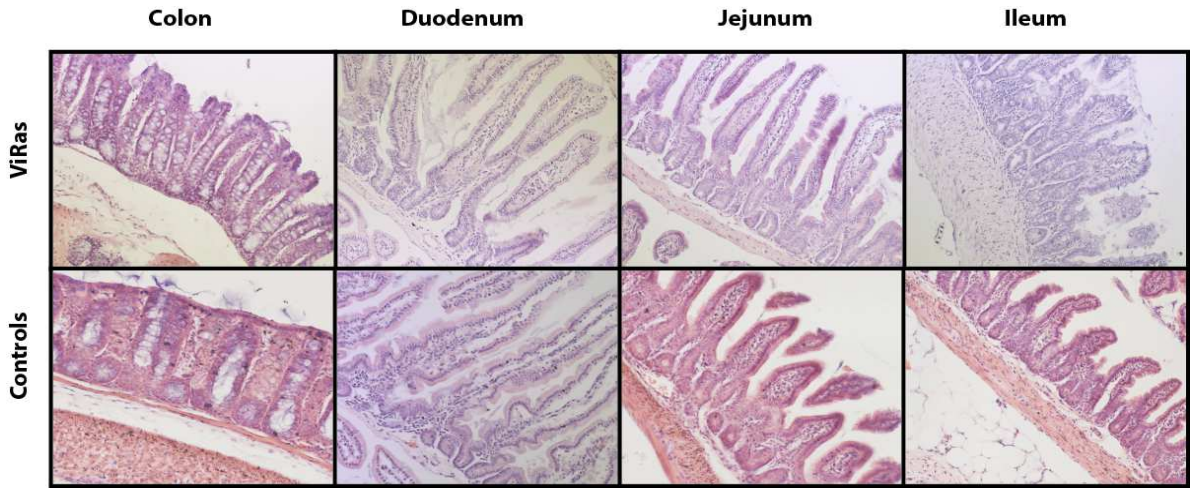

Figure 4.33: ViRas mice have hyperplastic polyps in the colon and longer and serrated villi. Histology of intestine from ViRas mice showing branched villi (duodenum ViRas). H&E staining magnification 20X.

Previously, microarray analysis performed with the duodenum of ViRas mice under both ND and HFD showed that ViRas mice under HFD had a down-regulation of genes involved in immune system. This down-regulation was confirmed via flow cytometry analysis in the lamina propria, Peyer's patches and mesenteric lymph nodes. More precisely, ViRas mice displayed a decrease in antigen presentation. Indeed, dendritic cells and $MHCII^{+}$ populations were significantly decreased in ViRas mice.

Our group showed that ViRas mice under HFD had a shift in the composition of intestinal bacteria leading to the hypothesis that commensal bacteria might be playing a causative role during carcinogenesis. Indeed, the treatment of mice with butyrate, a bacterial fermentation end-product, could block tumour development underscoring a role for intestinal bacteria in carcinogenesis. (Schulz *et al* in revision)

4.5 2 Microarray analysis of ViRas mice showed alteration in the expression of glycosyltransferases

Microarray analysis performed using duodenum samples from ViRas mice and controls following a ND or a HFD with or without supplementation of butyrate showed

significant alterations in gene expression. Among all the expression of glycosyltransferase genes was up-regulated in ViRas mice under HFD. (Figure 4.34) The expression profile for these genes under ND was similar between controls and ViRas mice leading to the hypothesis that glycosylation pattern is specifically altered in ViRas mice under HFD condition. Glycosylation is important in carcinogenesis (Varki *et al* Essentials of glycobiology Chapter 44) therefore the differences observed in glycosyltransferases' might be associated to tumour development in the ViRas mice. Moreover, as commensal bacteria are influencing glycosylation pattern and a shift in microbiota has been shown in ViRas mice one can think that this shift in microbiota might cause changes in the glycosylation pattern which in turn could promote carcinogenesis.

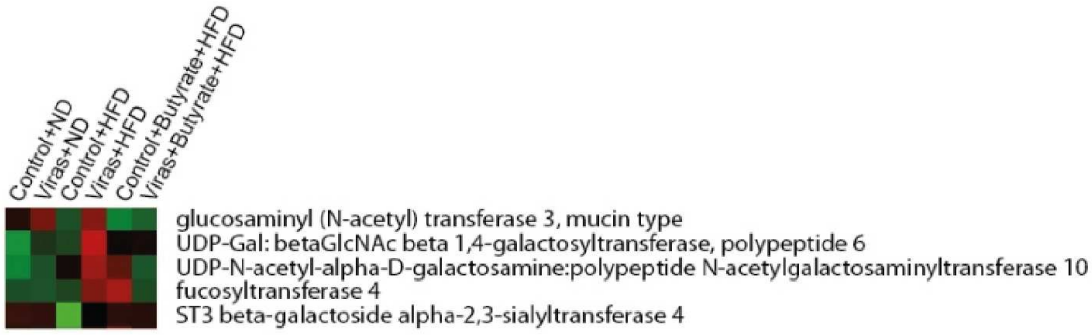

Figure 4.34: Glycosyltransferase gene expression is influenced by the diet and the genotype. Heat map from microarray analysis using RNA extracted from duodenum in ViRas ND/HFD and ViRas HFD+ butyrate groups. Red indicates an up-regulation while green shows a down-regulation. Controls ND n= 2, ViRas ND n=3, controls butyrate n=1, ViRas butyrate n=3, controls HFD n=2, ViRas HFD n=2

4.5.3 O-GlcNAc glycosylation pattern slightly differs between ND and HFD ViRas mice

Increasing evidence shows that modification of protein glycosylation is a feature of tumours and tumour cells. (Varki *et al* Essentials of glycobiology Chapter 44) In order to determine if protein glycosylation is different in control and ViRas mice, as was suggested by the microarray data, we performed a WB analysis with an antibody that recognises the glycosylation motif O-GlcNAc.

The O-GlcNAcylation motif was present in all mice. However, the glycosylation pattern between the different groups of mice was slightly changed. Indeed, a protein around 72 kDa was more glycosylated in the controls than in the ViRas under HFD. The glycosylation pattern of HFD ViRas mice was similar to the one of ViRas under ND.

Moreover, no difference was found between controls and ViRas under ND. Therefore, Kras activation cooperates with HFD to decrease O-GlcNAcylation pattern of the 72 kDa protein. The diet did not affect the O-GlcNAcylation as there were no differences between ViRas mice under HFD and ND.

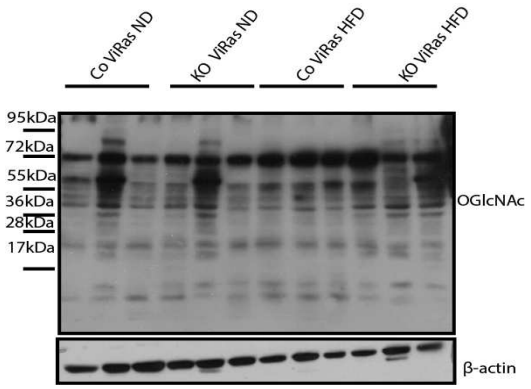

Figure 4.35: Diet and genotype lead to changes in O-GlcNAcylation. Detection of O-GlcNAcylated proteins in the duodenum of ND and HFD fed ViRas mice and controls.

4.5 4 St3GalIV gene deletion does not significantly affect tumour formation in ViRas mice but delay carcinogenesis

Among the genes that showed different expression pattern between controls and ViRas mice the glycosyltransferase ST3 Beta-Galactoside Alpha-2, 3-Sialyltransferase 4 (St3GalIV) was the most up-regulated one. The treatment with butyrate seemed to restore the expression of St3GalIV gene to the level seen in ND controls and ViRas. As mice treated with butyrate did not present cancer, the hypothesis that St3GalIV is implicated in the carcinogenesis was tempting.

To assess the hypothesis that St3GalIV is implicated in carcinogenesis, we crossed the ViRas mice with a strain bearing a whole body deletion of St3GalIV (named St3 ViRas mice).

During our study histological sections from the ViRas HFD and St3 ViRas mice had been evaluated by a pathologist. The pathologist determined the histological score of the different sections. Stage 1 and 2 were scored and defined as traditional serrated adenoma with low or high-grade intraepithelial neoplastic (TSA LGIEN and TSA HGIEN), while stages 3 and 4 were defined as invasive cancer and metastasis in distant tissues.

The evaluation showed that both ViRas and St3 ViRas mice developed adenocarcinoma. However, none of the mice had metastasis at that age. Among St3ViRas mice only one mouse presented adenocarcinoma while 4 mice were evaluated at this stage in

ViRas mice. Although not significant, we can notice a difference in the stage of the lesions seen in mice, with St3ViRas mice having lower grade lesions than ViRas mice. (Figure 4.36)

This tendency towards a better histological score in St3 ViRas mice suggests that genetic deletion of glycosyltransferase gene might have protected against, or at least delayed, carcinogenesis.

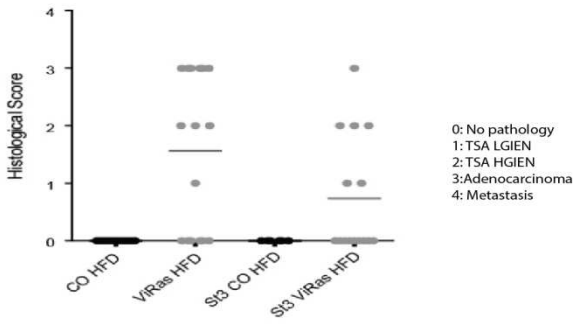

Figure 4.36: St3GalIV deletion delay carcinogenesis in ViRas mice. Histological score of ViRas and St3 ViRas mice under HFD.

4.5.5 St3ViRas mice show enlarged and serrated villi as the ViRas mice

Small intestine and colon sections from ViRas, St3ViRas and control mice have been stained by H&E. Macroscopically, the ViRas and St3ViRas showed an enlargement of the intestine and an increase in the length of the intestine. This macroscopic observation was as well found microscopically. Indeed, in ViRas and St3ViRas mice, the villi were longer than in the controls. Moreover, the villi of the ViRas and St3ViRas mice were serrated. (Figure 4.36)

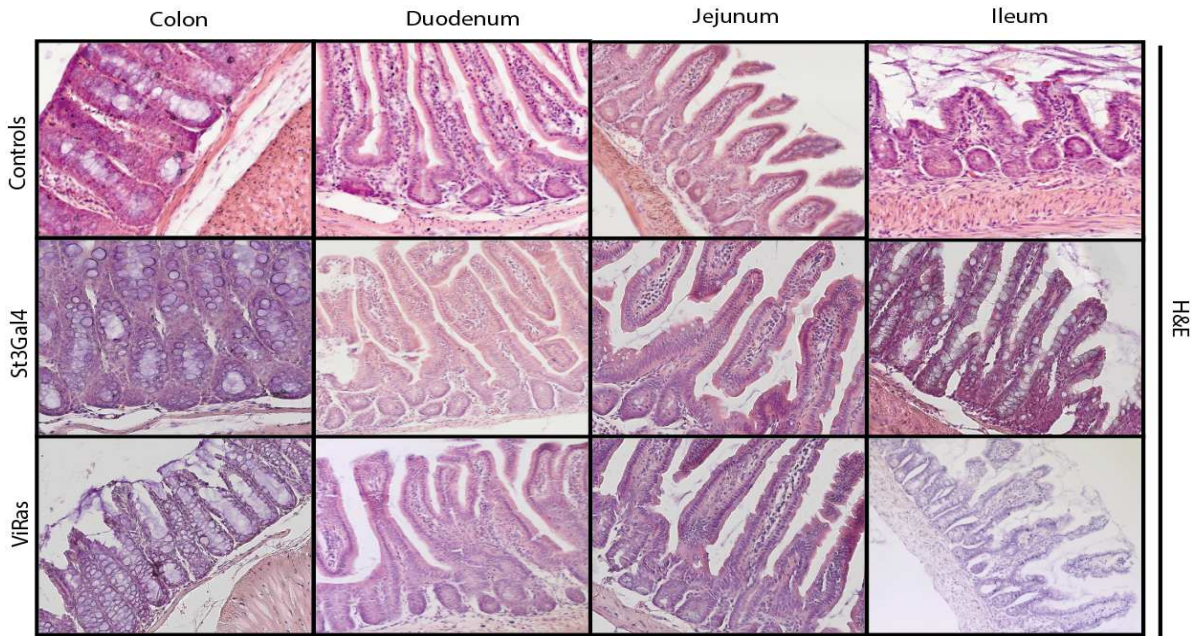

Figure 4.37: St3ViRas mice show the same villi elongation and hyperplastic polyps as the ViRas mice. H&E staining of small intestine and colonic sections from controls, ViRas mice and St3 ViRas mice. Magnification 20X.

4.5.6 St3ViRas mice produce mucus in amounts comparable to the one of controls

Mucus in the intestine is constituted by mucins, which are glycoproteins. Therefore, the St3 ViRas mice, which have a genetic deletion of a glycosyltransferase gene, might have less glycosylated proteins than the controls and therefore less mucus. In the intestine, mucus is produced by goblet cells and Alcian blue staining by colouring mucus in blue shed light on the goblet cells

The results showed that all the mice had mucus production in all the parts of the intestine. No difference in the amount of mucus and Goblet cell number could be seen in the different group of mice. Therefore, *Kras* activation or St3GalIV deletion did not alter Goblet cells. (Figure 4.37)

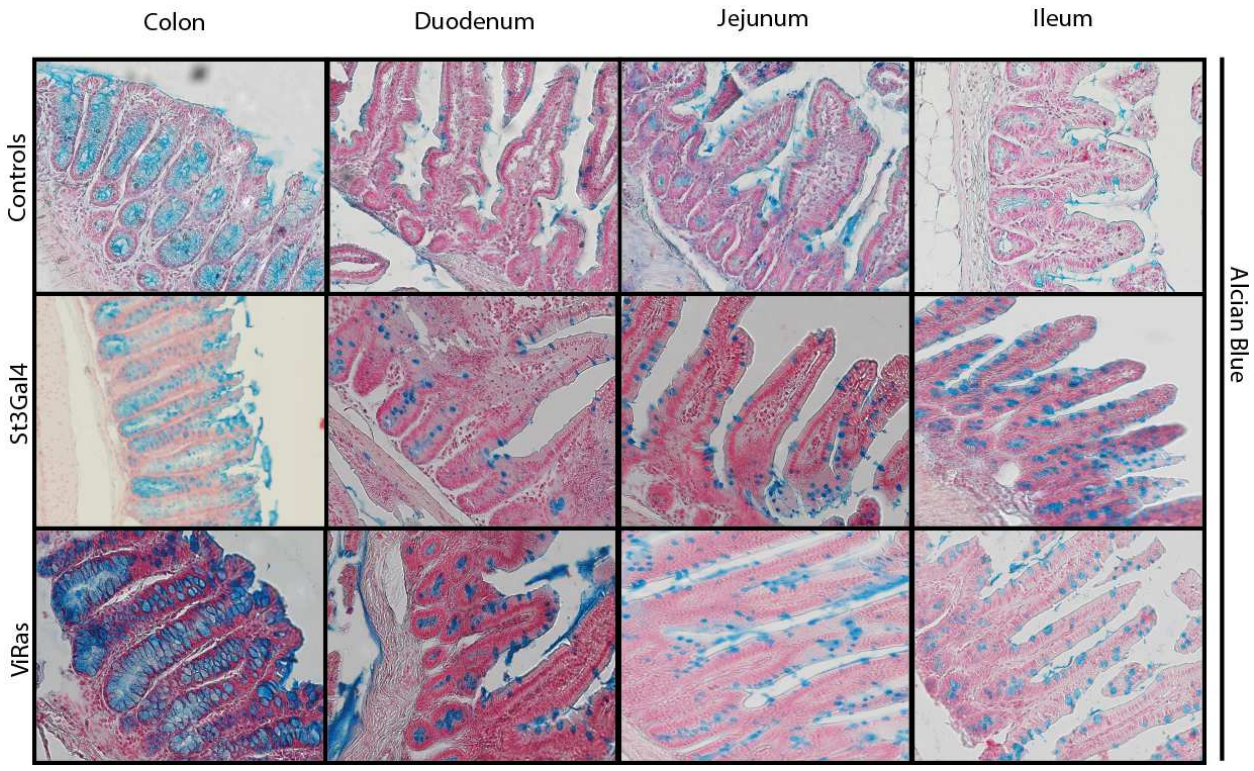

Figure 4.38: St3GalIV deletion does not lead to any mucus production impairment. Alcian blue staining from St3ViRas, ViRas and control mice.

4.5.7 Expression of glycosyltransferase is different between St3 ViRas mice and ViRas mice

The microarray data showed altered expression of glycosyltransferase genes. Therefore, we wanted to check if we could find a difference for some other genes involved in glycosylation at the mRNA level. Moreover, we compared it to the St3ViRas mice in order to see whether the deletion of St3GalIV had an impact on other glycosyltransferases genes.

St3GalIV was not detected in the St3ViRas mice showing that the genetic deletion of the gene was successfully achieved.

Concerning B4Galt6 (Beta-1,4-Galactosyltransferase 6), an enzyme transferring galactose, the microarray data showed increased expression in the KO mice compared to controls both under HFD and ND. The increase was confirmed by real-time PCR in the ND mice. However, a decrease was found in the HFD mice. St3-ViRas mice had less B4Galt6 expression than the ViRas mice suggesting a role for St3 Gal4 in the regulation of B4Galt6.

Tm4sf4 is a cell surface glycoprotein involved in cell proliferation and adhesion of intestinal epithelial cells. It was increased in St3ViRas mice compared to St3 controls mice

under ND. Similarly, it was as well increased in ViRas under ND compared to controls. Both in St3ViRas mice and ViRas mice, there was significantly more Tm4sf4 in the ND fed mice than in the HFD fed mice. This suggests that under HFD, the intestinal epithelial cells were less adherent than under ND.

Reg3a is a protein with similarities to the C-type lectin proteins. It is upregulated in pancreatic inflammation. Reg3a was more expressed in the St3 control mice under HFD than under ND. In the ViRas mice, there was a tendency towards a decrease in the ViRas mice compared to the controls both on HFD and ND.

Mgat4c is a glycosyltransferase, which transfer GlcNAc to N-linked glycans. This gene was significantly upregulated in the St3ViRas and ViRas mice under HFD compared to the controls or to the St3ViRas and ViRas mice under ND. This suggested more GlcNacylation in St3ViRas and ViRas mice under HFD.

Fut4, a fucosyltransferase, was overall upregulated in ViRas mice compared to St3 mice with the exception of St3ViRas mice under HFD.

Dgat1 is an acyltransferase involved in fatty acid synthesis. It was significantly upregulated in ViRas (controls and KO) under ND compared to St3 mice (controls and ViRas) under ND. It was down regulated in the ViRas compared to the controls both under ND and HFD. These results correlate with the leaner phenotype of ViRas mice under HFD compared to controls (previous results) and suggest that St3 mice have less fatty acid synthesis than ViRas mice. (Figure 4.39)

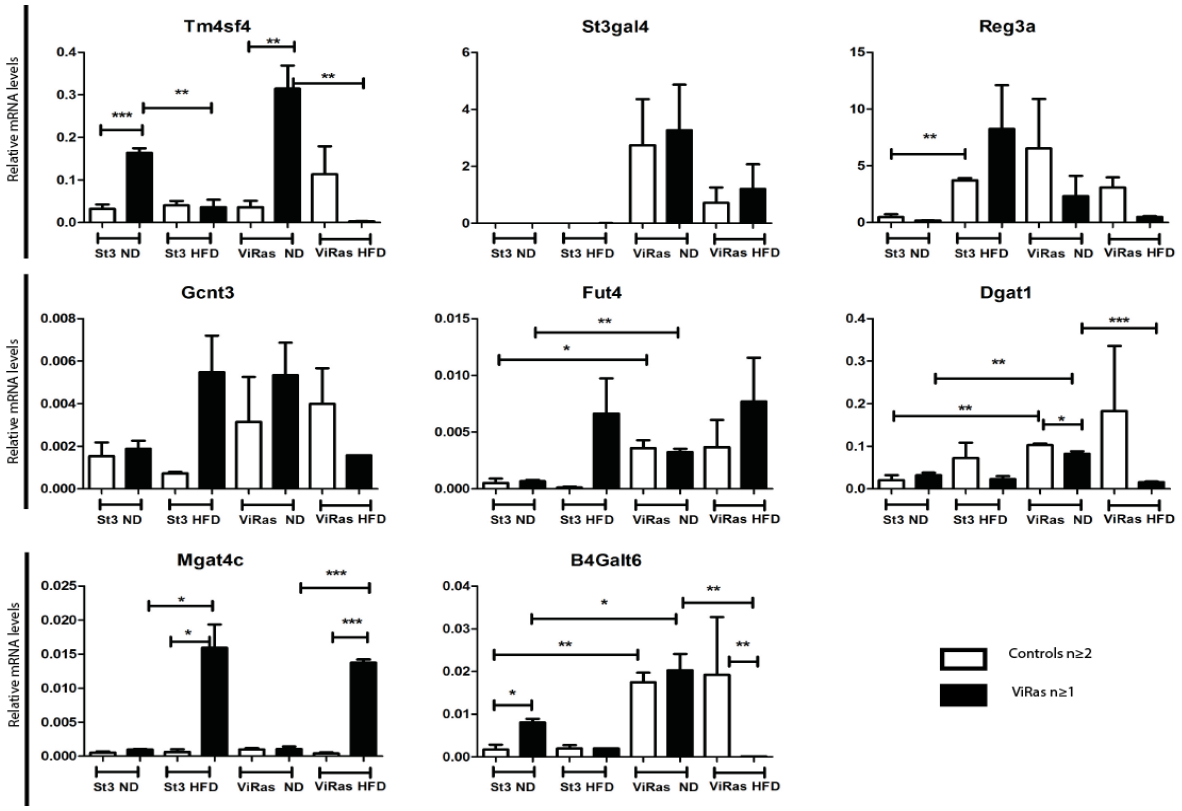

Figure 4.39: Glycosyltransferase gene expression is different between St3ViRas and ViRas mice. Real-time PCR for some genes involved in glycosylation in ViRas and St3-ViRas mice. Student's t-test, *: $p<0.05$; **: $p<0.01$; ***: $p<0.001$.

4.5 8 St3GalIV deletion has an impact on O-GlcNacylation

Age matched St3 ViRas mice had lower grade lesions compared to ViRas mice under HFD. Changes in glycosylation patterns have been shown to be present in cancer and thought to have a role to play in carcinogenesis. To determine if the glycosylation pattern in St3 ViRas mice is different than that of ViRas mice, we performed WB analysis detecting O-GlcNAcylation.

The deletion of St3GalIV gene in the whole body leads to a different glycosylation pattern. A protein around 95 kDa was less glycosylated in St3 controls and St3 ViRas mice than in ViRas mice and their controls. Moreover, there were proteins around 130 kDa and 72 kDa, which were highly glycosylated in the St3ViRas mice but not in the other groups of mice. This suggests that the deletion of a glycosyltransferase gene induces an increase in the glycosylation of proteins in the duodenum. The increased O-GlcNAcylation might be associated with the delayed carcinogenesis seen in St3ViRas mice. (Figure 4.40)

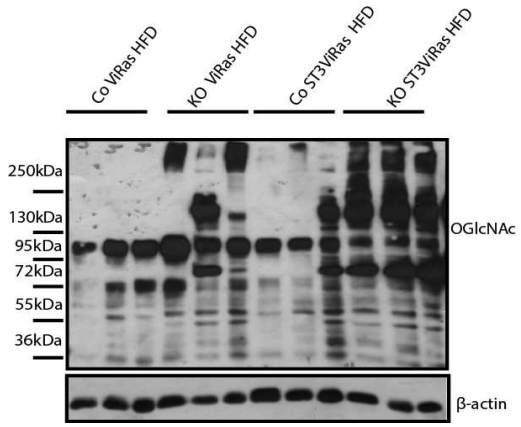

Figure 4.40: St3GalIV deletion leads to increased O-GlcNAcylation in the duodenum. O-GlcNacylation pattern of ViRas and St3 Viras mice.

4.5 9 Gallic acid protects ViRas mice against carcinogenesis

Genetic deletion of a glycosyltransferase gene leaded to a better histological score and differences in glycosylation. To determine if the pharmacological inhibition of glycosyltransferase might protect ViRas mice against carcinogenesis, we treated ViRas mice with Gallic acid, an inhibitor of fucosyltransferase 7, a protein responsible for glycosylation.

ViRas mice under HFD developed cancer more precisely in the duodenum.

Treatment with Gallic acid blocked the carcinogenesis in ViRas mice under HFD. Indeed, while treated ViRas mice showed LGIEN and HGIEN TSA and adenocarcinoma, none of the ViRas mice treated with Gallic acid showed any pathology in the small intestine. Only hyperplastic polyps were seen in the colon. Those hyperplastic polyps are not malignant and are typical feature of ViRas mice. (Figure 4.41)

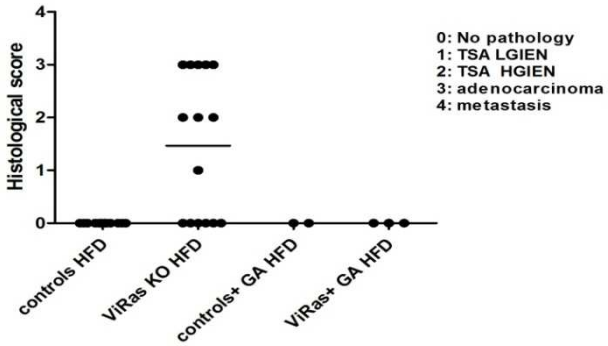

Figure 4.41: Gallic acid treatment protects against carcinogenesis. Histological score from ViRas HFD mice treated with Gallic acid and controls. Controls HFD n=7, ViRas HFD n=12, controls GA+HFD n=2, ViRas GA+HFD n=3.

4.5.10 Gallic acid, an inhibitor of Fucosyltransferase 7 does not protect against the weight loss seen in ViRas mice.

Our group showed previously that the weight of ViRas mice under HFD is significantly lower than their littermate controls. The same weight difference was found in ViRas mice treated with Gallic acid. Therefore, inhibition of Fucosyltransferase VII inhibited tumourigenesis but did not lead to a reversion of the weight difference. (Figure 4.42)

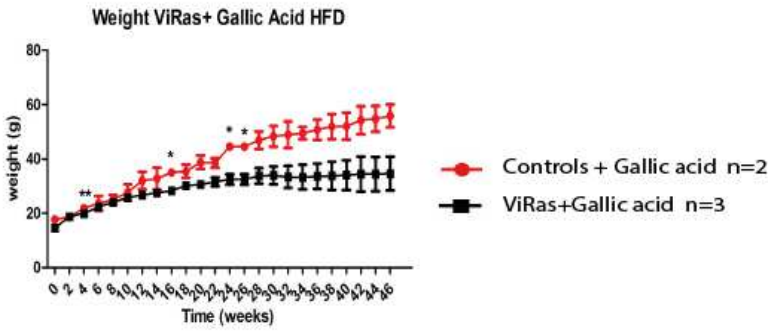

Figure 4.42: ViRas mice treated with Gallic acid remained leaner than their controls on HFD. Weight curve of female ViRas mice treated with Gallic acid under HFD. Student t-test, *: $p<0.05$, **: $p<0.01$.

4.5 11 ViRas mice treated with Gallic acid do not show any pathology or defect in mucus production in the intestine

The traditional phenotype of the histology of the colon and small intestine that is longer and serrated villi was still found in the ViRas mice treated with Gallic acid. The hyperplasia of the colon seen in ViRas mice was as well seen in ViRas mice treated with Gallic acid treatment.

Alcian blue staining revealed that the inhibition of Fucosyltransferase VII did not affect mucus production in the intestine. (Figure 4.43)

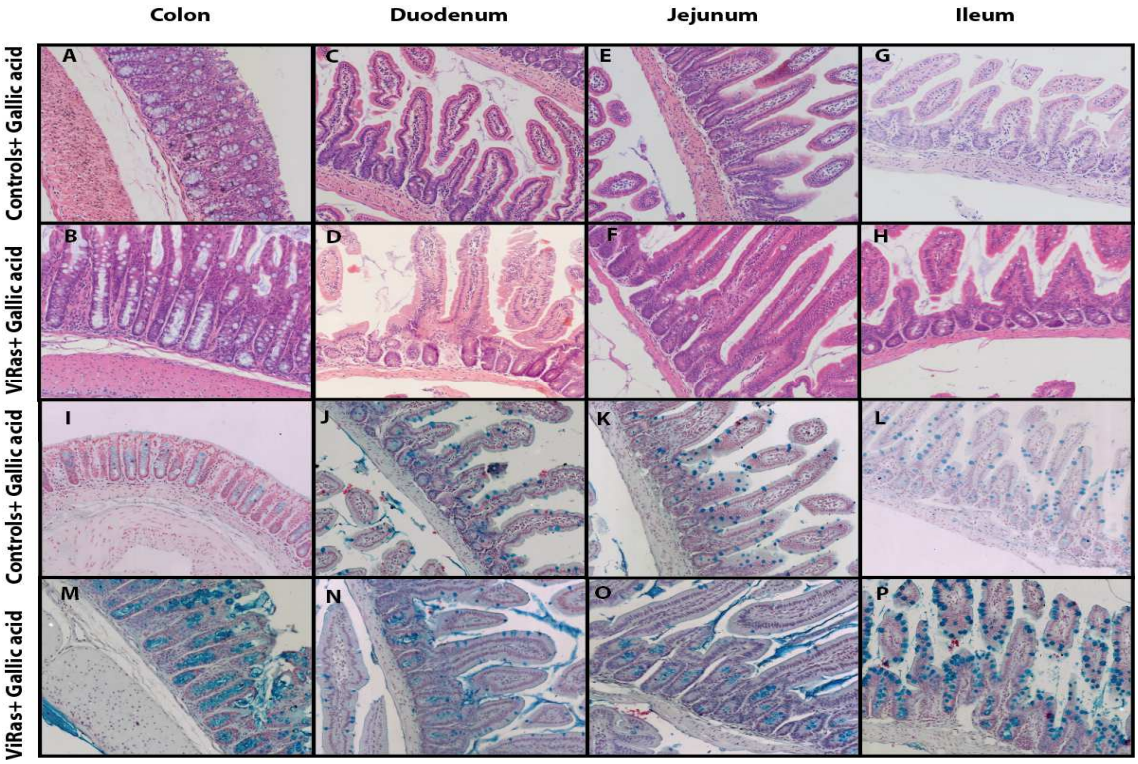

Figure 4.43: ViRas mice treated with Gallic acid had typical longer and serrated villi, hyperplasic colon and did not present any difference in mucus production. A to H: H&E staining and **I to P:** alcian blue staining of small intestine and colon of ViRas mice treated with Gallic acid and controls mice treated with Gallic acid.

4.5 12 Treatment with Gallic acid reverses anaemia seen in ViRas HFD mice

Previously we showed that accelerated tumourigenesis in ViRas mice under HFD was associated with anaemia and increased white blood cells. In order to see if Gallic acid treatment reversed anaemia as it did to tumourigenesis, we performed blood count.

The ViRas mice treated with Gallic acid were anaemic while the controls were not. However, the difference between red blood cells count between controls and KO was not significant as it was for untreated ViRas mice.

The increase in white blood cell count observed in ViRas mice under HFD was not found anymore when the mice were treated with Gallic acid. Therefore, Gallic acid treatment reversed the number of circulating lymphocytes as well as inhibited anaemia suggesting these were indeed a direct consequence of tumour development in ViRas animals. (Figure 4.44)

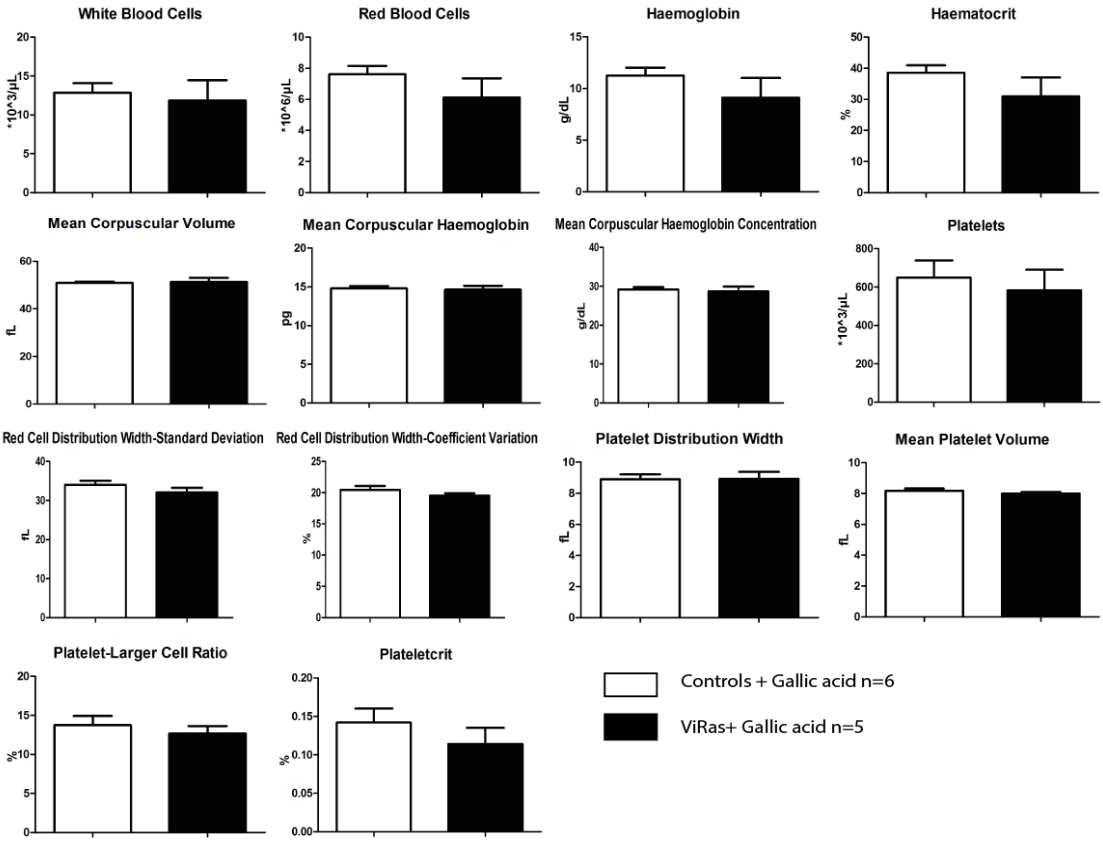

Figure 4.44: Treatment with Gallic acid correct anaemia and reverses the increased WBC counts in ViRas mice. Haemogram of ViRas mice treated with Gallic acid.

4.5 13 ViRas mice treated with Gallic acid have more O-glycosylated proteins than the other ViRas groups

In order to determine if there was a difference in the glycosylation pattern of the ViRas mice treated with Gallic acid in comparison to untreated ViRas mice, we performed Western Blot analysis.

ViRas mice treated with Gallic acid had a glycosylated protein around 95 kDa, which was not found in the others groups of mice. The same was observed for a protein around 55 kDa. Concerning the protein around 75 kDa, it seems that this protein was less glycosylated in ViRas mice after Gallic acid treatment compared to controls treated with Gallic acid.

Overall, Gallic acid seems to alter the O-glycosylated protein patterns in the duodenum. (Figure 4.45)

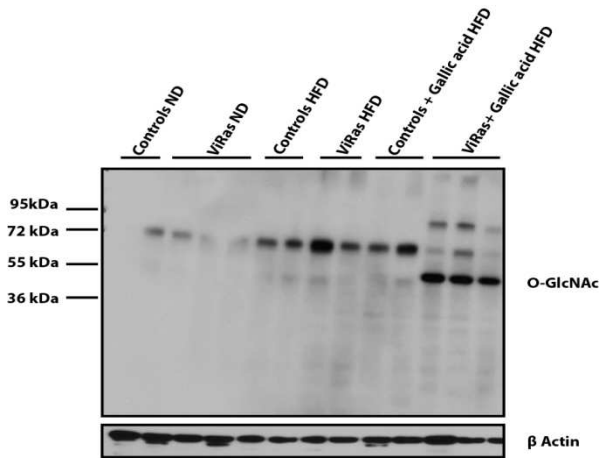

Figure 4.45: Treatment with Gallic acid leads to increased O-GlcNAcylation of proteins. Glycosylation patterns in duodenum samples from ViRas ND/HFD and ViRas mice treated with Gallic acid.

4.5.14 Oncogenic *Kras* activation in the epithelial cells of the intestine coupled with treatment with Gallic acid continue to lead to a decrease in immune responses

Inflammation is a hallmark of carcinogenesis. As our group showed that ViRas mice under HFD have a decrease in immune response in the lamina propria (LP), the peyer's patches (PP) and the mesenteric lymph nodes (MLN); we checked whether ViRas mice treated with Gallic acid with decreased tumour incidence reversed diminished immune response in the LP.

Two different sets of antibodies have been chosen. The first one in order to characterise the T cells populations, the second set to characterise antigen presenting cell populations.

CD45, a marker for haematopoietic cells is present on all cells from the myeloid or lymphoid lineage. The ViRas mice treated with Gallic acid had significantly less haematopoietic cells in the Peyer's patches than the controls. In the lamina propria and the mesenteric lymph nodes, the decrease in percentage of CD45+ cells was not significant.

CD25 is an activation marker of B and T cells. Overall, there was a tendency to a decrease in the activation of B and T cells in the ViRas mice treated with Gallic acid. In the Peyer's patches the CD45+/CD25+ cells were significantly decreased. Therefore, the immune system was less activated in the ViRas mice after Gallic acid treatment.

CD3 is a marker for T cells, CD4 a marker for T helper cells as well as for monocytes, macrophages and dendritic cells. CD8a is a marker specific for the cytotoxic T cells.

ViRas mice treated with Gallic acid had a decrease in T cell numbers in all the 3

tissues analysed: Peyer's patches, lamina propria and mesenteric lymph nodes, even if it was not always significant. CD45+/CD4+ and CD3+/CD4+ are double positive for T helper cells, were both significantly decreased in the Peyer's Patches.

The subset of cytotoxic T cells (CD45+/CD8a+ and CD3+/CD8a+ cells) was significantly decreased in PP and LP. The proportion of activated cytotoxic T cells (CD8a+/CD25+ cells) was also significantly decreased in the PP and MLN. Therefore, the Gallic acid seemed to increase the population and activation of cytotoxic T Cells. (Figure 4.46)

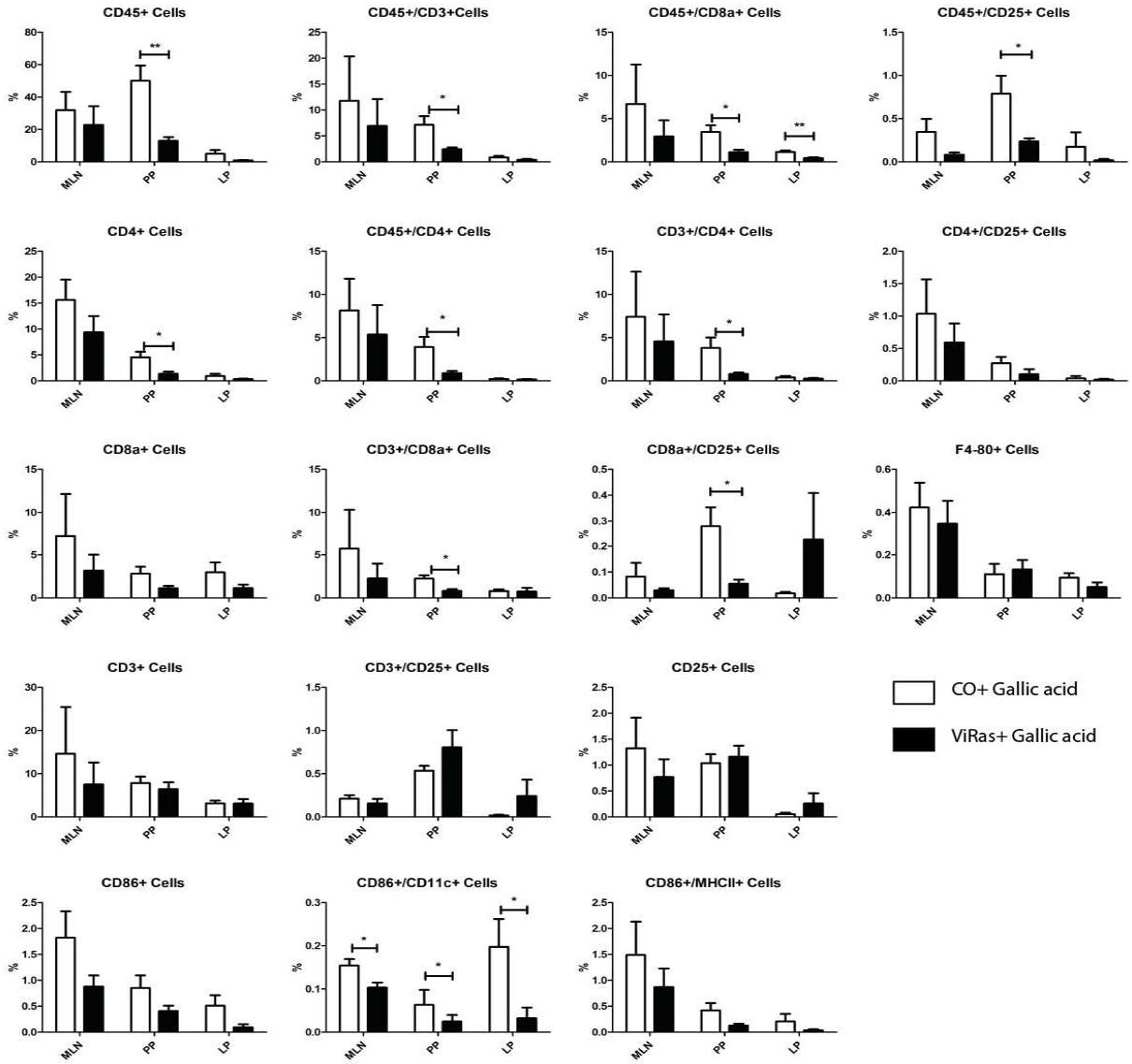

Figure 4.46: Treatment with Gallic acid induces a decrease in immune system activation. Flow cytometry analysis in the lamina propria (LP), peyer's patches (PP) and mesenteric lymph nodes (MLN) from controls and Viras mice treated with Gallic acid, controls n=5 ViRas n=5. Student's t-test, *: $p<0.05$, **: $p<0.01$.

MHCII is a marker of antigen presenting cells but MHCII is also found on lymphocytes. F4-80 is a marker for macrophages and CD11c a marker for dendritic cells.

The ViRas mice treated with Gallic acid had a significant but a similar decrease in CD11c+ dendritic cells as untreated ViRas mice on HFD. The decrease in antigen presenting dendritic cells was confirmed by the double positive cells CD86+/CD11c+ population and MHCII+/CD11c+ cells, which had a tendency to a decrease in all the tissues analysed. Concerning the macrophages, there was only a tendency towards a decrease in the ViRas mice treated with Gallic acid compared to the controls. (Figure 4.47) Interestingly, the decrease in immune system activation found previously in ViRas mice under ND and HFD compared to their littermate controls is further enhanced in the mice treated with Gallic acid. Therefore, we can conclude that the decrease in immune system activation is not responsible for tumour development in ViRas mice without Gallic acid treatment.

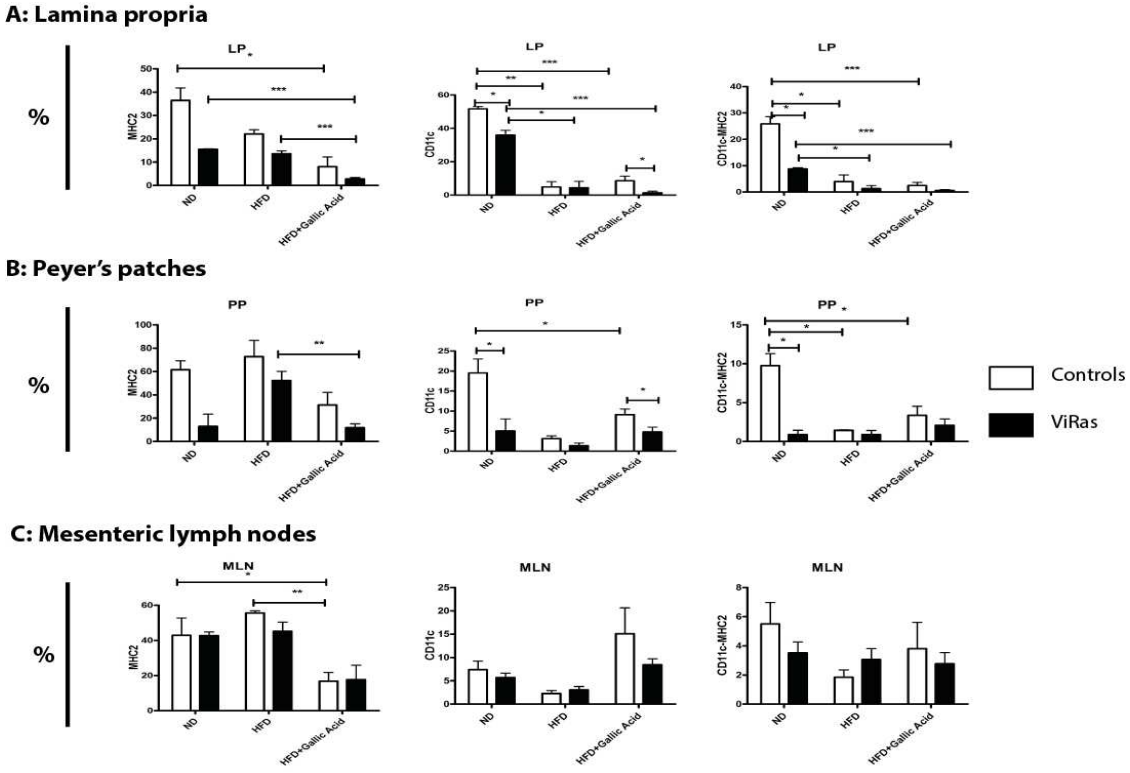

Figure 4.47: Gallic acid treatment further decrease the immune system activation seen in ViRas mice: Flow cytometry analysis from **A:** Lamina propria, **B:** Peyer's patches and **C:** mesenteric lymph nodes from controls and ViRas mice under ND, HFD and HFD + Gallic acid. ND controls n=2, ND ViRas n=2, HFD controls n=2, HFD ViRas n=2, HFD+ Gallic acid controls n=6, HFD+ Gallic acid ViRas n=5

4.5 15 Gallic acid treatment leads to a difference in the colonic gut microbiota

As it was shown previously (Schulz *et al* in revision) HFD-induces tumourigenesis was associated with a shift in the microbiota of Viras mice. Thus we wanted to know whether inhibition of carcinogenesis by Gallic acid was also related to microbial community changes. We could notice that some bacteria were present in the ViRas mice treated with Gallic acid while they were not present in the controls. (Figure 4.48) Capnocytophaga spp, Lactobacillus, Enterococcus, Proprionobacterium and Prevotella were found in the ViRas treated mice while there were not present in the controls treated mice. However, these results were achieved from *in vitro* culture system but not from 16S rRNA pyrosequencing. Therefore, it may have limitations in terms of actual changes in microbial communities.

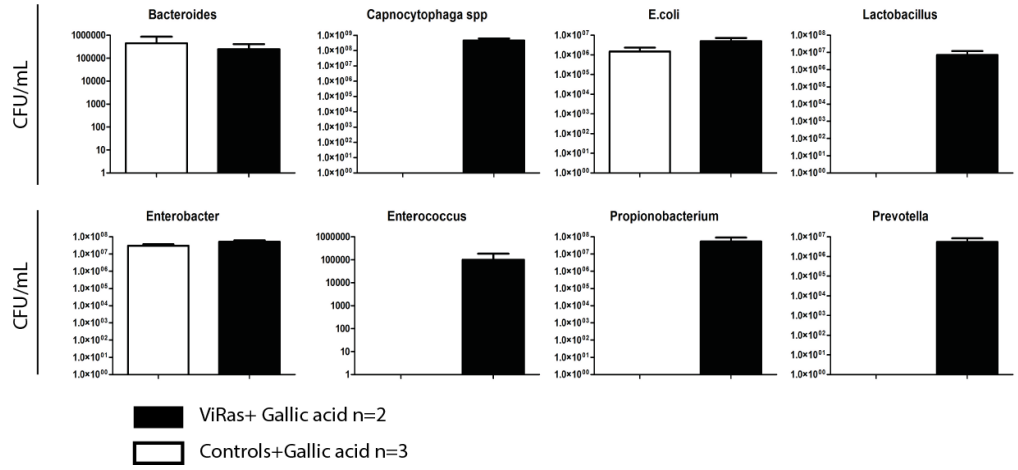

Figure 4.48: Treatment with Gallic acid provokes a change in colon microbiota. Analysis of colonic bacteria in ViRas mice treated with Gallic acid mice.

4.5 16 Treatment with ZP103 reverses the weight difference seen in ViRas mice under HFD

Acetylated Galβ1→4GlcNAcβ-O-naphthalenmethanol (ZP103) is an inhibitor of Sialyl Lewis X antigen, an important antigen for cell to cell recognition and interaction. We treated ViRas mice on HFD with ZP103 to determine if this inhibition will protect the mice from carcinogenesis.

Mice treated with ZP103 did not develop invasive cancer but only low and high grade TSA. However, the number of mice analysed was small therefore, we could not conclude that

the treatment with ZP103 decreased cancer incidence. (Figure 4.49)

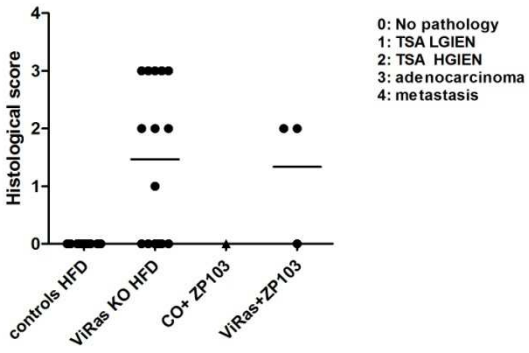

Figure 4.49: Histological score of ViRas mice treated with ZP103

Mice treated with ZP103 gained weight under HFD. However, the KO were heavier than the control. This was contrary to that seen in ViRas and ViRas mice treated with Gallic acid mice where KO were significantly leaner than controls. Therefore, treatment with ZP103 seems to reverse the weight difference of ViRas mice. (Figure 4.50)

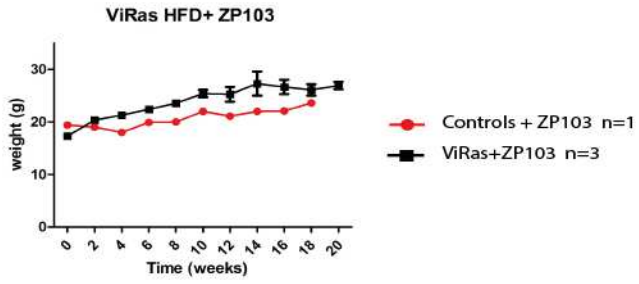

Figure 4.50: No weight difference is seen in ViRas mice treated with ZP103 compared to the controls. Weight curve of female ViRas mice and controls under HFD treated with ZP103.

4.5 17 Treatment with ZP103 disrupted colon architecture in ViRas mice

At the histological level, the architecture of the colon of the ViRas mice was destroyed. The crypts were no longer parallel to each other. The ileum of the control was also different than normal. The villi were thinner than normal and closer to each other.

In the duodenum of ViRas mice treated with ZP103 we could see some TSA HGIEN

areas but no invasive cancer. (Figure 4.51) Therefore, treatment with ZP103 seemed to delay carcinogenesis but not suppress it.

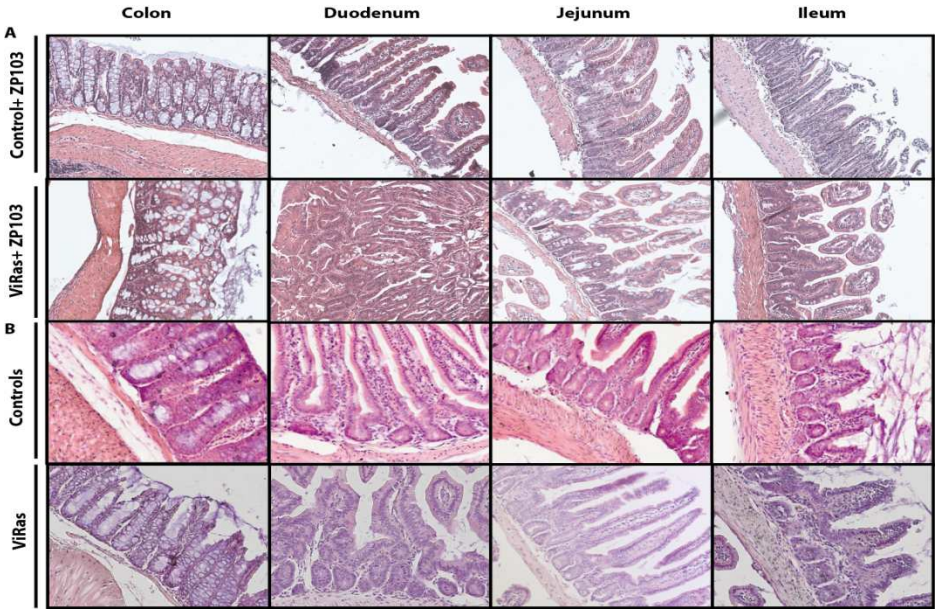

Figure 4.51: Disruption of colon architecture in mice treated with ZP103. Histology of small intestine and colon from control and ViRas mice A: treated with ZP103 and B: without ZP103.

4.5 18 Treatment with ZP103 does not affect mucus production

Both controls and ViRas mice treated with ZP103 were still abundantly producing mucus. Therefore ZP103 treatment did not affect mucus production. (Figure 4.52)

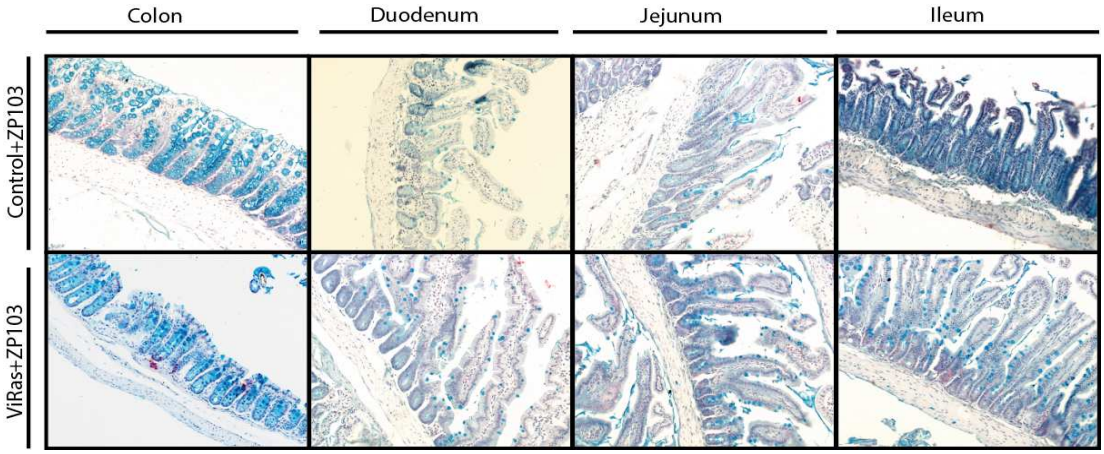

Figure 4.52: Mucus production is still present in ViRas mice treated with ZP103 mice. Alcian blue staining from ViRas mice treated withZP103 and controls+ZP103 mice.

4.5 19 Treatment with ZP103 decreases the number of platelets in the blood of the ViRas mice compared to the controls.

To evaluate whether ViRas mice treated with ZP103 similar to ViRas mice on HFD developed anaemia and showed increased WBC counts we checked whole blood cell count.

ViRas mice treated with ZP103 had a decreased platelet count than the control. They did not show anaemia as their red blood cell count although low, was still is the normal range. The increase of white blood cell count seen in ViRas mice was not either present in the mice treated with ZP103 suggesting that ZP103 was reversing typical phenotype of ViRas mice that was associated with increased tumourigenesis under HFD. (Figure 4.53) However, the number of animals was too small in order to make a final conclusion, the number of animals should be increased.

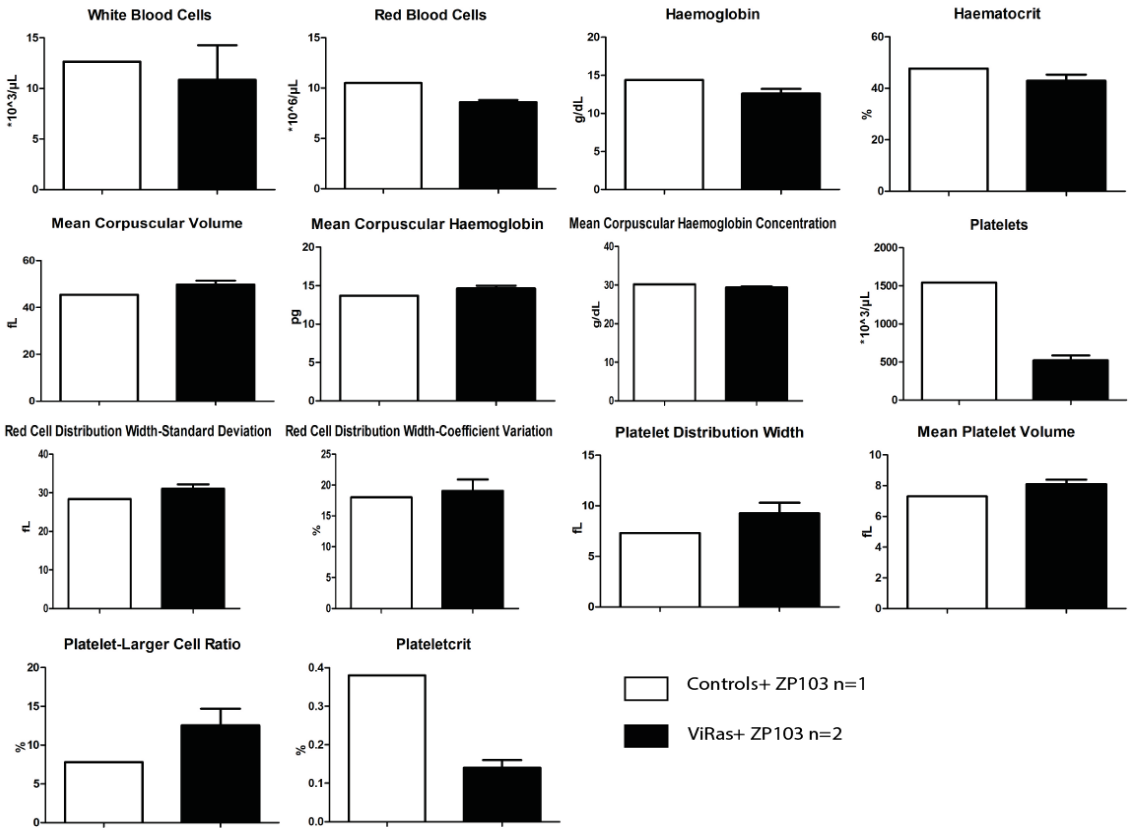

Figure 4.53: Treatment with ZP103 induces a decrease in platelet number but reverses anaemia. Haemogram of ViRas mice treated with ZP103.

4.5 20 Treatment with ZP103 does not affect colonic gut microbiota composition

As it has been shown that during obesity, cancer or diet, the microbiota is exposed to changes, we wanted to see if there was a difference in the colonic bacteria following treatment with ZP103, which appeared to decrease tumour incidence in ViRas mice after HFD. However, there was no significant difference between the control and the KO mice treated with ZP103. (Figure 4.54)

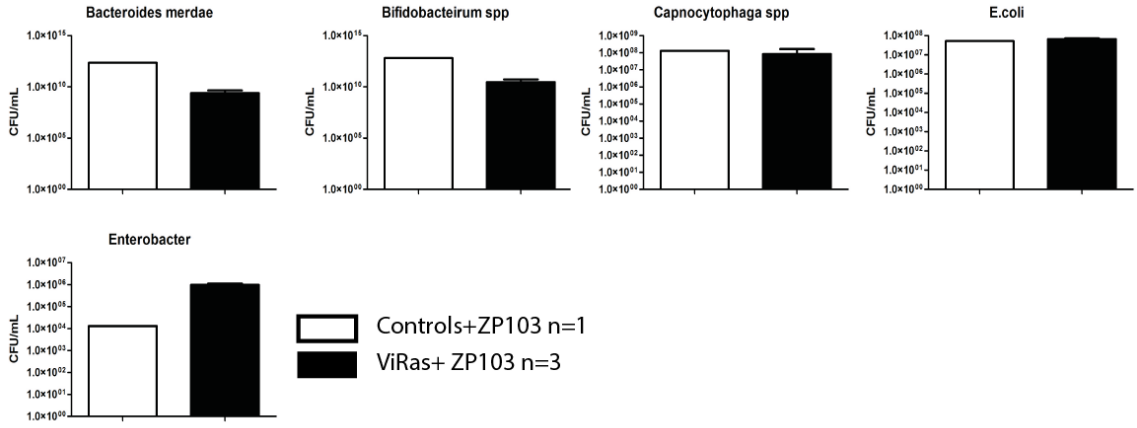

Figure 4.54: Colonic microbiota is not affected by treatment with ZP103. Bacterial analysis from colonic stool from control and ViRas mice treated with ZP103.

4.5 21 Treatment with ZP103 does slightly change O-GlcNacylation pattern

To determine glycosylation pattern, we performed WB analysis of O-GlcNacylation pattern on duodenum samples from ZP103 treated mice. The analysis showed that a protein around 72 kDa was less glycosylated in the ZP103 treated mice than in the non-treated mice. (Figure 4.55)

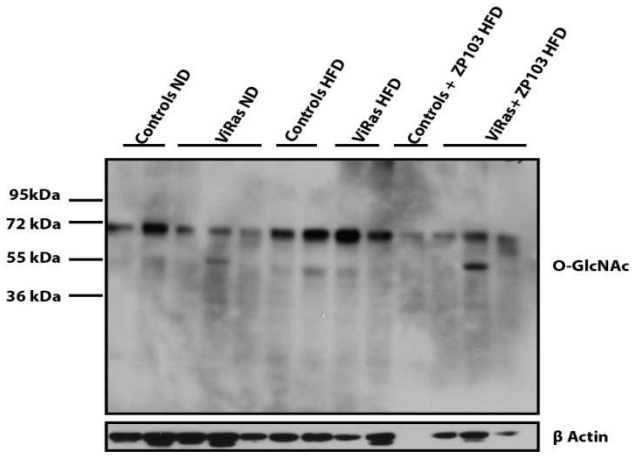

Figure 4.55: ZP103 treatment decreases O-GlcNAcylation. O-GlcNAcylation in ZP103 treated mice detected in the duodenum by western-blot.

5. DISCUSSION

Type 2 diabetes is a very common disease nowadays. While treatment is available, the molecular mechanisms underlying diabetes are not completely known. Type 2 diabetes has been shown to be a complication of obesity and inflammation and is characterised by insulin resistance and glucose intolerance. Moreover, obesity is a state of low chronic inflammation. The NF-κB pathway is a well-known inflammatory pathway responding to diverse stimuli like cytokines. Its two sub-pathways, the canonical one and the non-canonical one have different functions. The canonical NF-κB pathway has been shown to have a role in insulin sensitivity. Indeed, IKKβ is negatively regulating the insulin signalling pathway. Moreover, IKKβ deletion in liver protects mice from insulin resistance. (Arkan *et al* 2005) However, the role of the non-canonical NF-κB pathway in type 2 diabetes is not known at all.

Using conditional KO mice in the insulin sensitive tissues we assessed the role of IKKα, a component of both NF-κB pathways, in type 2 diabetes and glucose homoeostasis.

5.1 IKKα has different roles in body weight regulation in the different insulin sensitive tissues

IKKα deletion in β-cells but not muscle, exocrine pancreas or fat tissue leads to a leaner phenotype of the IKKα$^{fl/fl}$ Ins2-Cre mice both under ND and HFD. This weight difference might be a result of decreased food intake, increased energy expenditure or an increased energy release in the stools. We have shown that the energy content of the faeces was not different between IKKα$^{fl/fl}$ Ins2-Cre and IKKα$^{fl/fl}$ mice. This excludes the higher energy content of the faeces and therefore the less energy extraction from the diet as the reason for the leaner phenotype of the IKKα$^{fl/fl}$ Ins2-Cre mice.

However, mRNA level of some appetite regulating hormones had a tendency towards a decrease in IKKα$^{fl/fl}$ Ins2-Cre mice suggesting that they might eat less than the controls. However, since the Ins2 promoter is as well expressed in the brain (Song *et al* 2010), we cannot exclude that the deletion of IKKα in the brain, and more particularly in the hypothalamus, which is the place where appetite regulation takes place, may lead to the effects on appetite found in the IKKα$^{fl/fl}$ Ins2-Cre mice. In order to confirm the decreased appetite of the IKKα$^{fl/fl}$ Ins2-Cre animals, their metabolism should be analysed using metabolic cages.

Contrary to the leaner phenotype of the IKKα$^{fl/fl}$ Ins2-Cre animals, the mice having a deletion of IKKα in the fat tissue are bigger than their littermate controls under HFD. Therefore, IKKα does not regulate body weight in the exocrine pancreas or in the muscle but is important for body weight regulation in the fat tissue. In the fat tissue, IKKα deletion might increase the fat storage via the fatty acid synthesis.

5.2 IKKα deletion in the pancreas provokes an increased mitochondrial metabolism

NF-κB pathway has been shown to be involved in energy homoeostasis by up-regulating mitochondrial respiration (Mauro *et al* 2011). However, in this publication, they assessed the role of the classical pathway and not the role of the alternative pathway. Some studies investigated the role of the non-canonical pathway in mitochondrial metabolism. IKKα has been shown to promote mitochondrial biogenesis (Bakkar *et al* 2012) in skeletal muscle but so far there was no evidence of a role of IKKα in mitochondrial metabolism in the pancreas. In order to check if the reason of the leaner phenotype is higher energy expenditure, we performed RT-qPCR to assess lipid metabolism gene expression. The tendency towards an increased mitochondrial metabolism was seen by RT-PCR in the pancreas of the IKKα$^{fl/fl}$ Ins2-Cre mice suggesting that the difference in body weight is probably due to increased energy expenditure via the β-oxidation, which takes place in the mitochondria. Moreover, as we have already shown that the IKKα$^{fl/fl}$ p48-Cre mice have as well a tendency towards an increased mitochondrial metabolism, our findings show that IKKα promotes the β-oxidation in the pancreas.

5.3 IKKα in β-cells promotes insulin resistance and glucose intolerance

The improved glucose tolerance and insulin sensitivity might be due to the weight difference seen in the IKKα$^{fl/fl}$ Ins2-Cre mice. As they are leaner they might not develop diabetes and insulin resistance. However, one cannot exclude molecular mechanisms leading to a better glucose tolerance in the IKKα$^{fl/fl}$ Ins2-Cre mice. Most of the studies, which used the Ins2-Cre line to conditionally knock out genes in β-cells, showed that the deletion leads to a glucose intolerance. Those studies deleted genes involved in different pathways like insulin signalling (Kulkarni *et al* 2002; Choudhury *et al* 2005; Liu *et al* 2010; Postic *et al* 1999) and

Stat3 signalling (Gorogawa *et al* 2004; Cui *et al* 2003). However, two studies observed the contrary effect. Indeed, when knocking out FOXA2 (Sund *et al* 2001), a liver specific transcriptional activator, the mice suffered from a severe hypoglycaemia and a high secretion of insulin relative to the hypoglycaemia seen in those mice. The FOXA2 KO mice have a growth defect and do not survive after weaning. Interestingly, FOXA2 has been shown to be a target of IKKα (Liu *et al* 2012) after TNFα stimulation. Its phosphorylation by IKKα inactivates FOXA2. Therefore, it seems that deleting FOXA2 or its upstream kinase IKKα leads overall to the same effects even if the consequences of IKKα deletion in β-cells are not as dramatic as the deletion of FOXA2. The fact that IKKα phosphorylates FOXA2 upon stimulation by TNFα shows that the canonical NF-κB is involved in this regulation. The second study which showed an improvement in the glucose tolerance of the Ins2-Cre mice is the study by Liu *et al* in 2010 where they conditionally knocked out GSK3β from the β-cells. In that case, the improvement of glucose tolerance is due to an increase in β-cells mass via the PI3K/Akt pathway. However, in our study, the mice do not have a difference in β-cells mass; therefore, another mechanism is responsible for the lean phenotype of our mice.

More evidences point out a role of the NF-κB canonical pathway in body weight regulation and insulin sensitivity. Indeed, Tang *et al* showed that over-expression of p65 or knock down of p50 increases energy expenditure. (Tang *et al* 2010) Moreover, IKKε KO mice are leaner and more glucose tolerant than their controls (Chiang *et al* 2009). IKKε is a downstream effector of the PI3K-Akt pathway which targets the NF-κB pathway by phosphorylating IκBα or p65. A recent study showed that the pharmacological inhibition of IKKε and TBK1, a protein that can act as a NF-κB effector, provokes a weight loss and an improved insulin sensitivity in diet induced obesity mouse models (Reilly *et al* 2013). Moreover, this effect is independent of food intake. IKKα is a known kinase which as well phosphorylates IκBα. In our IKKα$^{fl/fl}$ Ins2-Cre mice we see the same phenotype than Chiang *et al* in the IKKε KO mice. Therefore, one can speculate that the same mechanism is used in both KO mice. IκBα and p65 are members of the canonical NF-κB pathway; therefore it suggests that the effect seen in the IKKα$^{fl/fl}$ Ins2-Cre mice is probably linked to the role of IKKα in the canonical pathway and not to its role in the alternative pathway.

Moreover, the IKKα$^{fl/fl}$ Ins2-Cre mice secrete overall less insulin than the controls, both during the GTT and during the time of the HFD feeding. This shows that the IKKα$^{fl/fl}$ Ins2-Cre mice require less insulin to regulate their glycaemia. Therefore, the IKKα$^{fl/fl}$ Ins2-Cre mice are more insulin sensitive than the controls. The IKKα$^{fl/fl}$ mice have a circulating level of insulin higher than the normal range of 0.4±0.1 ng/mL (Murphy *et al* 1997) showing

hyperinsulinaemia and insulin resistance while the IKKα$^{fl/fl}$ Ins2-Cre mice have an insulin secretion within the normal range. The deletion of IKKα in the other tissues leads to hyperinsulinaemia. However, the IKKα$^{fl/fl}$ Ckmm-Cre mice are insulin resistant while the IKKα$^{fl/fl}$ Fabp4-Cre and the IKKα$^{fl/fl}$ p48-Cre mice remain insulin sensitive. Moreover, the IKKα$^{fl/fl}$ Ckmm-Cre mice are insulin resistant while their controls are still insulin sensitive. Concerning the IKKα$^{fl/fl}$ Fabp4-Cre and IKKα$^{fl/fl}$ p48-Cre mice, both controls and KO show the same phenotype even if IKKα$^{fl/fl}$ Fabp4-Cre mice secrete more insulin than the controls. These results show that IKKα in the muscle is important for insulin sensitivity while it does not change the phenotype when deleted in the fat tissue or in the exocrine pancreas.

5.4 IKKα deletion in the fat tissue provokes kidney problems

Surprisingly, the IKKα$^{fl/fl}$ Fabp4-Cre mice developed kidneys problems. Fabp4 promoter is slightly expressed in the kidneys (Elmasri *et al* 2009) and therefore, the deletion of IKKα in the kidney might be the reason why the animals had cystic kidneys. However, we showed that the IKKα protein is still expressed in the abnormal kidneys of the IKKα$^{fl/fl}$ Fabp4-Cre mice. Therefore, the kidney problems are not due to a deletion of IKKα in the kidneys. The abnormal kidneys also have much more proliferation than the controls and the normal kidneys. They also have more infiltration of F4-80 and GR1 positive cells showing increased inflammation of the kidneys. In the abnormal kidneys, there are more IKKα positive cells than in the normal ones correlating with the increased infiltration and proliferation. Overall, inflammation is increased in the IKKα KO mice. Indeed, we have seen increased inflammation in the kidneys of the IKKα$^{fl/fl}$ Fabp4-Cre mice and the Ins2-IKKα mice have increased inflammation in the pancreas and in the fat tissue. The kidneys problems are probably due to the increased inflammation. Chronic kidney disease is a medical complication of obesity (Kalaitzidis and Siamopoulos 2011). In our model, we cannot exclude that the kidney problem encountered is a consequence of the obesity state. However, there is a higher incidence of those problems in IKKα$^{fl/fl}$ Fabp4-Cre fed on a ND mice than the HFD. This cannot be explained by the obesity status as the ND mice are leaner. Therefore, IKKα in the fat tissue seems to be responsible for the kidney disease seen in our mice.

We showed that IKKα has a variable role in the different insulin sensitive tissues. In the β-cells it seems that IKKα is very important for the regulation of blood glucose levels and for insulin sensitivity. IKKα promotes insulin resistance and hyperglycaemia as its deletion

leads to insulin sensitivity.

5.5 Glycosylation changes in intestinal cancer

Obesity leads to different medical complications such cancer or diabetes. Among obesity associated cancers, colorectal cancer is one of the most frequent. On the contrary, intestinal cancer is a very rare type of cancer which has been shown to have the same sequence of mutations as the colorectal cancer. As part of it, the oncogene *Kras* is important in the setting of carcinogenesis in both colorectal and small intestinal cancer (Delaunoit *et al* 2005). Therefore, in order to study the intestinal cancer, mice bearing an activation of *Kras* in the intestinal epithelial cells were used in our study (ViRas mice).

Glycosylation is a very important post translational modification required for, among others, cell interaction or immune system recognition. It has been shown that modifications in the glycosylation pattern occur in cancer. We therefore treated ViRas mice with Gallic acid, an inhibitor of fucosyltransferase VII or ZP103, an inhibitor of sialyl lewis X antigen to see if the glycosylation inhibition protects the mice from carcinogenesis. We assessed the differences in the O-GlcNAcylation pattern in treated mice to see if the inhibition of glycosylation leads to any changes in O-GlcNAcylation. Moreover, we checked the effect of a genetic deletion from a glycosyltransferase gene on carcinogenesis.

5.6 St3GalIV deletion in ViRas mice delayed carcinogenesis

Microarray results showed a difference in glycosyltransferase gene expression between ViRas mice under ND and HFD. The St3GalIV gene was the gene with the biggest up regulation in the ViRas HFD mice. There are some evidences that overexpression of sialyltransferase genes increases the cell motility and the metastatic potential of the cells. (Pérez-Garay *et al* 2010) Therefore, we thought that the deletion of St3GalIV gene would lead to the contrary effect, which means, a decrease in the incidence of invasive carcinoma. The genetic deletion of the St3GalIV gene in ViRas mice (St3ViRas mice) led to a delayed carcinogenesis in comparison to the ViRas mice but did not rescue completely the carcinogenesis. Therefore, it seemed that the deletion of a glycosyltransferase gene leads to a delayed carcinogenesis. This result correlates with the fact that overexpression of sialyltransferase gene enhances metastatic potential of the cells (Pérez-Garay *et al* 2010) and

that an over-expression of St3GalIV in gastric cancer cells increase the invasive phenotype (Gomes *et al* 2013). We further confirmed microarray results by RT-PCR using St3ViRas mice. Some other glycosyltransferase genes like Dgat1, Fut4 or B4Galt6 have a different expression in St3ViRas and ViRas mice. This effect might be a compensatory mechanism or St3GalIV might regulate directly those genes.

Moreover, a study showed that inhibitor of O-glycan leads to growth inhibition in colon cancer cell line (Patsos *et al* 2009). St3GalIV is implicated in both N and O-glycosylation (Varki *et al* Essential of glycobiology chapter 13). Therefore, as deletion of St3GalIV delays carcinogenesis our result correlates with the results of other groups.

5.7 St3GalIV deletion provokes an increased O-GlcNAcylation

O-GlcNAcylation has been proved to have a role in cancer progression. (Slawson and Hart 2011) Some studies showed that O-GlcNAcylation is decreased in tumour samples (Slawson *et al* 2001) while some other found out the contrary; an increase of O-GlcNAcylation in tumour tissues (Gu *et al* 2010; Mi *et al* 2011). To check whether the deletion of St3GalIV induces changes in the O-GlcNAcylation pattern, we first assessed the differences in O-GlcNAcylation in ViRas mice under ND and HFD. We showed that mice under HFD have more O-GlcNAcylation than under ND. Under HFD, there is a slight difference between controls and KO. When comparing the results of St3ViRas mice, we can notice that St3ViRas mice have more O-GlcNAcylation than ViRas mice. It seems that increase in O-GlcNAcylation is sometimes a feature of cancer (Slawson and Hart 2011) and is implicated in epithelial-mesenchymal transition process, which transform epithelial cell into mesenchymal cells with migratory and invasion properties. However, our study showed that St3ViRas mice have an increase in O-GlcNAcylation but the mice do have a delayed carcinogenesis. Mgat4c, which gene expression was shown to be up-regulated by microarray and RT-PCR suggests that the N-GlcNAcylation is as well increased in the St3ViRas mice.

5.8 Treatment of ViRas mice with Gallic acid delays carcinogenesis

When treating the ViRas mice with a pharmacological inhibitor of Fucosyltransferase VII, the Gallic acid, (Niu *et al* 2004) the mice did not develop cancer. Moreover, the mice were not anaemic, in contrast to untreated ViRas mice (Schulz *et al* unpublished data). ViRas

mice under HFD and treated with Gallic acid do not develop cancer while ViRas mice fed with HFD develop tumours in the duodenum. The histology of intestine from ViRas mice treated with Gallic acid is normal apart from some hyperplasic polyps in the colon, which are not malignant. Therefore, treatment with Gallic acid protects the mice from carcinogenesis. This correlates with other studiesthat suggests an anti-carcinogenic effect of Gallic acid principally in cancer cell lines. (Ho *et al* 2010) Nevertheless, we cannot exclude that the protective effect of Gallic acid is not related to the inhibition of fucosyltransferase but rather to another effect of Gallic acid such as enhancing apoptosis (Serrano *et al* 1998).

Mice treated with Gallic acid show as well more O-GlcNAcylation than ViRas mice without treatment. Therefore, in our case, the hyper-O-GlcNAcylation seems to correlate with a delayed carcinogenesis contrary to the studies, which found that hyper O-GlcNAcylation is a feature of cancer (Ma and Vosseller 2013). When treating ViRas mice with ZP103, an inhibitor of Sialyl Lewis X formation, the mice still develop TSA. Moreover, they have less O-GlcNAcylation than the other groups. This result is in agreement with our results, which shows that mice with more O-GlcNAcylation have a delayed carcinogenesis.

In our study, we show that there is more O-GlcNAcylation in mice bearing an activation of *Kras* and glycosyltransferase inhibition whether genetic (St3ViRas) or pharmacological (ViRas+ Gallic acid) correlating with the results of Slawson *et al* in 2001. As the increase in O-GlcNAcylation is only seen in mice with *Kras* activation, which were kept under HFD, we can conclude that *Kras* activation coupled with HFD is responsible for the effect on glycosylation when glycosyltransferase is inhibited. This result matches the result of the microarray data, which as well showed an increase in glycosyltransferase genes expression.

So far, no link between Gallic acid and O-GlcNAcylation modification has been depicted. Our study shows that treatment of ViRas mice bearing an activation of the oncogene *Kras*, with Gallic acid have a different pattern of O-GlcNAcylation in the duodenum than their controls. The O-GlcNAcylation pattern of ViRas mice and their controls is quite similar. As the difference is only found in ViRas mice treated with Gallic acid and not in the controls, this leads to the hypothesis that Gallic acid needs *Kras* activation to change the O-GlcNAcylation pattern. As the Gallic acid treated mice do not develop tumours, we can conclude that this modification of O-GlcNAcylation provokes at least partially the non-carcinogenic phenotype seen in the treated mice. One can also suggest that Gallic acid inhibits carcinogenesis and this inhibition provokes a change in the glycosylation pattern. This hypothesis is supported by the fact that control mice treated with Gallic acid have the same O-

GlcNAcylation pattern than ViRas and controls mice without Gallic acid treatment. Still the number of animals should be increased before drawing final conclusion.

5.9 Gallic acid treatment enhances the immune system down modulation seen in ViRas mice

Previous results showed that ViRas mice under HFD had a decrease in immune system activation with a down regulation of CD11c+cells (Schulz *et al* unpublished data). The flow cytometry analysis of ViRas mice treated with Gallic acid mice showed that the T -cells subset was decreased in ViRas compared to the controls. The dendritic cells were as well decreased suggesting that the immune system is down modulated. When comparing the results of ViRas+Gallic acid with the results of ViRas mice, we can notice that in the ViRas+ Gallic acid mice, the decrease in CD11c+ and MHCII+ cells is further enhanced compared to the ViRas untreated mice. Therefore, the treatment with Gallic acid does not reverse this down modulation. The anti-carcinogenic effect of Gallic acid is thus not due to an activation of the immune system which eliminates the tumour cells. ViRas mice under HFD develop more tumours than under ND and have a decrease in immune system activation. Therefore, it seems that *Kras* coupled to HFD provokes an immune escape of the cancer cells. In the Gallic acid treated ViRas mice, the mice do not develop tumours and have a further decrease of immune system activation. Moreover, they show more glycosylation than the ViRas mice without treatment. Therefore, in our model of ViRas+ Gallic acid, the immune system is further down regulated leading to think that the immune escape is more present than in untreated mice. However, the Gallic acid treated mice do not develop tumours. They as well present more glycosylation than the untreated mice. Consequently, one can suggest that *Kras* activation coupled to HFD provokes immune escape via down regulation of the immune system and that Gallic acid, by changing the glycosylation pattern provokes an enhancement of the immune system efficacy even if the down modulation of the immune system is still present. This improved immune system is efficient enough to eliminate the cancer cells and therefore, the mice do not develop tumours. However, we cannot exclude that Gallic acid provokes a tumour decrease and then a change in the glycosylation pattern.

The treatment with ZP103 as well led to changes in glycosylation. However, while treatment with Gallic acid increased the O-GlcNAcylation pattern, the treatment with ZP103 decreased it. Moreover, the treatment with ZP103 still leaded to presence of TSA and therefore did not protect against carcinogenesis. Therefore our hypothesis that glycosylation

changes and more especially increased O-GlcNAcylation, seems to be confirmed by the ZP103 treatment.

During intestinal cancer, *Kras* activation cooperates with HFD to develop carcinogenesis and down modulates immune system. The genetic deletion or pharmacological inhibition of some glycosyltransferase leads to an increase of O-GlcNAcylation and delayed carcinogenesis. The changes in glycosylation pattern might be the reason for the delayed carcinogenesis seen in these mice. Therefore, targeting glycosyltranferase in intestinal cancer in order to up-regulate the O-GlcNAcylation may be useful in clinic. However, as we started the treatment before the mice developed cancer, we cannot assure that targeting glycosyltransferase will eliminate or reduce tumours. Further studies, such that the treatment starts when the mice have already tumours are needed to assess this possibility.

6. CONCLUSION

In our study we could show that IKKα, a key kinase of the NF-κB pathway has different roles in the diverse insulin sensitive tissues. However, overall IKKα seems important for body weight regulation as well as for glucose tolerance. Moreover, in the endocrine pancreas, IKKα seems to affect body weight regulation via an increased mitochondrial metabolism, resulting in increased energy expenditure. Nevertheless, a decrease in appetite could as well result in the leaner phenotype of the IKKα$^{fl/fl}$ Ins2-Cre mice via the expression of the Ins2 promoter in the brain and more particularly in the hypothalamus, which is the centre of appetite regulation. Surprisingly, the deletion of IKKα in the fat tissue provokes kidneys problems, which are not due to a deletion of IKKα in the kidneys showing that IKKα has as well paracrine effects. The mechanism leading to kidney problem could not be determined.

In conclusion, IKKα is important for body weight regulation and glucose tolerance, revealing a new aspect of IKKα function and a role of the non-canonical NF-κB pathway in diabetes. Moreover, we highlighted that IKKα can as well act via a paracrine mechanism on the kidneys. IKKα is also a regulator of the mitochondrial metabolism in the pancreas, which can explain the weight difference.

We could show that during intestinal carcinogenesis, the expression of glycosyltransferase genes is increased. By genetic deletion or pharmacological inhibition of specific glycosyltransferases, the carcinogenesis is delayed and the O-GlcNAcylation pattern is altered. Therefore, our study showed that the glycosyltransferases are important for the development of tumours. Changes in O-GlcNAcylation pattern is as well an important factor for the carcinogenesis. Moreover, the inhibition of FuT VII by Gallic acid as well promotes a further enhanced down regulation of the immune system compared to the ViRas mice without Gallic acid treatment. Consequently, the proposed mechanism is that deletion or inhibition of specific glycosyltransferase causes an increased O-GlcNAcylation, which then can lead to an increased immune system efficacy, even with the down modulation seen, and therefore delayed carcinogenesis. Alternatively, the dampened immune responses may be independent of increased tumour incidence but rather a phenomenon associated with oncogene activation. Our study shows that the targeting of glycosyltransferase can be important in the treatment of cancer. However, we as well showed that not all the glycosyltransferases can be inhibited to

delay carcinogenesis as the inhibition of Sialyl Lewis X antigen did not result in delayed carcinogenesis. Moreover, we treated the mice before the development of tumours starting from the age of 6 weeks. In order to use glycosyltransferase inhibitors for cancer treatment, some studies need to be done by treating the mice after the beginning of tumour initiation and promotion to see if the treatment induces a regression of the tumour. However, our results still suggest a critical role for changes in glycosylation patterns and raised the possibility of using glycosyltransferase inhibitors during diet-associated tumour progression

7. REFERENCES

A

Abdul-Ghani, M.A., and DeFronzo, R.A. (2010). Pathogenesis of insulin resistance in skeletal muscle. Journal of biomedicine & biotechnology *2010*, 476279.

Adamczyk, B., Tharmalingam, T., and Rudd, P.M. (2012). Glycans as cancer biomarkers. Biochimica et biophysica acta *1820*, 1347-1353.

Agarwal, E., Brattain, M.G., and Chowdhury, S. (2013). Cell survival and metastasis regulation by Akt signaling in colorectal cancer. Cellular signalling *25*, 1711-1719.

Aghajan, M., Li, N., and Karin, M. (2012). Obesity, autophagy and the pathogenesis of liver and pancreatic cancers. Journal of gastroenterology and hepatology *27 Suppl 2*, 10-14.

Anandkumar, A., and Devaraj, H. (2013). Tumour immunomodulation: mucins in resistance to initiation and maturation of immune response against tumours. Scandinavian journal of immunology *78*, 1-7.

Antuna-Puente, B., Feve, B., Fellahi, S., and Bastard, J.P. (2008). Adipokines: the missing link between insulin resistance and obesity. Diabetes & metabolism *34*, 2-11.

Arber, N., Gammon, M.D., Hibshoosh, H., Britton, J.A., Zhang, Y., Schonberg, J.B., Roterdam, H., Fabian, I., Holt, P.R., and Weinstein, I.B. (1999). Overexpression of cyclin D1 occurs in both squamous carcinomas and adenocarcinomas of the esophagus and in adenocarcinomas of the stomach. Human pathology *30*, 1087-1092.

Arkan, M.C., Hevener, A.L., Greten, F.R., Maeda, S., Li, Z.W., Long, J.M., Wynshaw-Boris, A., Poli, G., Olefsky, J., and Karin, M. (2005). IKK-beta links inflammation to obesity-induced insulin resistance. Nature medicine *11*, 191-198.

B

Bakkar, N., Ladner, K., Canan, B.D., Liyanarachchi, S., Bal, N.C., Pant, M., Periasamy, M., Li, Q., Janssen, P.M., and Guttridge, D.C. (2012). IKKalpha and alternative NF-kappaB regulate PGC-1beta to promote oxidative muscle metabolism. The Journal of cell biology *196*, 497-511.

Barthel, S.R., Gavino, J.D., Descheny, L., and Dimitroff, C.J. (2007). Targeting selectins and selectin ligands in inflammation and cancer. Expert opinion on therapeutic targets *11*, 1473-1491.

Bastard, J.P., Maachi, M., Lagathu, C., Kim, M.J., Caron, M., Vidal, H., Capeau, J., and Feve, B. (2006). Recent advances in the relationship between obesity, inflammation, and insulin resistance. Eur Cytokine Netw *17*, 4-12.

Baud, V., and Karin, M. (2009). Is NF-kappaB a good target for cancer therapy? Hopes and pitfalls. Nature reviews Drug discovery *8*, 33-40.

Bennecke, M., Kriegl, L., Bajbouj, M., Retzlaff, K., Robine, S., Jung, A., Arkan, M.C., Kirchner, T., and Greten, F.R. (2010). Ink4a/Arf and oncogene-induced senescence prevent tumor progression during alternative colorectal tumorigenesis. Cancer cell *18*, 135-146.

Bjornholm, M., Kawano, Y., Lehtihet, M., and Zierath, J.R. (1997). Insulin receptor substrate-1 phosphorylation and phosphatidylinositol 3-kinase activity in skeletal muscle from NIDDM subjects after in vivo insulin stimulation. Diabetes *46*, 524-527.

Blander, J.M., Visintin, I., Janeway Jr. , C., and Medzhitov, r. (1999). α(1,3)-Fucosyltransferase VII and α(2,3)-Sialyltransferase IV Are Up-Regulated in Activated CD4 T

Cells and Maintained After Their Differentiation into Th1 and Migration into Inflammatory Sites.

Bonizzi, G., and Karin, M. (2004). The two NF-kappaB activation pathways and their role in innate and adaptive immunity. Trends in immunology *25*, 280-288.

Brüning, J.C., Michael, M.D., Winnay, J.N., Hayashi, T., Hörsch, D., Accili, D., Goodyear, L.J., and Kahn, C.R. (1998). A Muscle-Specific Insulin Receptor Knockout Exhibits Features of the Metabolic Syndrome of NIDDM without Altering Glucose Tolerance. Molecular Cell *2*, 559-569.

C

Capurso, C., and Capurso, A. (2012). From excess adiposity to insulin resistance: the role of free fatty acids. Vascular pharmacology *57*, 91-97.

Carmen, G.Y., and Victor, S.M. (2006). Signalling mechanisms regulating lipolysis. Cellular signalling *18*, 401-408.

Chariot, A. (2009). The NF-kappaB-independent functions of IKK subunits in immunity and cancer. Trends in cell biology *19*, 404-413.

Chen, H., Charlat, O., Tartaglia, L.A., Woolf, E.A., Weng, X., Ellis, S.J., Lakey, N.D., Culpepper, J., More, K.J., Breitbart, R.E., *et al.* (1996). Evidence That the Diabetes Gene Encodes the Leptin Receptor: Identification of a Mutation in the Leptin Receptor Gene in db/db Mice. Cell *84*, 491-495.

Chiang, S.H., Bazuine, M., Lumeng, C.N., Geletka, L.M., Mowers, J., White, N.M., Ma, J.T., Zhou, J., Qi, N., Westcott, D., *et al.* (2009). The protein kinase IKKepsilon regulates energy balance in obese mice. Cell *138*, 961-975.

Choi, K., and Kim, Y.B. (2010). Molecular mechanism of insulin resistance in obesity and type 2 diabetes. The Korean journal of internal medicine *25*, 119-129.

Choudhury, A.I., Heffron, H., Smith, M.A., Al-Qassab, H., Xu, A.W., Selman, C., Simmgen, M., Clements, M., Claret, M., Maccoll, G., *et al.* (2005). The role of insulin receptor substrate 2 in hypothalamic and beta cell function. The Journal of clinical investigation *115*, 940-950.

Colomb, F., Krzewinski-Recchi, M.A., El Machhour, F., Mensier, E., Jaillard, S., Steenackers, A., Harduin-Lepers, A., Lafitte, J.J., Delannoy, P., and Groux-Degroote, S. (2012). TNF regulates sialyl-Lewisx and 6-sulfo-sialyl-Lewisx expression in human lung through up-regulation of ST3GAL4 transcript isoform BX. Biochimie *94*, 2045-2053.

Cryer, P.E. (2007). Hypoglycemia, functional brain failure, and brain death. The Journal of clinical investigation *117*, 868-870.

Cui, Y., Huang, L., Elefteriou, F., Yang, G., Shelton, J.M., Giles, J.E., Oz, O.K., Pourbahrami, T., Lu, C.Y.H., Richardson, J.A., *et al.* (2003). Essential Role of STAT3 in Body Weight and Glucose Homeostasis. Molecular and Cellular Biology *24*, 258-269.

D

de Luca, C., and Olefsky, J.M. (2009). Inflammation and insulin resistance. FEBS letters *582*, 97-105.

Delaunoit, T., Neczyporenko, F., Limburg, P.J., and Erlichman, C. (2005). Pathogenesis and risk factors of small bowel adenocarcinoma: a colorectal cancer sibling? The American journal of gastroenterology *100*, 703-710.

Dohm, G.L., Elton, C.W., Friedman, J.E., Pilch, P.F., Pories, W.J., Atkinson, S.M., Jr., and Caro, J.F. (1991). Decreased expression of glucose transporter in muscle from insulin-resistant patients. The American journal of physiology *260*, E459-463.

Downward, J. (2003). Targeting RAS signalling pathways in cancer therapy. Nature reviews Cancer *3*, 11-22.

DS, N., and LF, S. (1960). Amino-acid sequence of human insulin. Nature, 483-485.

E

Ebert, D., Haller, R.G., and Walton, M.E. (2003). Energy contribution of octanoate to intact rat brain metabolism measured by 13C nuclear magnetic resonance spectroscopy. The Journal of neuroscience : the official journal of the Society for Neuroscience *23*, 5928-5935.

Eldor, R., Yeffet, A., Baum, K., Doviner, V., Amar, D., Ben-Neriah, Y., Christofori, G., Peled, A., Carel, J.C., Boitard, C., *et al.* (2006). Conditional and specific NF-kappaB blockade protects pancreatic beta cells from diabetogenic agents. Proceedings of the National Academy of Sciences of the United States of America *103*, 5072-5077.

Ellies, L.G., Ditto, D., Levy, G.G., Wahrenbrock, M., Ginsburg, D., Varki, A., Le, D.T., and Marth, J.D. (2002a). Sialyltransferase ST3Gal-IV operates as a dominant modifier of hemostasis by concealing asialoglycoprotein receptor ligands. Proceedings of the National Academy of Sciences of the United States of America *99*, 10042-10047.

Ellies, L.G., Sperandio, M., Underhill, G.H., Yousif, J., Smith, M., Priatel, J.J., Kansas, G.S., Ley, K., and Marth, J.D. (2002b). Sialyltransferase specificity in selectin ligand formation. Blood *100*, 3618-3625.

Elmasri, H., Karaaslan, C., Teper, Y., Ghelfi, E., Weng, M., Ince, T.A., Kozakewich, H., Bischoff, J., and Cataltepe, S. (2009). Fatty acid binding protein 4 is a target of VEGF and a regulator of cell proliferation in endothelial cells. FASEB journal : official publication of the Federation of American Societies for Experimental Biology *23*, 3865-3873.

Eriksson, J.W. (2007). Metabolic stress in insulin's target cells leads to ROS accumulation – A hypothetical common pathway causing insulin resistance. FEBS letters *581*, 3734-3742.

F

Freitas, M., Axelsson, L.G., Cayuela, C., Midtvedt, T., and Trugnan, G. (2002). Microbial-host interactions specifically control the glycosylation pattern in intestinal mouse mucosa. Histochemistry and cell biology *118*, 149-161.

Frommhold, D., Ludwig, A., Bixel, M.G., Zarbock, A., Babushkina, I., Weissinger, M., Cauwenberghs, S., Ellies, L.G., Marth, J.D., Beck-Sickinger, A.G., *et al.* (2008). Sialyltransferase ST3Gal-IV controls CXCR2-mediated firm leukocyte arrest during inflammation. The Journal of experimental medicine *205*, 1435-1446.

G

Garvey, W.T., Huecksteadt, T.P., Matthaei, S., and Olefsky, J.M. (1988). Role of glucose transporters in the cellular insulin resistance of type II non-insulin-dependent diabetes mellitus. The Journal of clinical investigation *81*, 1528-1536.

Gilmore, T.D. (2006). Introduction to NF-kappaB: players, pathways, perspectives. Oncogene *25*, 6680-6684.

Gomes, C., Osorio, H., Pinto, M.T., Campos, D., Oliveira, M.J., and Reis, C.A. (2013). Expression of ST3GAL4 leads to SLe(x) expression and induces c-Met activation and an invasive phenotype in gastric carcinoma cells. PloS one *8*, e66737.

Gorogawa, S., Fujitani, Y., Kaneto, H., Hazama, Y., Watada, H., Miyamoto, Y., Takeda, K., Akira, S., Magnuson, M.A., Yamasaki, Y., *et al.* (2004). Insulin secretory defects and

impaired islet architecture in pancreatic beta-cell-specific STAT3 knockout mice. Biochemical and biophysical research communications *319*, 1159-1170.

Grunfeld, C., Zhao, C., Fuller, J., Pollack, A., Moser, A., Friedman, J., and Feingold, K.R. (1996). Endotoxin and cytokines induce expression of leptin, the ob gene product, in hamsters. The Journal of clinical investigation *97*, 2152-2157.

Gu, Y., Ande, S.R., and Mishra, S. (2011). Altered O-GlcNAc modification and phosphorylation of mitochondrial proteins in myoblast cells exposed to high glucose. Archives of biochemistry and biophysics *505*, 98-104.

H

Hanahan, D., and Weinberg, R.A. (2000). The hallmarks of cancer. Cell *100*, 57-70.

Hanahan, D., and Weinberg, R.A. (2011). Hallmarks of cancer: the next generation. Cell *144*, 646-674.

Hayden, M.S., and Ghosh, S. (2004). Signaling to NF-kappaB. Genes & development *18*, 2195-2224.

Hayden, M.S., and Ghosh, S. (2008). Shared principles in NF-kappaB signaling. Cell *132*, 344-362.

He, W., Barak, Y., Hevener, A., Olson, P., Liao, D., Le, J., Nelson, M., Ong, E., Olefsky, J.M., and Evans, R.M. (2003). Adipose-specific peroxisome proliferator-activated receptor gamma knockout causes insulin resistance in fat and liver but not in muscle. Proceedings of the National Academy of Sciences of the United States of America *100*, 15712-15717.

Ho, H.H., Chang, C.S., Ho, W.C., Liao, S.Y., Wu, C.H., and Wang, C.J. (2010). Anti-metastasis effects of gallic acid on gastric cancer cells involves inhibition of NF-kappaB activity and downregulation of PI3K/AKT/small GTPase signals. Food and chemical toxicology : an international journal published for the British Industrial Biological Research Association *48*, 2508-2516.

J

Jackson, E.L., Willis, N., Mercer, K., Bronson, R.T., Crowley, D., Montoya, R., Jacks, T., and Tuveson, D.A. (2001). Analysis of lung tumor initiation and progression using conditional expression of oncogenic K-ras. Genes & development *15*, 3243-3248.

Jiao, P., Feng, B., Ma, J., Nie, Y., Paul, E., Li, Y., and Xu, H. (2012). Constitutive activation of IKKbeta in adipose tissue prevents diet-induced obesity in mice. Endocrinology *153*, 154-165.

Johnson, L., Mercer, K., Greenbaum, D., Bronson, R.T., Crowley, D., Tuveson, D.A., and Jacks, T. (2001). Somatic activation of the K-ras oncogene causes early onset lung cancer in mice. Nature *410*, 1111-1116.

K

Kalaitzidis, R.G., and Siamopoulos, K.C. (2011). The role of obesity in kidney disease: recent findings and potential mechanisms. International urology and nephrology *43*, 771-784.

Kamata, H., Honda, S.-i., Maeda, S., Chang, L., Hirata, H., and Karin, M. (2005). Reactive Oxygen Species Promote TNF±-Induced Death and Sustained JNK Activation by Inhibiting MAP Kinase Phosphatases. Cell *120*, 649-661.

Kanda, H., Tateya, S., Tamori, Y., Kotani, K., Hiasa, K., Kitazawa, R., Kitazawa, S., Miyachi, H., Maeda, S., Egashira, K., *et al.* (2006). MCP-1 contributes to macrophage infiltration into adipose tissue, insulin resistance, and hepatic steatosis in obesity. The Journal

of clinical investigation *116*, 1494-1505.

Kaneto, H., Matsuoka, T.A., Katakami, N., Kawamori, D., Miyatsuka, T., Yoshiuchi, K., Yasuda, T., Sakamoto, K., Yamasaki, Y., and Matsuhisa, M. (2007). Oxidative stress and the JNK pathway are involved in the development of type 1 and type 2 diabetes. Current molecular medicine *7*, 674-686.

Karin, M. (2008). The IkappaB kinase - a bridge between inflammation and cancer. Cell research *18*, 334-342.

Kawaguchi, Y., Cooper, B., Gannon, M., Ray, M., MacDonald, R.J., and Wright, C.V. (2002). The role of the transcriptional regulator Ptf1a in converting intestinal to pancreatic progenitors. Nature genetics *32*, 128-134.

Kelley, D.E., Goodpaster, B., Wing, R.R., and Simoneau, J.A. (1999). Skeletal muscle fatty acid metabolism in association with insulin resistance, obesity, and weight loss. The American journal of physiology *277*, E1130-1141.

Kim, Y.B., Nikoulina, S.E., Ciaraldi, T.P., Henry, R.R., and Kahn, B.B. (1999). Normal insulin-dependent activation of Akt/protein kinase B, with diminished activation of phosphoinositide 3-kinase, in muscle in type 2 diabetes. The Journal of clinical investigation *104*, 733-741.

Klok, M.D., Jakobsdottir, S., and Drent, M.L. (2006). The role of leptin and ghrelin in the regulation of food intake and body weight in humans: a review. Obesity reviews : an official journal of the International Association for the Study of Obesity *8*, 21-34.

Kulkarni, R.N., Holzenberger, M., Shih, D.Q., Ozcan, U., Stoffel, M., Magnuson, M.A., and Kahn, C.R. (2002). beta-cell-specific deletion of the Igf1 receptor leads to hyperinsulinemia and glucose intolerance but does not alter beta-cell mass. Nature genetics *31*, 111-115.

Kwak, Y.T., Li, R., Becerra, C.R., Tripathy, D., Frenkel, E.P., and Verma, U.N. (2005). IkappaB kinase alpha regulates subcellular distribution and turnover of cyclin D1 by phosphorylation. The Journal of biological chemistry *280*, 33945-33952.

Kwak, Y.T., Radaideh, S.M., Ding, L., Li, R., Frenkel, E., Story, M.D., Girard, L., Minna, J., and Verma, U.N. (2011). Cells lacking IKKalpha show nuclear cyclin D1 overexpression and a neoplastic phenotype: role of IKKalpha as a tumor suppressor. Molecular cancer research : MCR *9*, 341-349.

L

Lawrence, T., Bebien, M., Liu, G.Y., Nizet, V., and Karin, M. (2005). IKKalpha limits macrophage NF-kappaB activation and contributes to the resolution of inflammation. Nature *434*, 1138-1143.

Leahy, J.L. (2005). Pathogenesis of Type 2 Diabetes Mellitus. Archives of medical research *36*, 197-209.

Li, D., Morris, J.S., Liu, J., Hassan, M.M., Day, R.S., Bondy, M.L., and Abbruzzese, J.L. (2009). Body mass index and risk, age of onset, and survival in patients with pancreatic cancer. JAMA : the journal of the American Medical Association *301*, 2553-2562.

Li, Q., Lu, Q., Bottero, V., Estepa, G., Morrison, L., Mercurio, F., and Verma, I.M. (2005). Enhanced NF-kappaB activation and cellular function in macrophages lacking IkappaB kinase 1 (IKK1). Proceedings of the National Academy of Sciences of the United States of America *102*, 12425-12430.

Li, Q., Lu, Q., Hwang, J.Y., Buscher, D., Lee, K.F., Izpisua-Belmonte, J.C., and Verma, I.M. (1999). IKK1-deficient mice exhibit abnormal development of skin and skeleton. Genes & development *13*, 1322-1328.

Liu, B., Xia, X., Zhu, F., Park, E., Carbajal, S., Kiguchi, K., DiGiovanni, J., Fischer,

S.M., and Hu, Y. (2008). IKKalpha is required to maintain skin homeostasis and prevent skin cancer. Cancer cell *14*, 212-225.

Liu, M., Lee, D.F., Chen, C.T., Yen, C.J., Li, L.Y., Lee, H.J., Chang, C.J., Chang, W.C., Hsu, J.M., Kuo, H.P., *et al.* (2012a). IKKalpha activation of NOTCH links tumorigenesis via FOXA2 suppression. Mol Cell *45*, 171-184.

Liu, S., Chen, Z., Zhu, F., and Hu, Y. (2012b). IkappaB kinase alpha and cancer. Journal of interferon & cytokine research : the official journal of the International Society for Interferon and Cytokine Research *32*, 152-158.

Liu, Y., Tanabe, K., Baronnier, D., Patel, S., Woodgett, J., Cras-Meneur, C., and Permutt, M.A. (2010). Conditional ablation of Gsk-3beta in islet beta cells results in expanded mass and resistance to fat feeding-induced diabetes in mice. Diabetologia *53*, 2600-2610.

Lizcano, J.M., and Alessi, D.R. (2002). The insulin signalling pathway. Current biology : CB *12*, R236-238.

Loffreda, S., Yang, S.Q., Lin, H.Z., Karp, C.L., Brengman, M.L., Wang, D.J., Klein, A.S., Bulkley, G.B., Bao, C., Noble, P.W., *et al.* (1998). Leptin regulates proinflammatory immune responses. FASEB journal : official publication of the Federation of American Societies for Experimental Biology *12*, 57-65.

Luhn, K., and Wild, M.K. (2012). Human deficiencies of fucosylation and sialylation affecting selectin ligands. Seminars in immunopathology *34*, 383-399.

M

Ma, Z., and Vosseller, K. (2013). O-GlcNAc in cancer biology. Amino acids.

Madison, B.B., Dunbar, L., Qiao, X.T., Braunstein, K., Braunstein, E., and Gumucio, D.L. (2002). Cis elements of the villin gene control expression in restricted domains of the vertical (crypt) and horizontal (duodenum, cecum) axes of the intestine. The Journal of biological chemistry *277*, 33275-33283.

Malagolini, N., Santini, D., Chiricolo, M., and Dall'Olio, F. (2007). Biosynthesis and expression of the Sda and sialyl Lewis x antigens in normal and cancer colon. Glycobiology *17*, 688-697.

Malhi, H., Bronk, S.F., Werneburg, N.W., and Gores, G.J. (2006). Free fatty acids induce JNK-dependent hepatocyte lipoapoptosis. The Journal of biological chemistry *281*, 12093-12101.

Malumbres, M., and Barbacid, M. (2003). RAS oncogenes: the first 30 years. Nature reviews Cancer *3*, 459-465.

Mauro, C., Leow, S.C., Anso, E., Rocha, S., Thotakura, A.K., Tornatore, L., Moretti, M., De Smaele, E., Beg, A.A., Tergaonkar, V., *et al.* (2011). NF-kappaB controls energy homeostasis and metabolic adaptation by upregulating mitochondrial respiration. Nature cell biology *13*, 1272-1279.

MD, S., C, A., J, H., FK, R., Aydin B, Schwitalla S, Ziegler P, Reindl W, O, P.d.C., Buch T, *et al.* High-fat diet-mediated dysbiosis cooperates with oncogenic K-Ras activation to promote intestinal carcinogenesis independently of obesity

Mi, W., Gu, Y., Han, C., Liu, H., Fan, Q., Zhang, X., Cong, Q., and Yu, W. (2011). O-GlcNAcylation is a novel regulator of lung and colon cancer malignancy. Biochimica et biophysica acta *1812*, 514-519.

Moody, T.W., Ito, T., Osefo, N., and Jensen, R.T. (2011). VIP and PACAP: recent insights into their functions/roles in physiology and disease from molecular and genetic studies. Current opinion in endocrinology, diabetes, and obesity *18*, 61-67.

Murphy, J.E., Zhou, S., Giese, K., Williams, L.T., Escobedo, J.A., and Dwarki, V.J. (1997). Long-term correction of obesity and diabetes in genetically obese mice by a single

intramuscular injection of recombinant adeno-associated virus encoding mouse leptin. Proceedings of the National Academy of Sciences of the United States of America *94*, 13921-13926.

N

Nguyen, M.T., Satoh, H., Favelyukis, S., Babendure, J.L., Imamura, T., Sbodio, J.I., Zalevsky, J., Dahiyat, B.I., Chi, N.W., and Olefsky, J.M. (2005). JNK and tumor necrosis factor-alpha mediate free fatty acid-induced insulin resistance in 3T3-L1 adipocytes. The Journal of biological chemistry *280*, 35361-35371.

Niu, X., Fan, X., Sun, J., Ting, P., Narula, S., and Lundell, D. (2004). Inhibition of fucosyltransferase VII by gallic acid and its derivatives. Archives of biochemistry and biophysics *425*, 51-57.

O

Oeckinghaus, A., Hayden, M.S., and Ghosh, S. (2011). Crosstalk in NF-kappaB signaling pathways. Nature immunology *12*, 695-708.

Oleinika, K., Nibbs, R.J., Graham, G.J., and Fraser, A.R. (2013). Suppression, subversion and escape: the role of regulatory T cells in cancer progression. Clinical and experimental immunology *171*, 36-45.

Ouchi, N., Kihara, S., Arita, Y., Okamoto, Y., Maeda, K., Kuriyama, H., Hotta, K., Nishida, M., Takahashi, M., Muraguchi, M., *et al.* (2001). Adiponectin, an Adipocyte-Derived Plasma Protein, Inhibits Endothelial NF- B Signaling Through a cAMP-Dependent Pathway. Circulation *102*, 1296-1301.

P

Pan, D.A., Lillioja, S., Kriketos, A.D., Milner, M.R., Baur, L.A., Bogardus, C., Jenkins, A.B., and Storlien, L.H. (1997). Skeletal muscle triglyceride levels are inversely related to insulin action. Diabetes *46*, 983-988.

Park, S.Y., Ryu, J., and Lee, W. (2005). O-GlcNAc modification on IRS-1 and Akt2 by PUGNAc inhibits their phosphorylation and induces insulin resistance in rat primary adipocytes. Experimental & molecular medicine *37*, 220-229.

Patsos, G., Hebbe-Viton, V., Robbe-Masselot, C., Masselot, D., San Martin, R., Greenwood, R., Paraskeva, C., Klein, A., Graessmann, M., Michalski, J.C., *et al.* (2009). O-glycan inhibitors generate aryl-glycans, induce apoptosis and lead to growth inhibition in colorectal cancer cell lines. Glycobiology *19*, 382-398.

Pederson, T.M., Kramer, D.L., and Rondinone, C.M. (2001). Serine/threonine phosphorylation of IRS-1 triggers its degradation: possible regulation by tyrosine phosphorylation. Diabetes *50*, 24-31.

Perez-Garay, M., Arteta, B., Pages, L., de Llorens, R., de Bolos, C., Vidal-Vanaclocha, F., and Peracaula, R. (2010). alpha2,3-sialyltransferase ST3Gal III modulates pancreatic cancer cell motility and adhesion in vitro and enhances its metastatic potential in vivo. PloS one *5*.

Phillips, D.I., Caddy, S., Ilic, V., Fielding, B.A., Frayn, K.N., Borthwick, A.C., and Taylor, R. (1996). Intramuscular triglyceride and muscle insulin sensitivity: evidence for a relationship in nondiabetic subjects. Metabolism: clinical and experimental *45*, 947-950.

Popkin, B.M., Adair, L.S., and Ng, S.W. (2011). Global nutrition transition and the pandemic of obesity in developing countries. Nutrition reviews *70*, 3-21.

Portela, S.V., Martin, C.V., Romay, L.M., Cuevas, E., Martin, E.G., and Briera, A.F. (2011). sLea and sLex expression in colorectal cancer: implications for tumourigenesis and disease prognosis. Histology and histopathology *26*, 1305-1316.

Postic, C., Shiota, M., Niswender, K.D., Jetton, T.L., Chen, Y.J., Moates, J.M., Shelton, K.D., Lindner, J., Cherrington, A.D., and Magnuson, M.A. (1999). Dual roles for glucokinase in glucose homeostasis as determined by liver and pancreatic beta cell-specific gene knock-outs using Cre recombinase. Journal of Biological Chemistry *274*, 305-315.

R

Rabinovich, G.A., van Kooyk, Y., and Cobb, B.A. (2012). Glycobiology of immune responses. Annals of the New York Academy of Sciences *1253*, 1-15.

Rachagani, S., Torres, M.P., Moniaux, N., and Batra, S.K. (2009). Current status of mucins in the diagnosis and therapy of cancer. BioFactors *35*, 509-527.

Ran, R., Lu, A., Zhang, L., Tang, Y., Zhu, H., Xu, H., Feng, Y., Han, C., Zhou, G., Rigby, A.C., *et al.* (2004). Hsp70 promotes TNF-mediated apoptosis by binding IKK gamma and impairing NF-kappa B survival signaling. Genes & development *18*, 1466-1481.

Razani, B., Reichardt, A.D., and Cheng, G. (2011). Non-canonical NF-kappaB signaling activation and regulation: principles and perspectives. Immunological reviews *244*, 44-54.

Razani, B., Zarnegar, B., Ytterberg, A.J., Shiba, T., Dempsey, P.W., Ware, C.F., Loo, J.A., and Cheng, G. (2010). Negative feedback in noncanonical NF-kappaB signaling modulates NIK stability through IKKalpha-mediated phosphorylation. Science signaling *3*, ra41.

Reaven, G. (2012). Insulin resistance and coronary heart disease in nondiabetic individuals. Arteriosclerosis, thrombosis, and vascular biology *32*, 1754-1759.

Reilly, S.M., Chiang, S.H., Decker, S.J., Chang, L., Uhm, M., Larsen, M.J., Rubin, J.R., Mowers, J., White, N.M., Hochberg, I., *et al.* (2013). An inhibitor of the protein kinases TBK1 and IKK-varepsilon improves obesity-related metabolic dysfunctions in mice. Nature medicine *19*, 313-321.

Rowland, A.F., Fazakerley, D.J., and James, D.E. (2011). Mapping insulin/GLUT4 circuitry. Traffic *12*, 672-681.

S

Scarpellini, E., and Tack, J. (2012). Obesity and metabolic syndrome: an inflammatory condition. Digestive diseases *30*, 148-153.

Schenk, S., Harber, M.P., Shrivastava, C.R., Burant, C.F., and Horowitz, J.F. (2009). Improved insulin sensitivity after weight loss and exercise training is mediated by a reduction in plasma fatty acid mobilization, not enhanced oxidative capacity. The Journal of physiology *587*, 4949-4961.

Sen, R., and Baltimore, D. (1986). Multiple nuclear factors interact with the immunoglobulin enhancer sequences. Cell *46*, 705-716.

Senftleben, U., Cao, Y., Xiao, G., Greten, F.R., Krahn, G., Bonizzi, G., Chen, Y., Hu, Y., Fong, A., Sun, S.C., *et al.* (2001). Activation by IKKalpha of a second, evolutionary conserved, NF-kappa B signaling pathway. Science *293*, 1495-1499.

Serrano, A., Palacios, C., Roy, G., Cespon, C., Villar, M.L., Nocito, M., and Gonzalez-Porque, P. (1998). Derivatives of gallic acid induce apoptosis in tumoral cell lines and inhibit lymphocyte proliferation. Archives of biochemistry and biophysics *350*, 49-54.

Shembade, N., Pujari, R., Harhaj, N.S., Abbott, D.W., and Harhaj, E.W. (2011). The kinase IKKalpha inhibits activation of the transcription factor NF-kappaB by phosphorylating

the regulatory molecule TAX1BP1. Nature immunology *12*, 834-843.

Shoelson, S.E., Lee, J., and Yuan, M. (2003). Inflammation and the IKK beta/I kappa B/NF-kappa B axis in obesity- and diet-induced insulin resistance. International journal of obesity and related metabolic disorders : journal of the International Association for the Study of Obesity *27 Suppl 3*, S49-52.

Slawson, C., and Hart, G.W. (2011). O-GlcNAc signalling: implications for cancer cell biology. Nature reviews Cancer *11*, 678-684.

Slawson, C., Pidala, J., and Potter, R. (2001). Increased N-acetyl-beta-glucosaminidase activity in primary breast carcinomas corresponds to a decrease in N-acetylglucosamine containing proteins. Biochimica et biophysica acta *1537*, 147-157.

Smitka, K., Papezova, H., Vondra, K., Hill, M., Hainer, V., and Nedvidkova, J. (2013). The Role of "Mixed" Orexigenic and Anorexigenic Signals and Autoantibodies Reacting with Appetite-Regulating Neuropeptides and Peptides of the Adipose Tissue-Gut-Brain Axis: Relevance to Food Intake and Nutritional Status in Patients with Anorexia Nervosa and Bulimia Nervosa. International journal of endocrinology *2013*, 483145.

Solinas, G., and Karin, M. (2010). JNK1 and IKKbeta: molecular links between obesity and metabolic dysfunction. FASEB journal : official publication of the Federation of American Societies for Experimental Biology *24*, 2596-2611.

Solinas, G., Naugler, W., Galimi, F., Lee, M.S., and Karin, M. (2006). Saturated fatty acids inhibit induction of insulin gene transcription by JNK-mediated phosphorylation of insulin-receptor substrates. Proceedings of the National Academy of Sciences of the United States of America *103*, 16454-16459.

Song, J., Xu, Y., Hu, X., Choi, B., and Tong, Q. (2010). Brain expression of Cre recombinase driven by pancreas-specific promoters. Genesis *48*, 628-634.

Sperandio, M. (2006). Selectins and glycosyltransferases in leukocyte rolling in vivo. The FEBS journal *273*, 4377-4389.

Sperandio, M. (2012). The expanding role of alpha2-3 sialylation for leukocyte trafficking in vivo. Annals of the New York Academy of Sciences *1253*, 201-205.

Suerbaum, S., and Michetti, P. (2002). Helicobacter pylori infection. The New England journal of medicine *347*, 1175-1186.

Sun, S.C. (2011). Non-canonical NF-kappaB signaling pathway. Cell research *21*, 71-85.

Sund, N.J., Vatamaniuk, M.Z., Casey, M., Ang, S.L., Magnuson, M.A., Stoffers, D.A., Matschinsky, F.M., and Kaestner, K.H. (2001). Tissue-specific deletion of Foxa2 in pancreatic beta cells results in hyperinsulinemic hypoglycemia. Genes & development *15*, 1706-1715.

Sundsten, T., and Ortsäter, H. (2009). Proteomics in diabetes research. Molecular and Cellular Endocrinology *297*, 93-103.

Sung, M.K., and Bae, Y.J. (2010). Linking obesity to colorectal cancer: application of nutrigenomics. Biotechnology journal *5*, 930-941.

T

Tang, T., Zhang, J., Yin, J., Staszkiewicz, J., Gawronska-Kozak, B., Jung, D.Y., Ko, H.J., Ong, H., Kim, J.K., Mynatt, R., *et al.* (2010). Uncoupling of inflammation and insulin resistance by NF-kappaB in transgenic mice through elevated energy expenditure. The Journal of biological chemistry *285*, 4637-4644.

Thomsen, J., Kristiansen, K., Brunfeldt, K., and Sundby, F. (1972). The amino acid sequence of human glucagon. FEBS letters *21*, 315-319.

V

van Gisbergen, K.P., Ludwig, I.S., Geijtenbeek, T.B., and van Kooyk, Y. (2005). Interactions of DC-SIGN with Mac-1 and CEACAM1 regulate contact between dendritic cells and neutrophils. FEBS letters *579*, 6159-6168.

Varki A, Cummings RD, and JD, E., eds. (2009). Essentials of Glycobiology. 2nd edition (Cold Spring Harbor (NY): Cold Spring Harbor Laboratory Press).

W

Weiss, Y.G., Bromberg, Z., Raj, N., Raphael, J., Goloubinoff, P., Ben-Neriah, Y., and Deutschman, C.S. (2007). Enhanced heat shock protein 70 expression alters proteasomal degradation of IkappaB kinase in experimental acute respiratory distress syndrome. Critical care medicine *35*, 2128-2138.

Y

Yamaguchi, N., Argueta, J.G., Masuhiro, Y., Kagishita, M., Nonaka, K., Saito, T., Hanazawa, S., and Yamashita, Y. (2005). Adiponectin inhibits Toll-like receptor family-induced signaling. FEBS letters *579*, 6821-6826.

Z

Zhang, Y., Proenca, R., Maffei, M., Barone, M., Leopold, L., and Friedman, J.M. (1994). Positional cloning of the mouse obese gene and its human homologue. Nature *372*, 425-432.

8. ACKNOWLEDGEMENTS

First of all I would like to thanks P.D. Dr Canan Arkan for the opportunity she gave me to work in her laboratory on those subjects. Thank you for the supervision throughout my whole PhD.

Then I would like to thank you Prof Dr Florian Greten for being part of my thesis committee and for the technical support during those years.

I also would like to thank Prof Dr Gabriele Multhoff for being part of my thesis committee and her suggestions during the committee meetings.

Thank you to Prof Dr Martin Klingenspor for the collaboration and the technical assistant of his team for performing an experiment of this thesis.

I would as well like to thank Dr Katrin Offe and the medical faculty of TUM for the administrative help as well as for the one year fellowship.

Thanks to the Krebshilfe and the DFG for the financial support.

A PhD thesis would not be possible without the support of colleagues. I had the chance to have great colleagues. So many thanks to Dr Çiğdem Atay, Dr Manon Schulz, Dr Franziska Romrig for the friendship, the good atmosphere and the help with the experiments when I needed it. Çiğdem, thank you for the Turkish lesson, I still know some words! Manon thank you for your great help and simply for your presence. Franzi thank you for your help during the difficult moments.

Thanks a lot to Saskia Ettl for the technical support and her help during those years in Munich.

Thanks to Kerstin Burmeister, who is a little bit the “mum” of the lab, for the chocolate she always brought us! Thanks as well for the technical support.

I would like to thanks as well all the members of Prof Dr Florian Greten team for their friendship and the great international atmosphere: Dr Hsin-Yu Fang, the energy-full Taiwanese, Dr Tiago de Oliveira, the only one who understood me about French cuisine, Dr Sarah Schwitalla and her great travels around the world, Dr Özge Canlı and Emine, Dr Abdelhamid Beji, my French speaking colleague, Dr Charles Pallyango, the tall guy with a big heart, Michaela Diamanti, the “MAD” girl, Jùlia Varga: I didn’t forget Budapest!, Paul Ziegler: you will be a great MD! and Olga Goncharova, our colleague who comes from the cold!

Thank a lot to all former members of the lab: Dr Arun Mankan, Begüm Alankuş, Gülfem Öner, Michael Willert and Kristin Retzlaff.

Thank you to all my friends, in Germany, France or even Canada for the support. A particular thanks to Marie who was around all the time.

Pour finir, j’aimerai remercier du fond du cœur ma famille: mes parents, Amandine ainsi que Pascal. Sans vous je ne serais pas là où j’en suis. Je vous aime très fort. Pour finir je profite de cette thèse pour souhaiter la bienvenue dans notre famille au petit dernier, Tom. J’espère que quand tu seras assez grand pour lire ceci tu seras fier de ta marraine.